2009-12

Characterization of transient plasma ignition flame kernel growth for varying inlet conditions

Hawkes, Neil C.

Monterey, California. Naval Postgraduate School

NAVAL POSTGRADUATE SCHOOL

MONTEREY, CALIFORNIA

THESIS

CHARACTERIZATION OF TRANSIENT PLASMA IGNITION FLAME KERNEL GROWTH FOR VARYING INLET CONDITIONS

By

Neil C. Hawkes

December 2009

Thesis Advisor:	Christopher M. Brophy
Second Reader:	Jose O. Sinibaldi

THIS PAGE INTENTIONALLY LEFT BLANK

REPORT DOCUMENTATION PAGE			*Form Approved OMB No. 0704-0188*
Public reporting burden for this collection of information is estimated to average 1 hour per response, including the time for reviewing instruction, searching existing data sources, gathering and maintaining the data needed, and completing and reviewing the collection of information. Send comments regarding this burden estimate or any other aspect of this collection of information, including suggestions for reducing this burden, to Washington headquarters Services, Directorate for Information Operations and Reports, 1215 Jefferson Davis Highway, Suite 1204, Arlington, VA 22202-4302, and to the Office of Management and Budget, Paperwork Reduction Project (0704-0188) Washington DC 20503.			
1. AGENCY USE ONLY ***(Leave blank)***	**2. REPORT DATE** December 2009	**3. REPORT TYPE AND DATES COVERED** Master's Thesis	
4. TITLE AND SUBTITLE Characterization of Transient Plasma Ignition Flame Kernel Growth for Varying Inlet Conditions		**5. FUNDING NUMBERS**	
6. AUTHOR(S) Neil C. Hawkes			
7. PERFORMING ORGANIZATION NAME(S) AND ADDRESS(ES) Naval Postgraduate School Monterey, CA 93943-5000		**8. PERFORMING ORGANIZATION REPORT NUMBER**	
9. SPONSORING /MONITORING AGENCY NAME(S) AND ADDRESS(ES) N/A		**10. SPONSORING/MONITORING AGENCY REPORT NUMBER**	
11. SUPPLEMENTARY NOTES The views expressed in this thesis are those of the author and do not reflect the official policy or position of the Department of Defense or the U.S. Government.			
12a. DISTRIBUTION / AVAILABILITY STATEMENT Approved for public release; distribution is unlimited		**12b. DISTRIBUTION CODE** A	

13. ABSTRACT (maximum 200 words)

Pulse detonation engines (PDEs) have the potential to significantly improve the efficiency of a variety of internal combustion engine designs. This efficiency improvement hinges on the ability of the engine to detonate fuel/air mixture through deflagration-to-detonation transitions at 60 to 100 times a second. A major break through in reducing the cycle time of a pulse detonation device is through the use of a Transient Plasma Ignition (TPI) system vice the normal Capacitive Discharge Ignition (CDI) system. The TPI system deposits an equivalent amount of energy as the CDI system but in a fraction of the time and over a larger combustor volume. The TPI also creates high quantities of OH due to the high density of energetic electrons produced by the TPI event. The combination of decreased energy deposition time, larger ignition volume, and a high density of free radicals reduces the flame kernel growth time which in turn creates a choked flame condition more rapidly. This thesis characterized the flame kernel growth following a transient plasma ignition event for various combustor inlet configurations so as to better understand the flame patterns within the combustion chamber. High speed images of the combustor were taken from a side profile and end view to observe the flame growth. Time from ignition event until initial flame kernel observation and from ignition event until fully developed flame were gathered from the images and plotted to find the most favorable inlet condition.

14. SUBJECT TERMS Transient Plasma Ignition, Pulse Detonation Engine, Flame Kernel Growth			**15. NUMBER OF PAGES** 103
			16. PRICE CODE
17. SECURITY CLASSIFICATION OF REPORT Unclassified	**18. SECURITY CLASSIFICATION OF THIS PAGE** Unclassified	**19. SECURITY CLASSIFICATION OF ABSTRACT** Unclassified	**20. LIMITATION OF ABSTRACT** UU

NSN 7540-01-280-5500 Standard Form 298 (Rev. 2-89)
Prescribed by ANSI Std. 239-18

THIS PAGE INTENTIONALLY LEFT BLANK

Approved for public release; distribution is unlimited

CHARACTERIZATION OF TRANSIENT PLASMA IGNITION FLAME KERNEL GROWTH FOR VARYING INLET CONDITIONS

Neil C. Hawkes
Lieutenant, United States Navy
B.S., Rensselaer Polytechnic Institute, 2000

Submitted in partial fulfillment of the
requirements for the degree of

MASTER OF SCIENCE IN ASTRONAUTICAL ENGINEERING

from the

NAVAL POSTGRADUATE SCHOOL
December 2009

Author: Neil C. Hawkes

Approved by: Christopher M. Brophy
Thesis Advisor

Jose O. Sinibaldi
Second Reader

Knox T. Millsaps
Chairman, Department of Mechanical & Astronautical Engineering

THIS PAGE INTENTIONALLY LEFT BLANK

ABSTRACT

Pulse detonation engines (PDEs) have the potential to significantly improve the efficiency of a variety of internal combustion engine designs. This efficiency improvement hinges on the ability of the engine to detonate fuel/air mixture through deflagration-to-detonation transitions at 60 to 100 times a second. A major breakthrough in reducing the cycle time of a pulse detonation device is through the use of a Transient Plasma Ignition (TPI) system vice the normal Capacitive Discharge Ignition (CDI) system. The TPI system deposits an equivalent amount of energy as the CDI system but in a fraction of the time and over a larger combustor volume. The TPI also creates high quantities of OH due to the high density of energetic electrons produced by the TPI event. The combination of decreased energy deposition time, larger ignition volume, and a high density of free radicals reduces the flame kernel growth time, which in turn creates a choked flame condition more rapidly. This thesis characterized the flame kernel growth following a transient plasma ignition event for various combustor inlet configurations so as to better understand the flame patterns within the combustion chamber. High-speed images of the combustor were taken from a side profile and end view to observe the flame growth. Time from ignition event until initial flame kernel observation and from ignition event until fully developed flame were gathered from the images and plotted to find the most favorable inlet condition.

THIS PAGE INTENTIONALLY LEFT BLANK

TABLE OF CONTENTS

THIS PAGE INTENTIONALLY LEFT BLANK

LIST OF FIGURES

THIS PAGE INTENTIONALLY LEFT BLANK

LIST OF TABLES

THIS PAGE INTENTIONALLY LEFT BLANK

LIST OF ACRONYMS, ABBREVIATIONS, AND SYMBOLS

CEQUEL	-	Chemical Equilibrium in Excel
CDI	-	Capacitive Discharge Ignition
DDT	-	Deflagration-To-Detonation Transition
GUI	-	Graphical User Interface
NI	-	National Instruments
NPS	-	Naval Postgraduate School
PDC	-	Pulse Detonation Combustor
PDE	-	Pulse Detonation Engine
Phi		The Greek letter Φ
PSIA	-	Pounds per Square Inch Absolute
TPI	-	Transient Plasma Ignition
ISP	-	Specific Impulse
A	-	area
C	-	carbon
C_2H_4	-	ethylene
c	-	speed of sound
e	-	electron
eV	-	electron volt
Hz	-	hertz
I_{sp}	-	specific impulse
msec	-	millisecond
M	-	Mach number
$\dot{m}$	-	mass flow rate
$\dot{m}_f$	-	mass flow rate of fuel
$\dot{m}_a$	-	mass flow rate of air
$\dot{m}_{tot}$	-	total mass flow rate
O	-	oxygen
P	-	Pressure

R	-	specific gas constant
s	-	second
t	-	time
T	-	temperature
u	-	velocity
μsec	-	microsecond
v	-	velocity
ϕ	-	equivalence ratio
γ	-	specific heat ratio
ρ	-	density

ACKNOWLEDGMENTS

The author would like to express his sincere gratitude to Dr. Christopher Brophy for his support and direction throughout the experimentation process. His depth of knowledge of all the lab systems and through handle of the workings of Pulse Detonation Engines made short work of any complications that arose. His ability to challenge results and ask questions enabled more meaningful results that will enhance the future of the PDE. Additionally, a show of gratitude is owed to George Hageman and David Dausen for their support during testing and test rig component change outs.

The author would also like to express his gratitude to Doug Learned and Doug Learned Jr. from Intercity Manufacturing. Without their expertise in precision machining this thesis would not have been possible. Their countless hours spent making sure that the parts for this experiment were not only made to my specifications, but would fit together seamlessly, was invaluable.

Finally, and most importantly, the author would like to express his heartfelt gratitude to his lovely wife, Shelley, sons, Joshua and Caleb, and daughter, Emma. Without their support this educational opportunity would not have been possible.

THIS PAGE INTENTIONALLY LEFT BLANK

I. INTRODUCTION

Pulse detonation combustors (PDCs) have recently received a large amount of attention from the military and civilian research institutions due to their potential to achieve increased thermodynamic efficiency with little to no moving parts. Military uses include propulsion systems capable of speeds up to Mach 4 and increased fuel efficiencies for hybrid PDC-gas turbine engines. The civilian sector is looking at PDCs for use in hybrid gas turbine electric power generation systems and eventually the core combustor on advanced engines for commercial airline applications.

The last 40 years have produced little to no new chemical propulsion developments; only improvements to existing architectures. The Pulse Detonation Engine (PDE) is a unique next step in engine system design. Figure 1 graphically depicts the operating envelopes for existing primary propulsion systems and shows where a basic PDE system would operate. The advantage of the PDE is that it has a moderately high specific impulse (Isp), effective thrust per fuel flow rate, and can be operated over a wide flight Mach number range up to Mach 4.

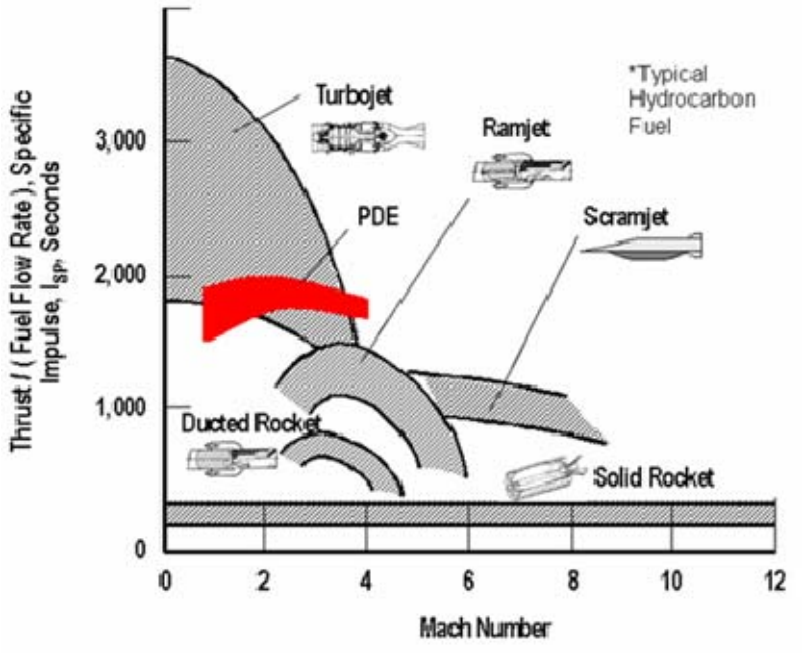

Figure 1. Propulsion Comparison Chart (From [1])

Turbofan and turbojet engines are capable of much higher Isp values at lower speeds than the PDE but, due to structural and thermodynamic limitations, their max speed is typically limited to Mach 2.5–3. Turbojet engines are also extremely complex machines that require hundreds of moving parts, making the engine more costly to produce and maintain, and may reduce reliability at high flight Mach number conditions. Ramjets and scramjets have a higher top speeds, but have reduced Isp values due to Brayton cycle limitations.

PDEs combine attractive features from both Turbojet and ram/scramjet engines. Detonation-based combustion shockwaves compress the air fuel mixture there by removing the need for a complex compressor section, which significantly simplifies the engine design. Elimination of the compressor section also allows the power that would normally be needed to turn the compressor to be used for propulsion. The PDE removes the Brayton cycle limitations by using constant-volume combustion instead of constant-pressure combustion. Most PDE designs also use almost no moving parts, which lends higher reliability and a reduction in manufacturing and maintenance costs.

To realize the benefits of PDEs, the formation of a detonation shock wave needs to be achieved at the rate of 60 to 100 times per second. Since PDEs operate in a cyclic manner, two major stages of the PDE cycle: the combustor fill time and the time from ignition until a fully-choked flame is developed, require the most amount of time. The use of obstacles in the combustor, to hasten the formation of detonations, is currently being investigated by numerous groups. This will decrease the overall tube length and allow for shorter fill times. The object of this research is to investigate the use of a Transient Plasma Ignition system to improve the time from ignition until the flame is fully developed. A reduction in both these processes will allow the PDE to be operated at a frequency at which a near-constant thrust profile can be attained.

II. BACKGROUND

A. PULSE DETONATION ENGINE OPERATION

1. Basic Engine Operation

The PDE operates in a cycle much like that of a typical car engine. It has four distinct phases each of which is vital to the overall operation of the engine. Figure 2 shows the basic processes of each phase. In order for the engine to produce any usefully work, this cycle must be repeated as often as possible, but preferably at close to 80–100 times a second. In order for the engine to be able to operate at these frequencies each phase needs to be completed as quickly as possible.

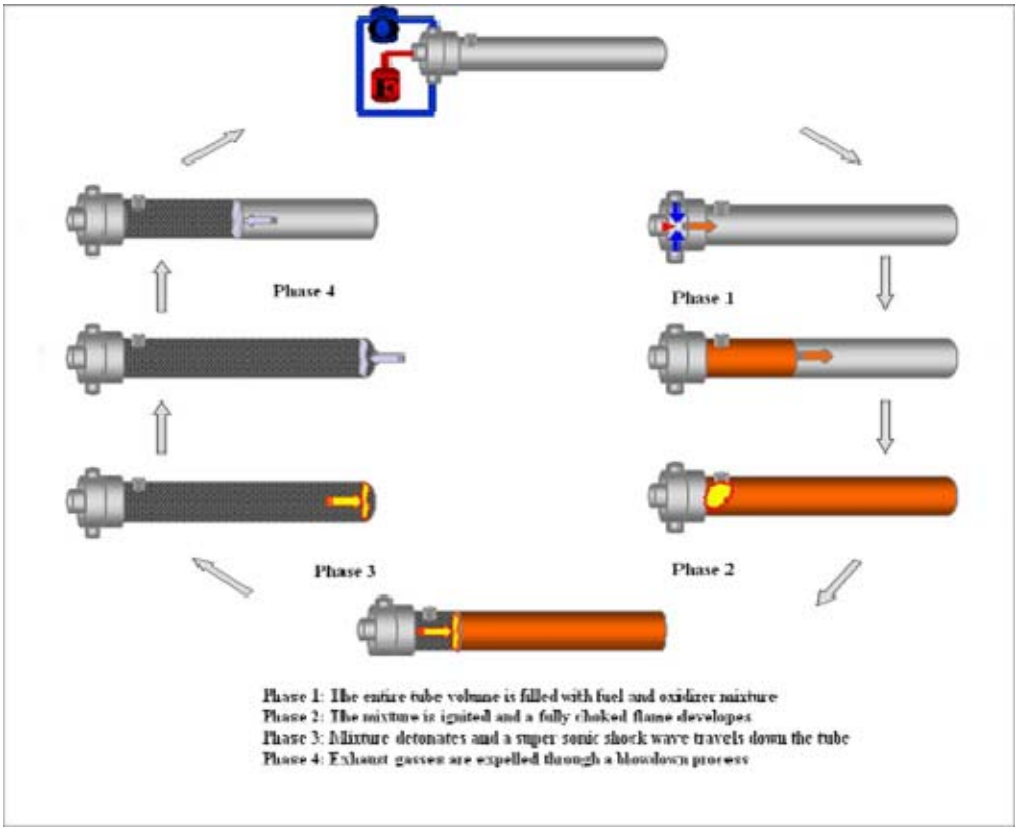

Figure 2. PDE Cycle (From [1])

The first step in the PDE cycle is filling the entire tube volume with the fuel/oxidizer mixture. This is necessary to ensure that there are enough reactants in the combustor to sustain the flame front until the shockwave has formed and exited the tube. The time required to fill the entire volume is a function of the tube length, cross sectional area, and mass flow rate of the incoming fuel/oxidizer mixture. For a fixed mass flow rate, the shorter the tube the faster it can be filled and the sooner the mixture can be ignited. A typical fill time for a 1 meter tube at a Mach number of 0.2 is on the order of 15 milliseconds.

Once the fuel/oxidizer mixture has filled the entire tube, it is ignited near the forward end. Early PDE systems have used Capacitive Discharge Ignition (CDI) systems which produce a relatively long lived (~0.1ms) arc of hot plasma to initiate the combustion process. The effectiveness and associated ignition delay with this type of igniter makes it difficult to run a pulsed engine at the required frequency. Transient Plasma Ignition (TPI) systems are now used due to their improved effectiveness from the dramatically shorter energy deposition timescales. The TPI system is capable of delivering the same amount of energy as the CDI system, but in one thousandths of the time. The ignition portion of the cycle can be broken down into to distinct time segments. The first is the time it takes from the ignition energy discharge until a flame kernel is formed (ignition delay), and the second is the time it takes from the initial flame kernel formation until the flame is fully developed (flame growth time). Phase 2 ends once the flame has become fully developed and a detonation shockwave has been formed. However, for this thesis the flame growth time will be considered complete when the flame is fully choked because further development of the flame does not depend on the ignition system any more. Typical ignition delay times, from this thesis, were 1.6 msec and 500 μsec for the CDI and TPI systems respectfully.

Once the flame is fully choked, a process called deflagration-to-detonation transition (DDT) takes place. Under proper conditions, this process takes the aggressively burning reactants and creates a detonation shockwave, which rapidly moves down the remainder of the tube and exits out the exhaust end. The detonation wave will be produced somewhere within the combustor due to the time required to produce the

required conditions, and will be travelling at near Mach 5 speeds for most hydrocarbon fuel/air mixtures. The time required for this wave to traverse a typical combustor is approximately 300 μsec. The conditions produced by this detonation wave provide the thrust for the engine.

The final phase of the cycle is known as blowdown, and it consists of exhausting combustion products out the end of the tube. Blowdown occurs when the detonation wave exits the tube and the combustion products sense the surrounding atmospheric pressure. This sudden drop in pressure creates a rarefaction wave that travels forward in the combustor. The blowdown time for a 1 meter long tube is approximately 3 msec. Combustion products are then forced out of the chamber as a fresh fuel/oxidizer mixture is added in preparation for the next cycle. The total cycle time formula can be represented by in the following formula:

Cycle time: $$t_{cycle} = t_{fill} + t_{ignition\,delay} + t_{flame\,growth} + t_{detonation} + t_{blowdown} \quad (1)$$

Max Operating Frequency: $f = 1/t_{cycle}$

Typical CDI Cycle Time: $$t_{\sec} = 15_{m\sec} + 1.6_{m\sec} + 0.3_{m\sec} + 3_{m\sec} = 19.9_{m\sec} \quad (2)$$
$$f = 1/19.9_{m\sec} = 50.25Hz$$

Typical TPI Cycle Time: $$t_{\sec} = 15_{m\sec} + 0.5_{m\sec} + 0.3_{m\sec} + 3_{m\sec} = 18.8 \quad (3)$$
$$f = 1/18.8_{m\sec} = 53.19Hz$$

2. Deflagration vs. Detonation Combustion

The most widely used and studied form of combustion is deflagration. Deflagration is a constant-pressure combustion reaction in which a flame front propagates at sub-sonic speeds though a reactive mixture. This is the combustion process that occurs in ramjet engines, turbojet engines, and even in rocket engines. Temperature and pressure strongly affect the chemical reactions needed for combustion, but because deflagration is a constant pressure event, it is unable to fully harness the reactants potential energy.

Detonation is a combustion event in which a supersonic shockwave propagates though a mixture causing it to become compressed. This compression leads to a rapid rise in temperature, pressure, and density. This highly energized mixture develops just behind the shockwave and erupts in a violent exothermic reaction which helps to support the preceding wave. Once this reaction takes place the system becomes self sustaining and will continue as long as there are reactants ahead of the combustion wave.

A simple way to explain the combustion wave dynamics is to look at the one-dimensional planar wave in Figure 3. This model takes the reference frame of the combustion wave (hence the combustion wave is now stationary). Unburned reactants travel from left to right into the wave with a speed of u_1 and burned gasses would travel away from the wave at speed u_2.

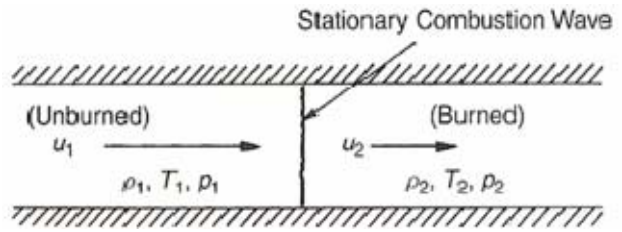

Figure 3. Diagram of 1-D Combustion Wave (From [1])

Table 1 shows the how Temperature (T), density (ρ), pressure (p) and reactant velocity (u) are affected by the different types of combustion. The 1 subscript denotes unburned reactants and the 2 subscript represents combustion products. The greatest factor affecting the reactants in a detonation is the u_1/c_1, speed of unburned reactants to that of the local speed of sound. It can be seen that a detonation produces a Mach 5-10 shock wave which is propagating at velocities 2 to 3 orders of magnitude higher than for deflagration. It is this shockwave that compresses the unburned gasses, adds a large amount of temperature, and increases the density of the mixture all of which contribute to a more efficient combustion process.

	Detonation	Deflagration
u_1/c_1	5-10	0.0001-0.03
u_2/u_1	0.4-0.7 (deceleration)	4-16
p_2/p_1	13-55 (compression)	0.98-0.976 (slight expansion)
T_2/T_1	8-21 (heat addition)	4-16 (heat addition)
ρ_2/ρ_1	1.4-2.6	0.06-0.25

Table 1. Comparison of Sonic and Subsonic Combustion Waves (From [2])

B. TRANSIENT PLASMA IGNITION

The Transient Plasma Ignition system (TPI) plays a major roll in the success of a multiple cycle PDE. TPI systems have the ability to reduce the ignition delay time over a wide range of temperatures and pressures, as well as the ability to combust leaner mixtures as seen in reference 7. The TPI system also promotes initial combustion over a larger volume of reactants, which leads to a more robust initial combustion. All these factors allow the faster formation of a choked flame front, which in turn reduces the time for detonation thus allowing the engine to be operated at a frequency that will allow for a near constant thrust profile.

Figure 4 shows an end and side view of a transient plasma (pulsed Corona) discharge from a threaded rod. When the electrode is stressed with high voltages, thin plasma filaments, called streamers, are formed and travel to the opposite electrode. Once the distance between the two electrodes has been bridged, the further evolution of a plasma channel is controlled by the amount of applied voltage. If the voltage is too high the streamer will give way to a spark which will result in a large increase in gas temperature and free radicals. This spark is also know as thermal plasma, and has been found to be less efficient at initiating combustion than the streamer phase. By controlling the voltage applied to the electrode, the TPI system is kept from developing into thermal plasma thereby increasing the efficiency of the ignition process.

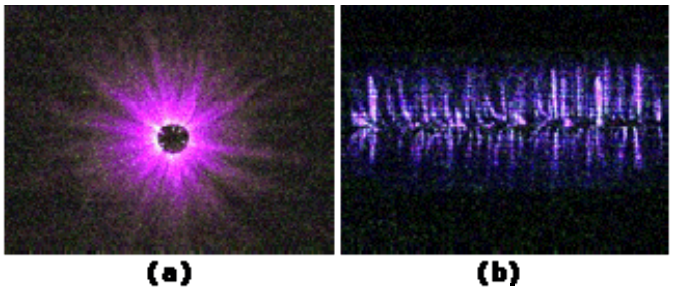

Figure 4. Transient Plasma Discharge with Threaded Rod Electrode (From [3])

An important process in the combustions of hydrocarbons is the formations of free radicals, namely CH, OH, H, and O. During a TPI event it is theorized that an initial formation of radicals is due to highly energized electron interactions with the hydrocarbons. Equations 4 and 5 show the theorized dissociation reactions:

$$RH + e \rightarrow R + H + e \quad (4)$$

$$O_2 + e \rightarrow O + O + e \quad (5)$$

Due to the non-equilibrated state of the plasma, a higher fraction of the electrons produced have energies in the 10–15 eV range. This energy level is high enough to produce the dissociative reactions of hydrocarbons over the entire length of the electrode. This large volume of free radicals enables the production of significantly more ignition kernels which promote a more rapidly expanding flame front.

C. FLAME KERNEL GROWTH

While there has been much research into the TPI system, little is known about how a TPI generated flame kernel develops once ignited. This thesis is specifically interested in this process and how various combustor inlet configurations affect the overall spreading of the flame. The goal of this research is to find the best inlet geometry to support a three tube PDE configuration with each tube having only a single inlet. Three different inlet angles (90°, 60° and 45°) were investigated with both the capacitive discharge and Transient Plasma ignition systems. The flame front was imaged both radially and axially using a high speed camera to observe the flame growth. A light probe

was used to measure the time from the ignition event until combustion was present and until the flame was fully developed. Delay times for all the inlet configurations were graphed for equivalence ratios varying from 1 to 1.5. The high-speed images were compiled into movies (in ".avi" format) and viewed to determine flame spreading path.

THIS PAGE INTENTIONALLY LEFT BLANK

III. DESIGN/EXPERIMENTAL SETUP

The experimental research for this thesis was conducted in-house at the Rocket Propulsion Laboratory in Monterey, California. The test assembly was housed in Cell #1 and is show in Figure 5. The test assembly consisted of a combustor section, an exhaust section and a fuel delivery system. Gaseous ethylene (C_2H_4) was premixed with air and injected into the combustor. The ignition portion for this test rig was designed to allow for both a CDI and TPI systems and was located at the head end of the combustor. A high speed data acquisition system was used to record fuel pressure, air pressure, initial event trigger and light probe data. A Shimadzu high-speed camera capable of imaging up to one million frames per second was used to capture the ignition event and flame kernel growth. All valve manipulation and trigger events were controlled from inside the control room via LabView and externally at the test rig via a BNC. The test rig was designed to accommodate inlet angles of 45°, 60°, and 90° relative to the horizontal axes. The entire assembly was mounted on a Newport Research Corporation optical table.

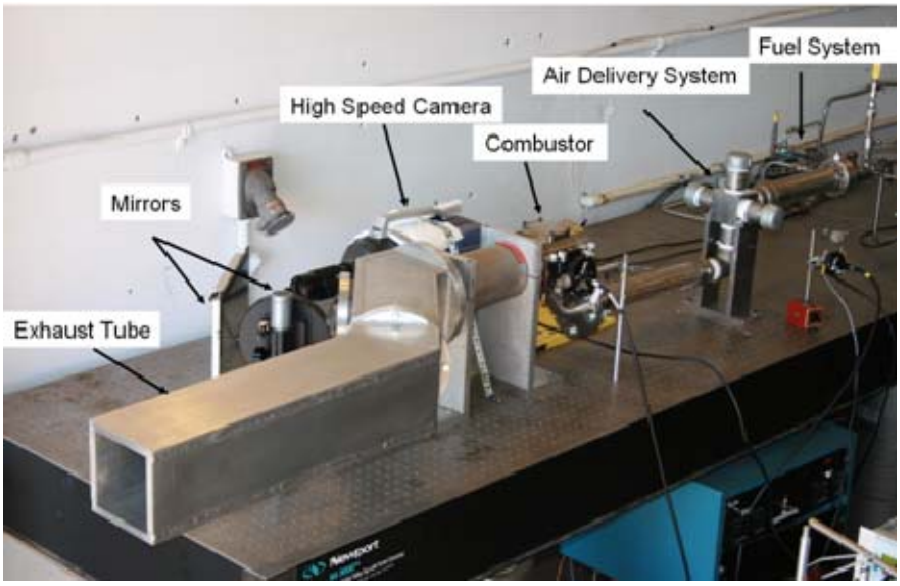

Figure 5. Test Assembly with One 45° Inlet on Test Bench in Test Cell #1

A. DESCRIPTION OF EXPERIMENTAL ASSEMBLY

1. Combustor Section

The combustor section for this experiment was a 4.25 inch long stainless steel section with a 4 inch inner diameter that housed the igniter and combustor can assembly (Figure 6). This section has four 2.5x3.25 inch rectangles cut into the main body which were used to house the optical windows as well as allow for multiple inlets to be attached to it. The combustor igniter can was attached to the combustor head section, was used to mount the combustor can, and allowed the two different ignition systems to be positioned within the combustor.

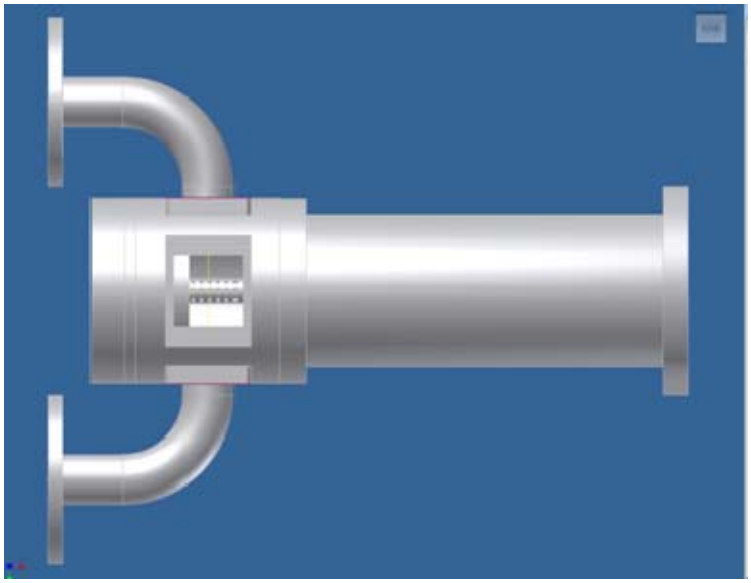

Figure 6. Combustor Viewing Section

The igniter can is a 0.63 inch diameter 3 inch long stainless steel tube with 48 perforated 0.13 inch holes distributed near the forward end. The can surrounds the electrode and protects the igniter from receiving excessive flow velocities of the incoming gasses while still allowing the air/fuel mixture to fill the volume with the electrode. Figure 7 is a picture of the combustor can as it is attached to the head

assembly. A 12 inch section of 4 inch ID pipe was attached to the downstream end of the combustor to provide a means of directing the combustion products toward an exhaust section.

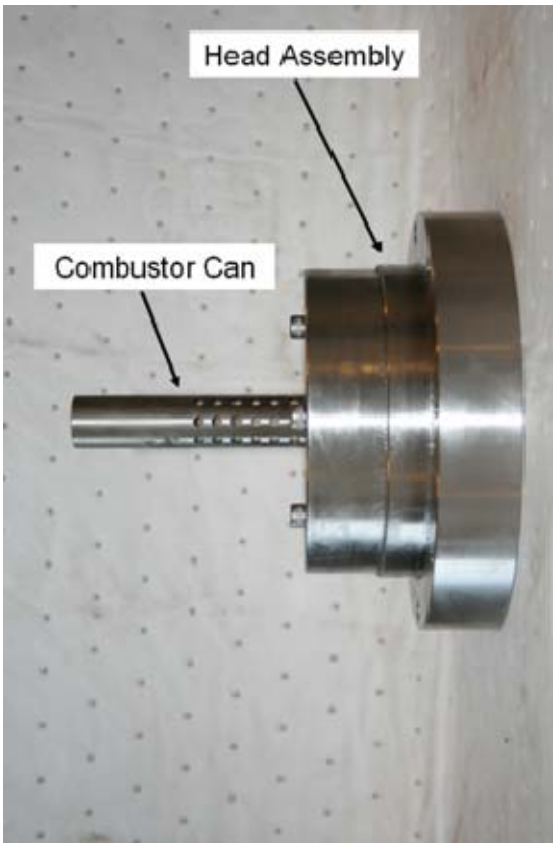

Figure 7. Combustor Can and Head Assembly

The TPI assembly in Figure 8 consists of a stainless steel housing, insulator, conductor and electrode. This system, designed in collaboration with the University of Southern California, provides the interface between the pulse generator control box and the electrode. The conductor connects the electrode to the pulse generator via a shielded low impedance cable. The insulator consists of 2 concentric tubes one made of Teflon and the other made of nylon which provides a tortuous leakage path that provides sufficient insulation and prevents unwanted grounding to the housing while traveling to the threaded portion of the electrode.

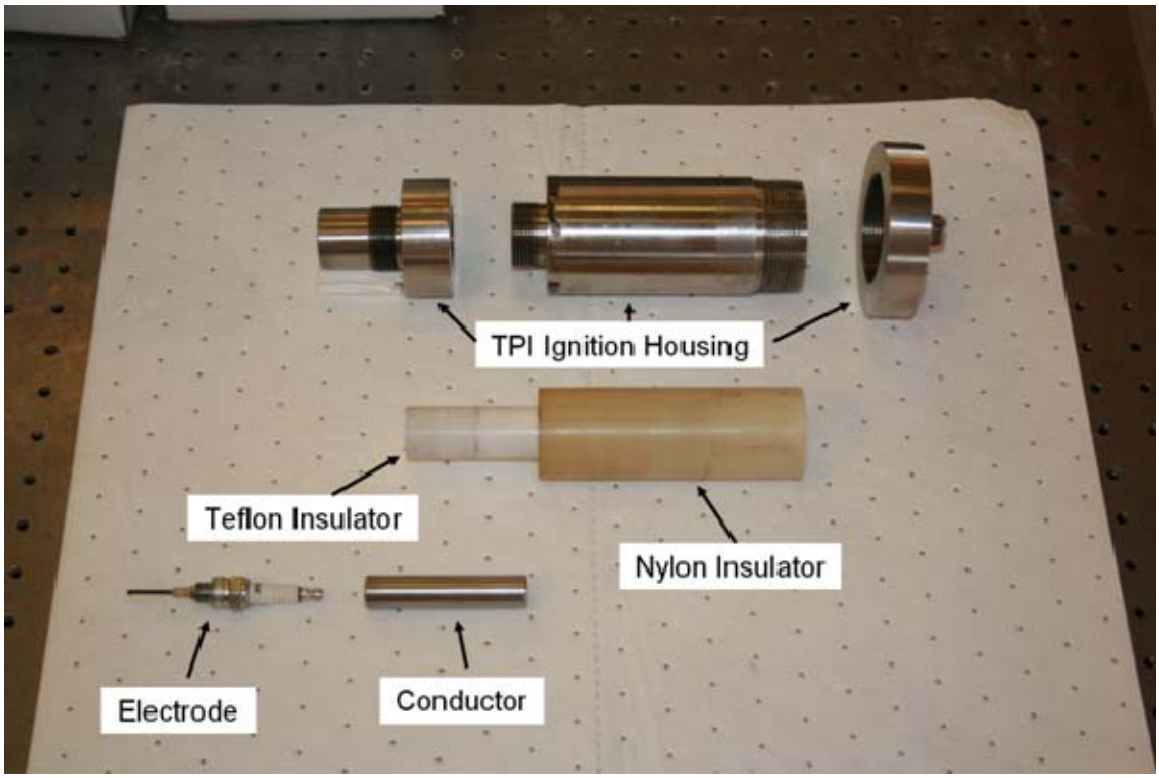

Figure 8. TPI Assembly

The High-Repetition Solid State Pulse Generator in Figure 9, built by the University of Sothern California, is used as the power source for the TPI system. The pulse generator operates using a 0–225 VDC power source (Figure 9) which is connected to the HV DC supply connector on the front of the pulse generator. The pulse generator requires two trigger signals. The fist signal commences the rapid charging sequence, and the second triggers the discharge event. The pulse generator is capable of delivering a 65kV, 12 ns pulse into a 200Ω resistive load. The amplitude is scalable down to 20kV while still retaining the 12ns pulse width. The maximum repetition rate for the pulse generator is 1 kHz.

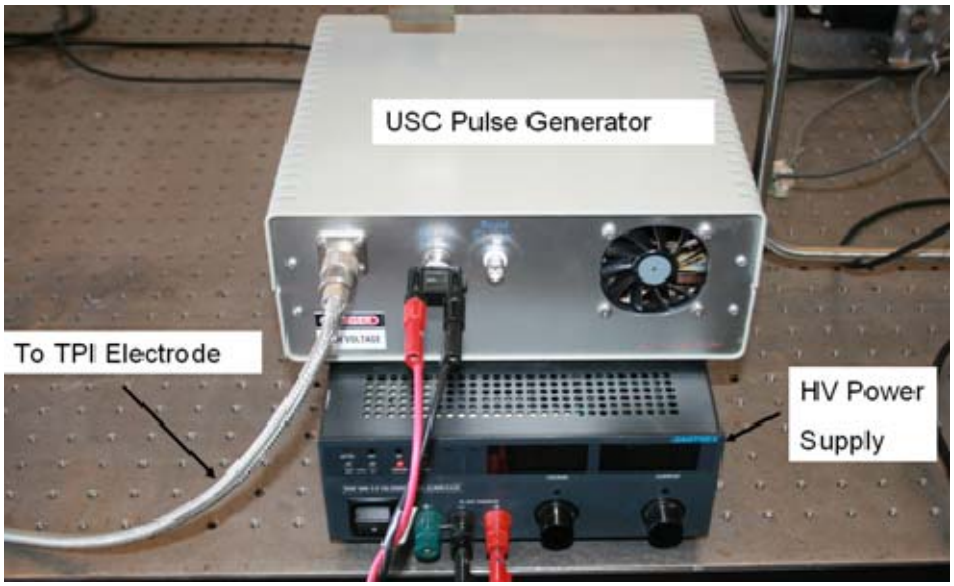

Figure 9. TPI Pulse Generator and High Voltage Boxes

The electrode is a standard motorcycle spark plug that has been modified to accommodate a single threaded electrode (Figure 10). The electric (E) field on the electrode is enhanced due to the discontinuities of the threading creating dense electric fields at the tip of the thread. This non-equilibrated state causes ionized electrons to be excited to energy levels in the 10–15 eV range.

The capacitive discharge igniter is a standard gas turbine plug (Figure 10). This igniter utilizes a thermal plasma arc which heats the combustible mixture to initiate the combustion event. A Unison Vision-8 Variable Ignition System (VIS-8) (Figure 11) was used to run the capacitive discharge spark plug, and is triggered via the BNC.

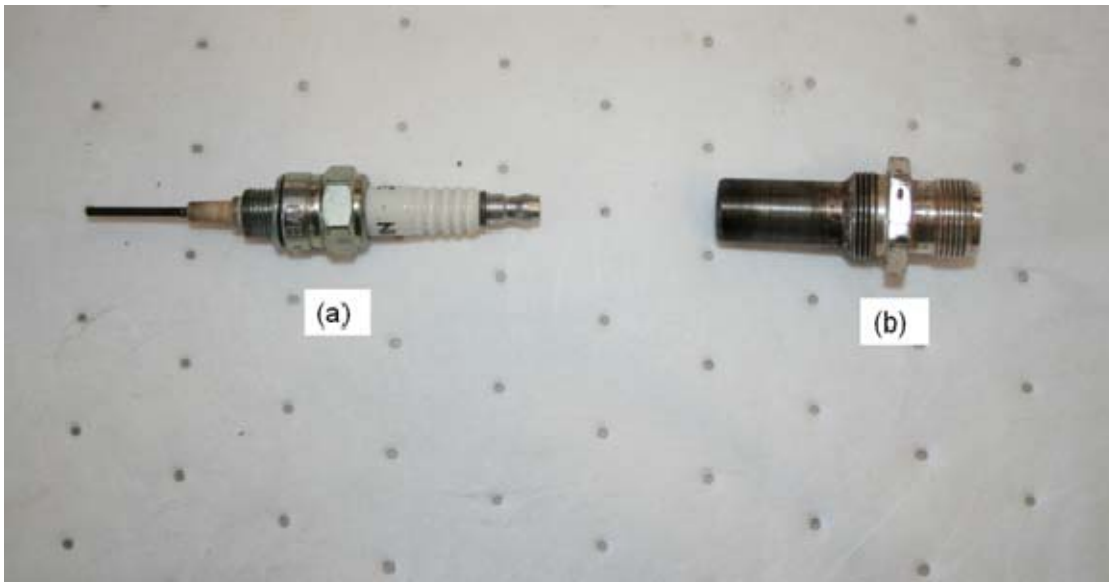

Figure 10. (a) TPI Electrode, (b) Capacitive Discharge Spark Plug

Figure 11. Unison Ignition System

2. Air and Fuel Delivery System

High pressure air was provided by a high pressure air system via 0.5 inch high pressure tubing and regulators, and ethylene (C_2H_4) was provide to the system via a dedicated bottle and regulator system. The Tescom ER3000 Version 2 software was located on the main lab computer and was used to control the delivery pressures of both air and C_2H_4. The high pressure air was sent to a 0.15625 inch diameter choke to achieve the desired mass flow for testing using Equations 6 and 7. The C_2H_4 was routed through an electro-pneumatic ball valve and then through a 0.0938 inch choke. Once the fuel exited the choke it was directed to the delivery manifold.

Choked Mass Flow Rate:
$$\dot{m} = \left(\frac{A_2 P_t}{\sqrt{T_t}} \right) \Gamma_2 K_\Gamma \tag{6}$$

Where:
$$K_\Gamma = \sqrt{\left[\left(\frac{g_c}{R} \right) \left(\frac{2\gamma}{\gamma - 1} \right) \left(\frac{2}{\gamma + 1} \right)^{\frac{2}{\gamma - 1}} \left(\frac{\gamma - 1}{\gamma + 1} \right) \right]} \tag{7}$$

and $\Gamma_2 = 1$ (choked flow)

A range of air flow rates between Mach 0.025 and 0.05 were selected for testing due to the exposure time of the Shimadzu Hyper-vision 2 camera. The Shimadzu camera is not intensified, therefore the exposure time needed to be long enough to capture the small amount of light that would be present during early combustion. The frame rate selected for side imaging was 8k frames per second which corresponded to a 125 μsec exposure time. An exposure time of 125 μsec showed that although the combustor would shield some of the light given off by the ignition event it was long enough to capture the initial combustion event. The 8k frame rate associated with a 125 μsec exposure time was fast enough to capture the flame growth allowing for evaluation of how it spread within the combustor.

Total mass flow rate for each of the six Mach numbers was calculated and the desired equivalence ratio (φ) was used to calculate the air and fuel mass flow rates. Equivalence ratio is the ratio of a fuel/oxidizer mixture to that of the ideal stoichiometric ratio of that mixture and is defined by Equation 8:

Equivalence Ratio:
$$\varphi = \frac{\dot{m}_f / \dot{m}_o}{\left[\dot{m}_f / \dot{m}_o\right]_{stoichiometric}} \tag{8}$$

The stoichiometric ratio is the exact ratio of fuel and oxidizer so as to turn all of the reactants into combustion products. The stoichiometric chemical equation for ethylene and air is as follows:

$$C_2H_4 + 3(O_2 + 3.76N_2) \rightarrow 2CO_2 + 3(3.76N_2) + 2H_2O \tag{9}$$

A φ less than one indicates that the mixture is lean, while a φ greater than one indicates a rich mixture. The φs used in these experiments were 1, 1.2, and 1.5. Table 2 is a matrix of the six Mach numbers used and the air and fuel pressures needed to achieve each of the φs.

Air and Fuel Pressure Sheet								
Mach .05			**Mach .045**			**Mach .04**		
Phi	**Air Press**	**Fuel Press**	**Phi**	**Air Press**	**Fuel Press**	**Phi**	**Air Press**	**Fuel Press**
1	765.769	142.515	1	689.1921	128.2635	1	612.6152	114.012
1.2	756.267	170.65	1.2	680.6403	153.585	1.2	605.0136	136.52
1.5	742.096	212.607	1.5	667.8864	191.3463	1.5	593.6768	170.0856
Mach .035			**Mach .03**			**Mach .025**		
Phi	**Air Press**	**Fuel Press**	**Phi**	**Air Press**	**Fuel Press**	**Phi**	**Air Press**	**Fuel Press**
1	536.0383	99.7605	1	459.4614	85.509	1	382.8845	71.2575
1.2	529.3869	119.455	1.2	453.7602	102.39	1.2	378.1335	85.325
1.5	519.4672	148.8249	1.5	445.2576	127.5642	1.5	371.048	106.3035

Table 2. Air and Fuel Pressure Sheet for Various Mach Numbers and φs

The delivery manifold was a 2 inch diameter by 12 inch long pipe that housed a high pressure air choke as well as the fuel inlet port. The choke size of 0.15625 was selected to achieve a Mach of 0.05 in the combustor section. Once the fuel and air were mixed they were sent to the 4-way manifold which sent the mixture to the combustion section via 1.5 inch flexible tubing. This manifold could be configured for any inlet configuration from single inlet to quad inlet. The 4-way manifold is made of aluminum and contained five 1.5 inch NPT threaded holes. The manifold is supported by an aluminum structure that is securely attached to the table. Figure 12 shows the air delivery and 4-way manifolds.

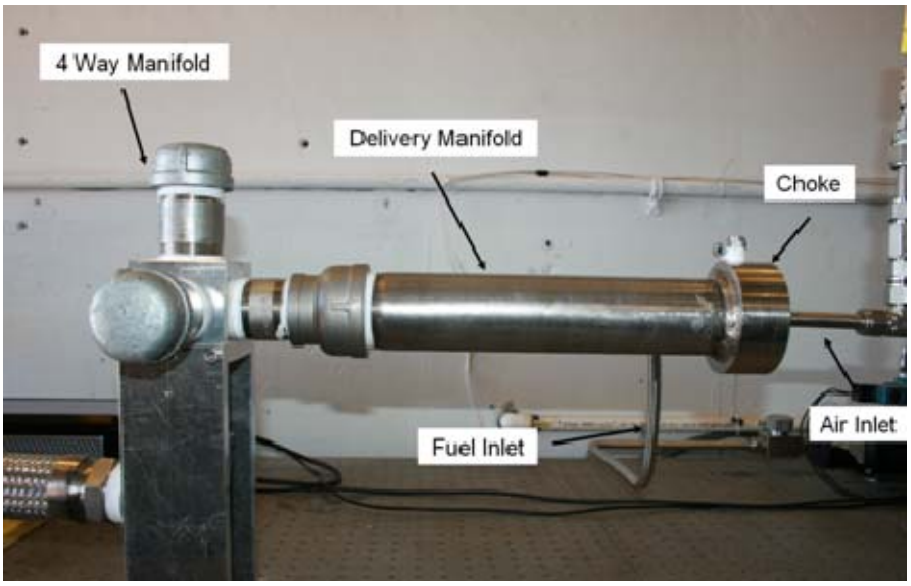

Figure 12. Fuel/Air Delivery System

The air inlet pipes were constructed to fit into the rectangular cutouts in the combustor section and connect to the flexible tubing. Due to the size constraints of the openings and the angle at which the inlets entered the combustor section, the inlet pipe size was limited. As seen in Figures 13 and 14 the 45-degree inlet had the smallest diameter at 1 inch. The 90-degree inlet did not have the constraints of the other two and therefore was able to have a diameter of 1.5 inches. Custom flanges were manufactured to ensure a smooth transition from the 1.5-inch flexible tubing down to the 1.38 and 1 inch inlet pipes of the 60 and 45-degree inlet arms.

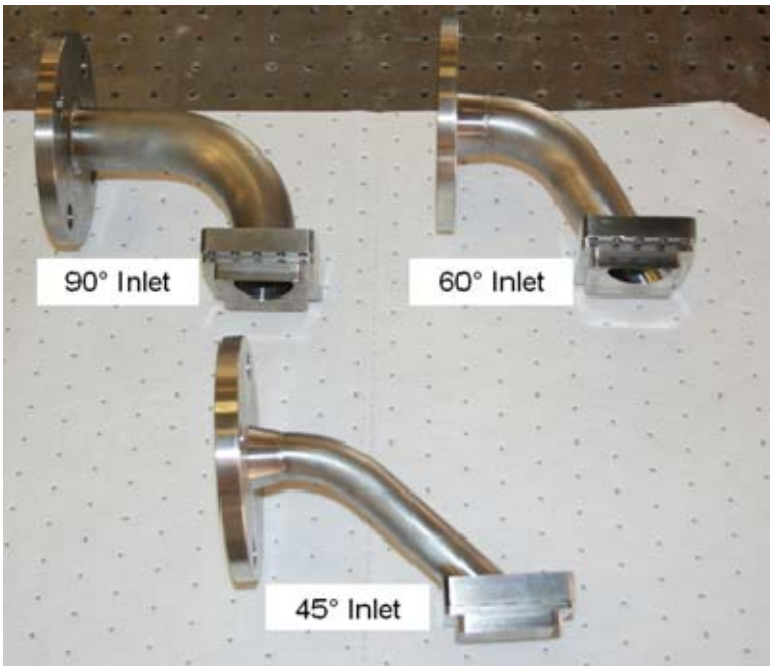

Figure 13. 90, 60, 45 Degree Inlet Assemblies

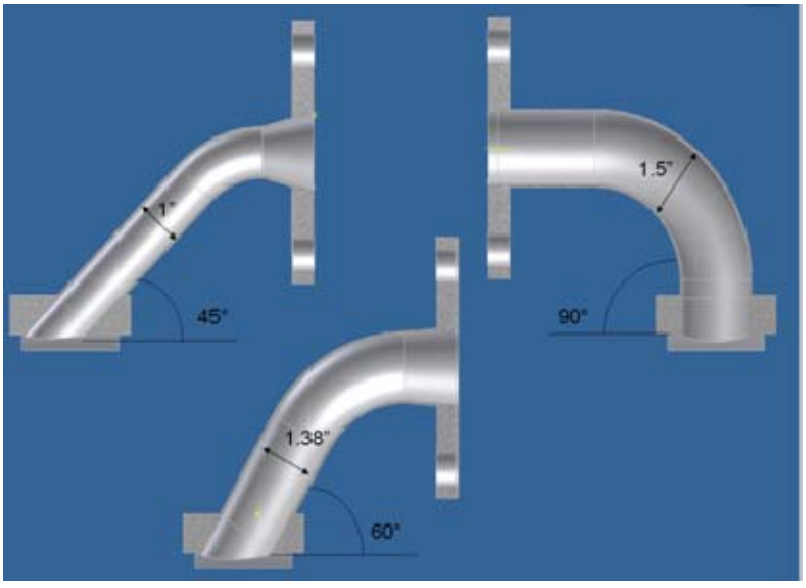

Figure 14. Cut Away of Inlet Arms

Ethylene was provided to the apparatus through 0.5 inch tubing from a dedicated bottle via a pneumatic regulator located in the flammable gas storage room. The desired ethylene pressure was set using the ER3000 software in the control room, and a pneumatic ball valve was operated via a LabView Graphical User Interface (GUI) during

the run sequence. When the valve was opened the ethylene flowed through the 0.0938 inch choke and check valve and then into the delivery manifold. Figure 15 shows the fuel delivery system.

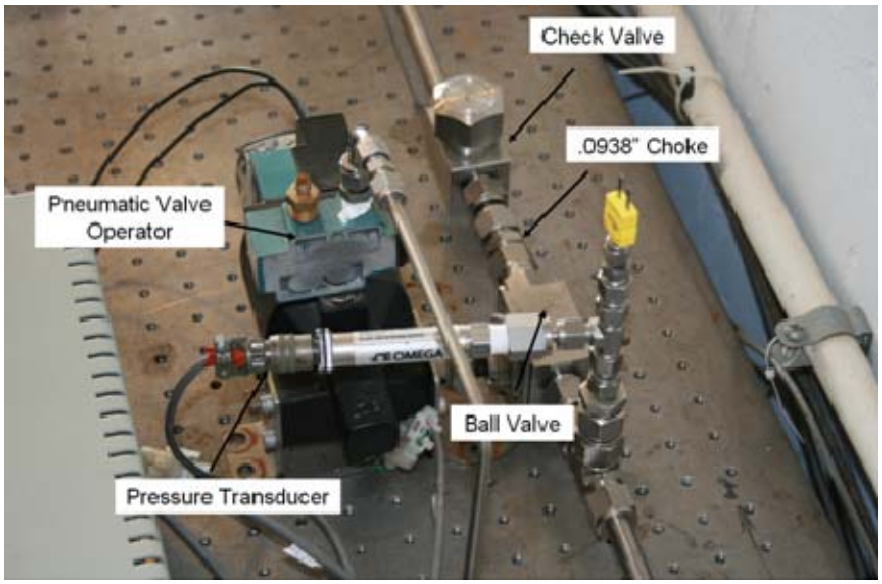

Figure 15. Fuel Delivery and Metering System

3. Exhaust Section

The exhaust section takes the burned reactants and routes them outside of the test cell as well as allow for axial imaging of the combustor head end section. A square design was used because it allowed the viewing window to be placed on a flat surface vice a round section of pipe. A 0.25 inch by 6 inch aluminum plate was used to manufacture the exhaust assembly which allowed for the 5 inch diameter optical window to be placed directly on the exhaust wall. Aluminum was used to reduce the weight and need for a separate support assembly. In order to view the head end of the combustor the exhaust section was turned 45 degrees and the optical viewing window was placed on the 45° section. The exhaust tube was then turned back 45 degrees to ensure that the exhaust gases were expelled outside of the test cell (refer to Figure 16).

Figure 16. Exhaust Section

B. CONTROL AND DATA ACQUISITION

Control of the test rig and high-speed data acquisition was accomplished through the use of LabVIEW 8.5 located on a computer in the control room and National Instruments 14-bit PXI-6115 cards located in the test cell. The LabVIEW control program was designed to open the fuel valve for the amount of time determined by the operator and then shut. Once the fuel valve began to shut, a trigger signal was sent to the test cell and the high speed data acquisitions system was commanded to start taking data. The trigger signal was also used as the external trigger of a Berkeley Nucleonics Corporation (BNC) model 555 Pulse Generator. The BNC was used to trigger the rapid charging of the TPI pulse generator and to send the firing command to the TPI system. The BNC also allowed a delay in the start of the ignition sequence to allow the high speed data system to commence taking data prior to the trigger signal being sent. Figure 17 shows the LabVIEW control screen that was used.

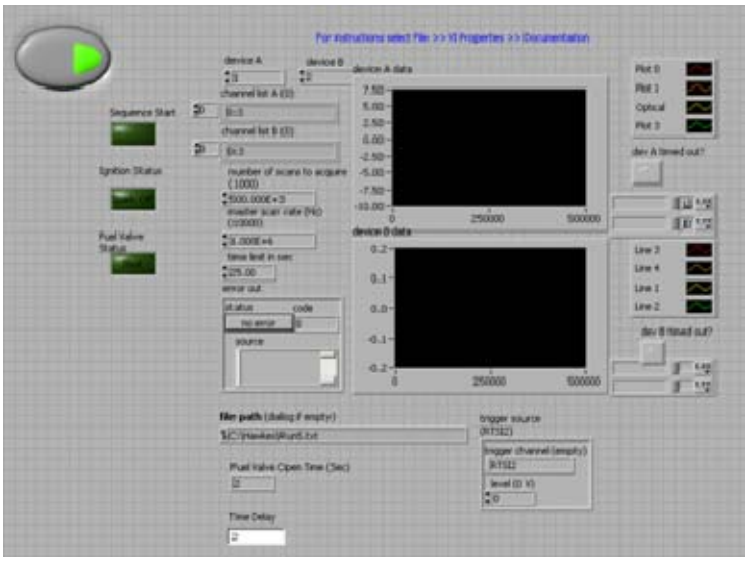

Figure 17. LabVIEW Control Console GUI

The data acquisition portion of this experiment consisted of two pressure transducers, which were used to monitor fuel and air inlet pressures. Each transducer had a pressure range from 0 to 1000 psig and a corresponding voltage of 1 to 5 volts DC. Each transducer was calibrated from 0 to 1000 psig and plotted in Excel. The equation of the line was calculated in Excel, and used in Tecplot to display the actual pressure in psia. These pressures were needed to calculate the actual Mach number of the mixture flowing through the test rig as well as calculate the equivalence ratio, φ, of the mixture.

An optical probe was used to detect the ignition event and the onset of combustion. Due to the limited amount of light produced from transient plasma event, the output of the light sensor was fed through a Stanford Research Center SR560 amplifier, amplified 200 times then sent to the data acquisition system. Along with the light sensor a trigger signal from the BNC was sent to the data acquisition system. This signal recorded the beginning of the trigger event for both the TPI and CDI systems and allowed the time from the trigger signal until the ignition spark was initiated and evaluated.

C. IMAGING

To better understand what was happening inside the combustion chamber, radial and axial images were taken. The Shimadzu Hyper-vision 2 high speed camera was used to take the images (Figure 18). This camera is capable of taking one million frames per second, and can store up to 102 frames. The camera was positioned parallel to the combustor and a mirror was placed at 45 degrees to the viewing window to obtain the side view of. A Nikon L37c 52mm lens and PK-13 27.5mm extender was used to get the proper framing and focal plane for side viewing.

For axial viewing, a Nikon L1A 52mm lens was used and focused via two mirrors midway down the center of the combustor can. The first mirror was positioned 90 degrees to the viewing window while the second mirror was place parallel with the viewing window. This allowed the camera to be parallel with the test rig due to space constraints. The camera speed was set to 16k fps allowing a 64 μsec exposure time. This reduced exposure time from that of side viewing was sufficient because the combustor can did not obstruct the view of the inner electrode therefore more light was visible to the camera. The camera was triggered using one of the BNC channels, and was delayed via software in the control room to allow the camera to capture entire ignition event.

Figure 18. Shimadzu Hyper-vision 2 Camera with Power Supply and Software

THIS PAGE INTENTIONALLY LEFT BLANK

IV. EXPERIMENTAL RESULTS

A. CAPACITIVE DISCHARGE IGNITION RESULTS

1. Ignition Delay and Flame Growth Development

Gas turbine capacitive discharge spark plugs are widely used in the industry and well characterized, therefore they were a good choice to use for a baseline configuration. Each of the six inlet configurations (45° dual inlet, 45° single inlet, 60° dual inlet, etc.) were tested at an average combustor flow Mach number of 0.05 as seen at the exit of the exhaust chamber. Light probe data was taken acquired by a National Instruments PXI-6115 14-bit board via a LabVIEW GUI and then plotted using Tecplot 10. Ignition delay and flame growth times were extracted from the plot and verified via the high speed images. Figure 19 shows the ignition command, ignition discharge and subsequent flame development data for the ignition event.

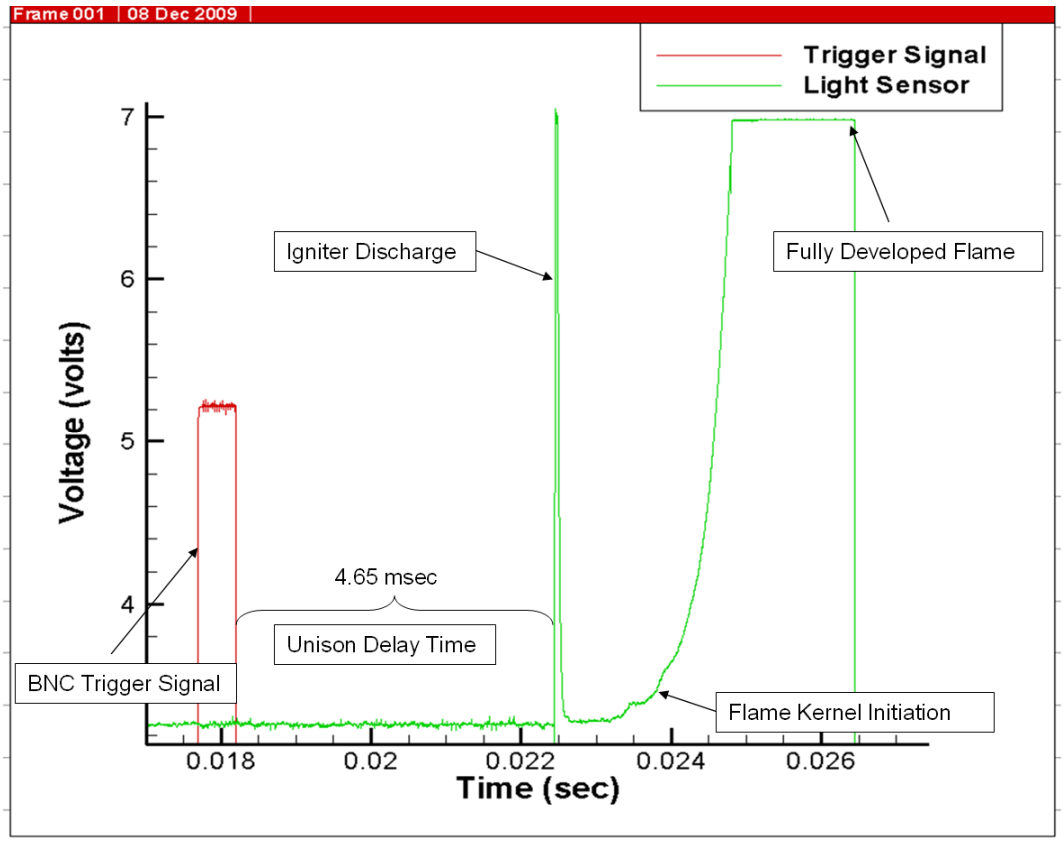

Figure 19. Typical Plot of CDI Ignition Event

Along with the light probe data, air and fuel supply pressures to the mass metering chokes were collected and used to calculate Mach number and stoichiometry of the test run. The voltage output from the pressure transducers was collected by LabVIEW and converted into pressures in Tecplot using their respective calibration equations (Appendix B). The stiochiometry of the mixture, φ, was then calculated using the determined mass flow rates and the equivalence ratio definition. Figure 20 shows the stability of the supply pressures during a typical test and resulting φ. Ignition delay time and flame growth time were plotted against this calculated value of φ to see how the mixture ratio affected ignition and flame growth times (Figures 21 and 22).

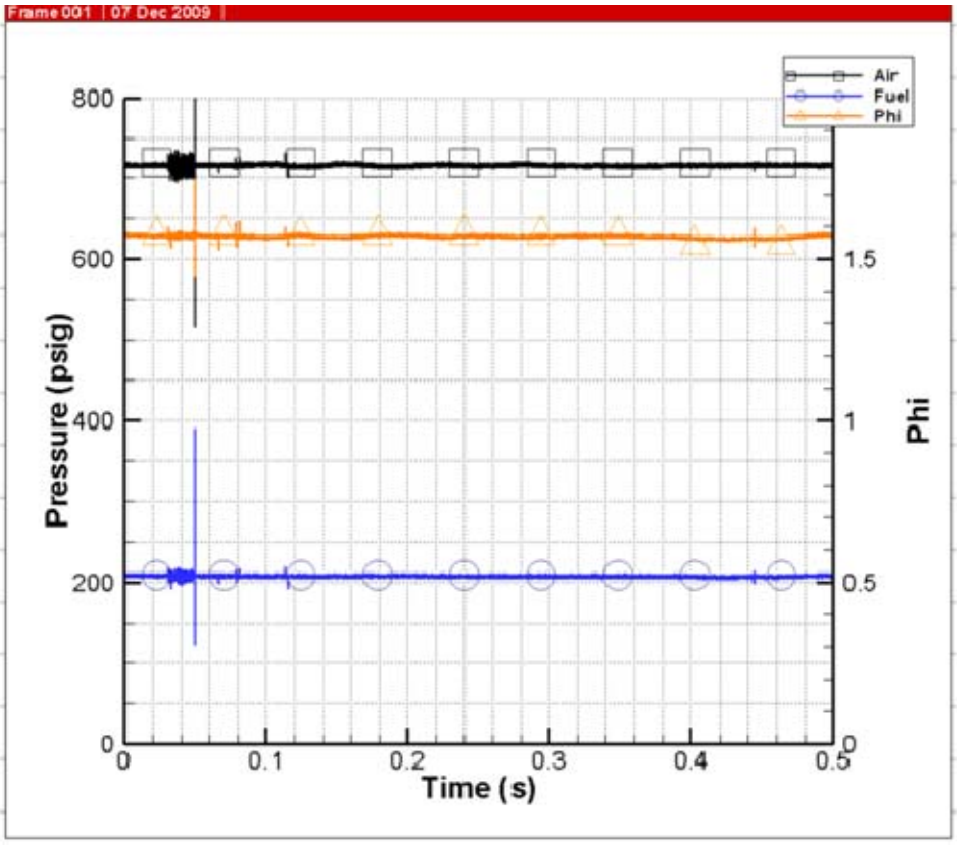

Figure 20. Typical Plot of Air Pressure, Fuel Pressure and Phi

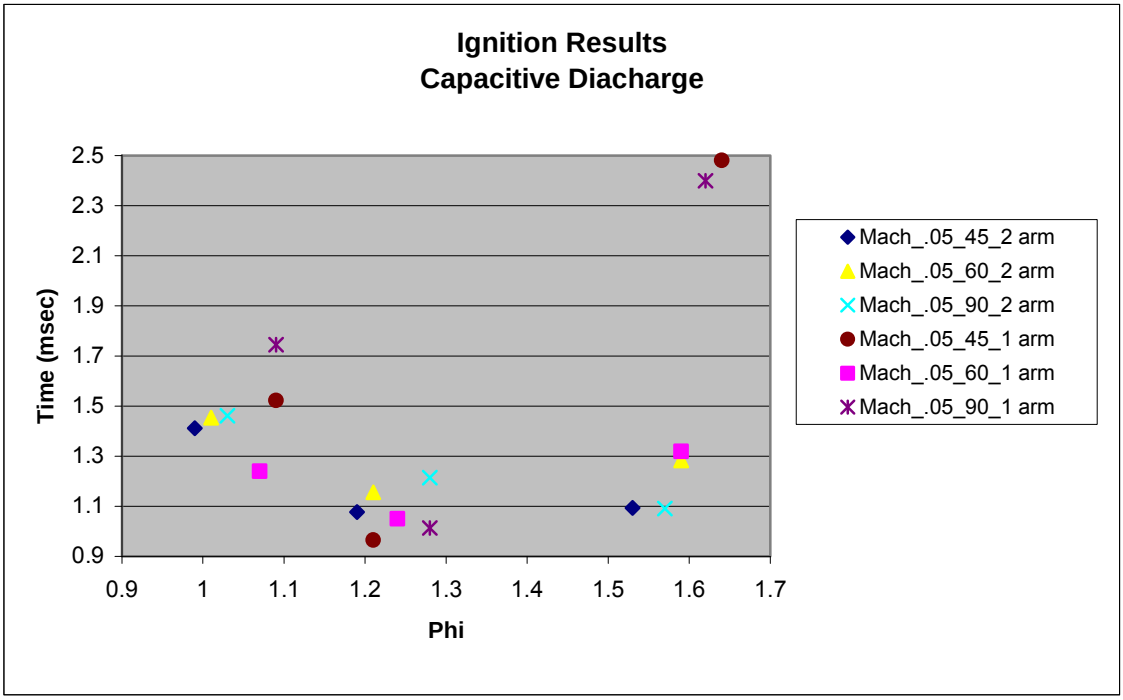

Figure 21. CD Ignition Delay Times vs. Phi for Varying Inlet Conditions

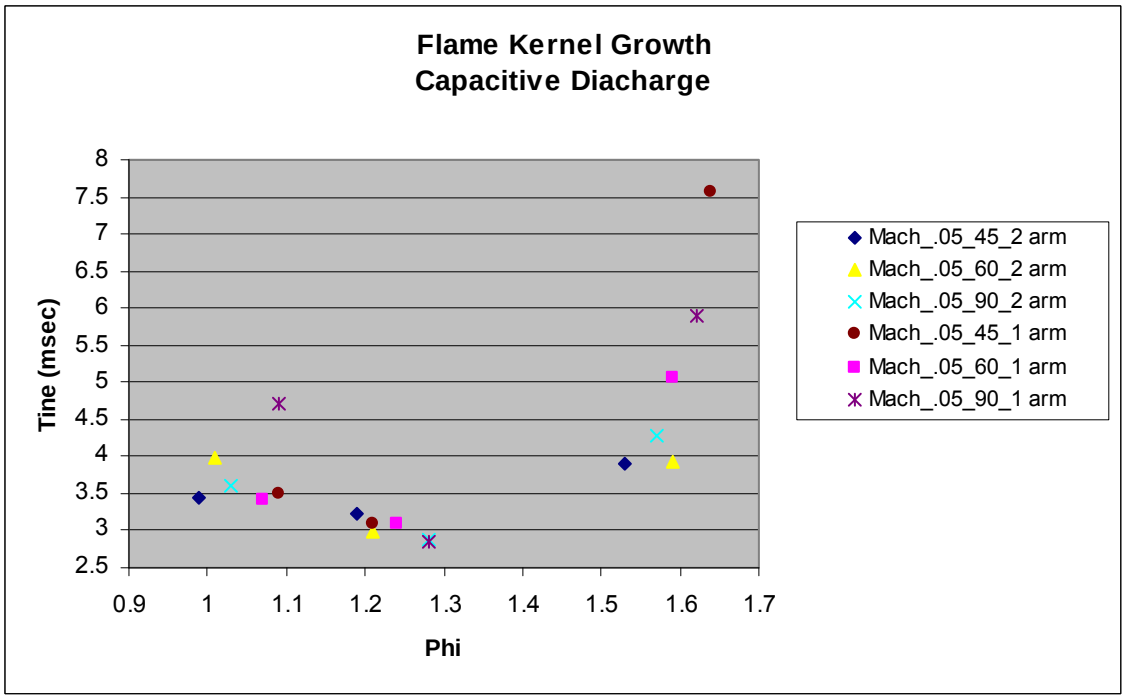

Figure 22. CD Flame Kernel Growth Times vs. Phi for Varying Inlet Conditions

For the purpose of this thesis, the ignition delay time is defined as the time from igniter discharge until the optical sensor voltage increases by 0.25 volts. This voltage increase was enough to ensure that the increase was due to light emission form combustion and not background noise. Flame growth time is defined as the time from igniter discharge until the light sensor reverses polarity. The high-speed images of the event were examined to ensure that the flame fully filled the combustion chamber at the time corresponding to the polarity reversal.

It is clear from the plots of ignition delay and flame growth times that an equivalence ratio near 1.2 (slightly rich) provides the fastest ignition and flame growth times. This is primarily due to the unique nature of ethylene. Ethylene has a positive heat of formation, which tends to cause the peak reactivity of ethylene/air mixtures to occur at slightly fuel rich conditions.

By examining the plot of ignition delay time it can be determined that the single 45° inlet configuration provided the fastest ignition time at a Phi of 1.2, but rapidly increases as the mixture stoichiometry deviates from a Phi of 1.2. The single 60° inlet provided the fastest ignition time over the range of mixtures tested. The plot of flame growth time shows that at a Phi of 1.2 all inlet configurations had a flame growth time between 2.75 and 3.5 msecs, but the early ignition cases did not necessarily have the fastest growth times. It can also be noted that for a stoichiometric ratio of 1.5 and greater the ignition times and flame growth times for dual inlet configurations were faster than for single inlet configurations.

2. Flame Growth Characterization

In order to better understand what takes place within the combustor, images from an axial and radial vantage point were taken. With these images the flame kernel could be viewed from inception until the flame was fully developed. Figure 23 is a series of images taken of the capacitive discharge spark discharge with no fuel present. Each frame has a 64 μsec exposure time making the total event time 576 microseconds long. Due variances in the electrical hardware of the Unison control unit, the discharge event and subsequent after glow times varied between 576 and 768 μsec. Following the CD

spark, the flame kernel begins to form and Figures 24 and 25 show this development. Figure 24 shows time lapse images of a 60°dual inlet configuration with a Phi of 1.5, while Figure 25 is a single 90° inlet configuration with a Phi of 1.5.

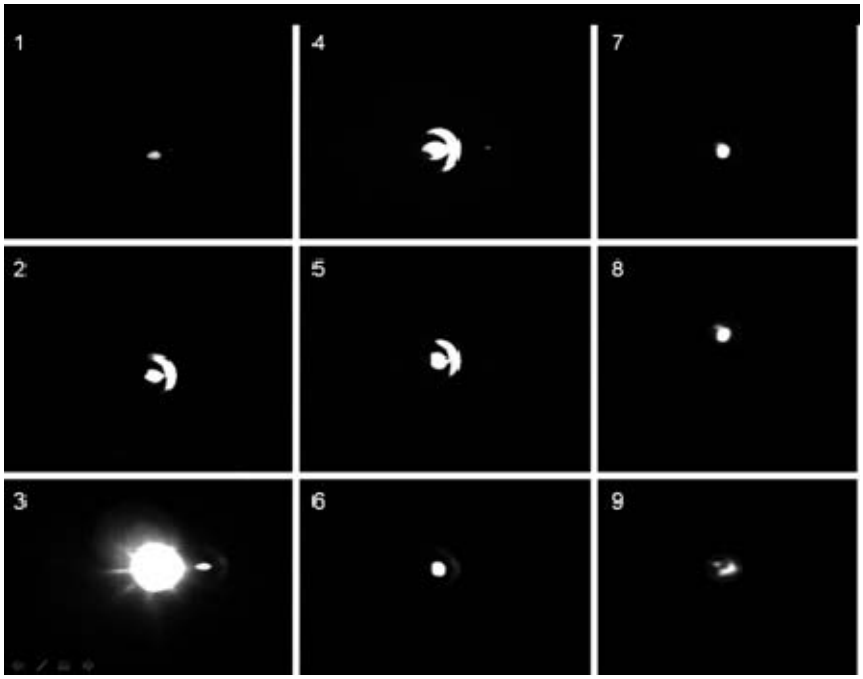

Figure 23. Axial Images of CD Igniter Spark Discharge (Air Only)

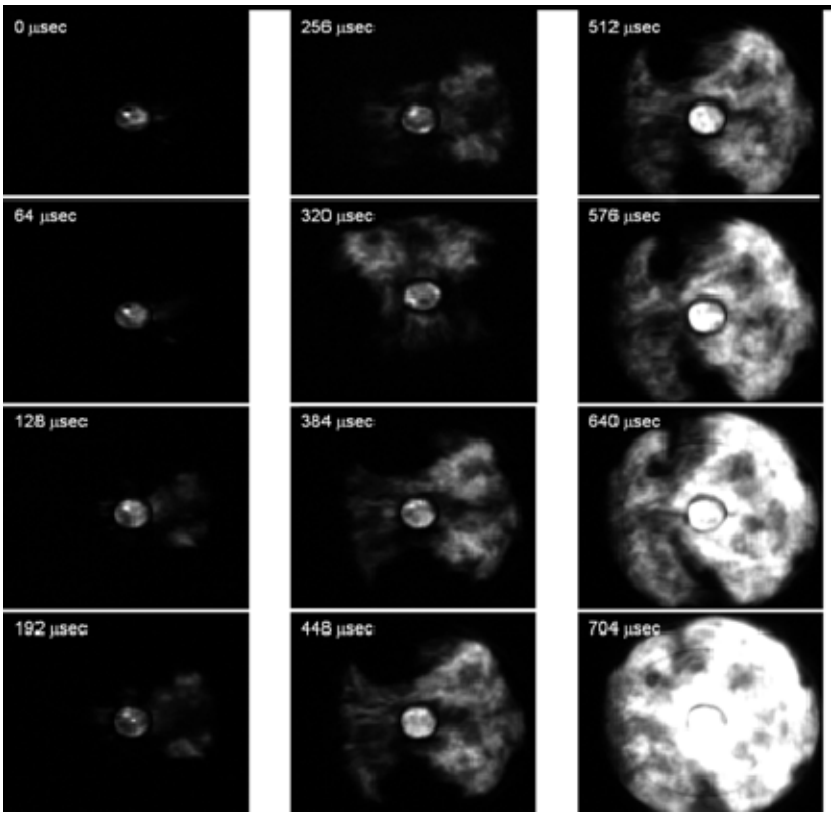

Figure 24. 60° Dual Inlet Flame Growth (C_2H_4, Phi=1.5, T=280k, P=101325Pa)

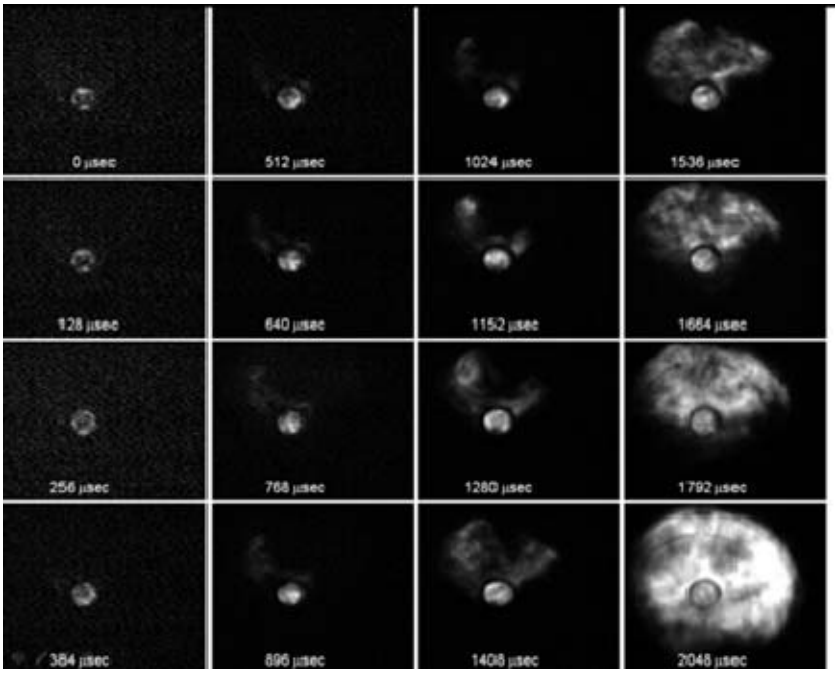

Figure 25. 90° Single Inlet Flame Growth (C_2H_4, Phi=1.5, T=280k, P=101325Pa)

Reviewing all of the images taken form each of the six inlet configurations yielded a few unique flame spreading patterns. The first of these patterns was that for the dual inlet configurations the flame was forced out the side holes in the can and spread out ward toward the tube outer wall and then rolled up into four vortices as depicted in Figure 26. The single inlet configurations tended to trap the flame within the can causing a rotating motion of the flame. The flame then exits the can on the opposite side of the inlet and develops into two vortices which then move toward the opposite side of the tube until the entire volume is filled (Figure 26).

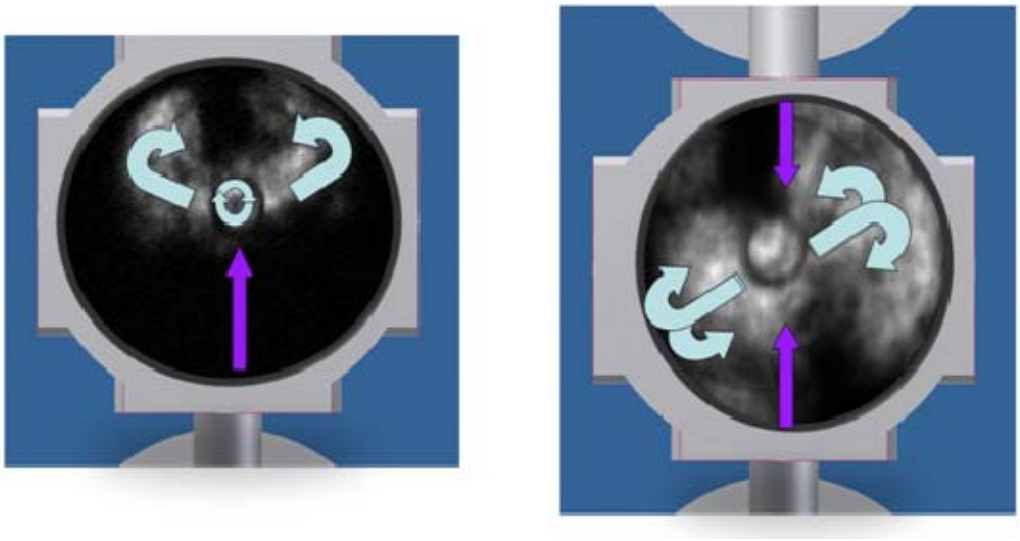

Figure 26. Single and Dual Inlet Flame Spreading Pattern

The side view images were not as reveling as the end view due to the limited area that could be viewed and the slower exposure time used, but did yield some interesting results. One characteristic that was noticed was that the thermal plasma ball from the CD spark was drawn away from the igniter and traveled down the combustor can igniting the reactants as it went. When this happened the flame front began at the head end of the combustor and rapidly filled the tube volume as it move toward the exhaust end. This flame front pattern is beneficial because it utilizes the entire tube length to reach a fully developed flame condition thus meeting the requirements for detonation earlier in the tube. Figure 27 illustrates this flame front spreading path with two 90° inlets. The 60°

and 45° inlets showed an even more pronounced movement of the thermal plasma through the combustor can due to the angle at which the air entered the combustor volume.

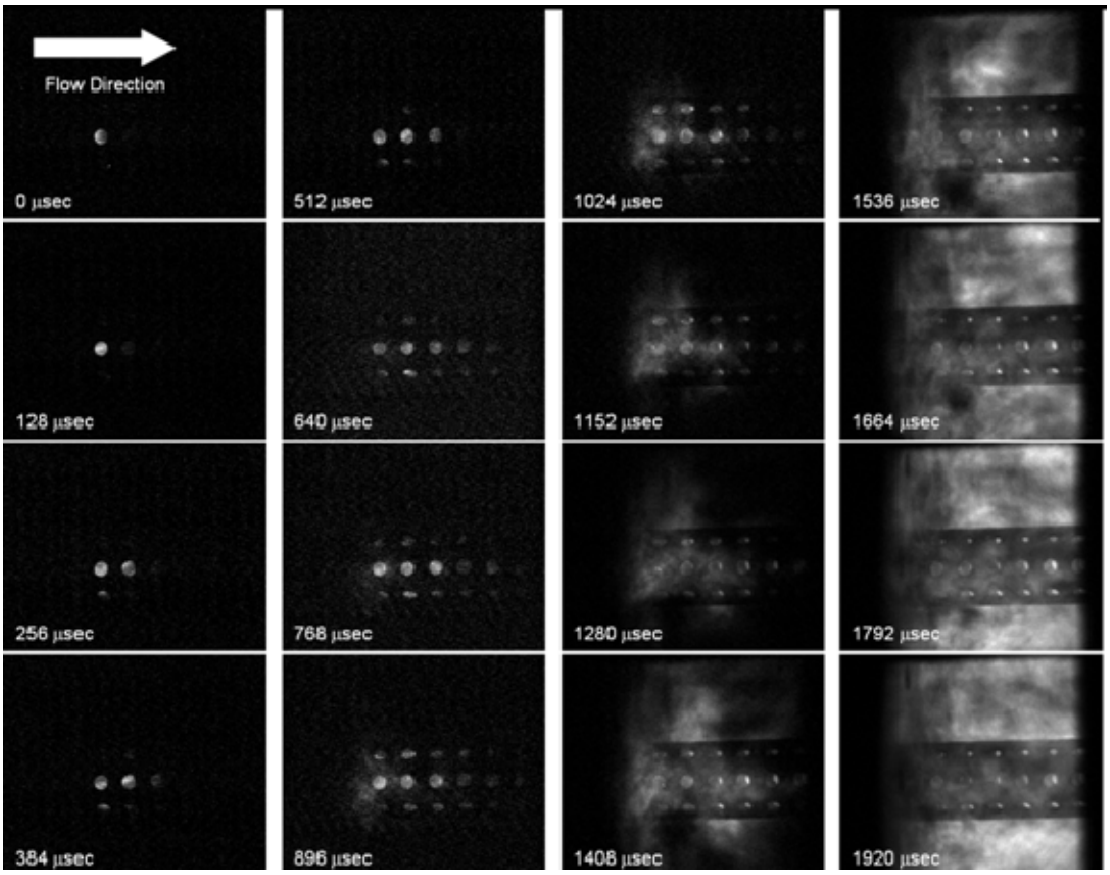

Figure 27. Side View of CD Ignition Event (C_2H_4, Phi=1.5, T=280k, P=101325Pa)

B. TRANSIENT PLASMA IGNITION RESULTS

With the capacitive discharge base line completed, the TPI system was installed and the six inlet configurations were tested again. Once again fuel pressure, air pressure and light probe data was taken. Figure 28 shows the typical light probe plot. Of note with this plot is the shortened time from trigger signal until electrode discharge. The USC pulse generator cut this time down from 4.65 msec to 210 µsec. This significant savings in time allows the PDE to be operated at frequencies closer to the 60100 Hz range.

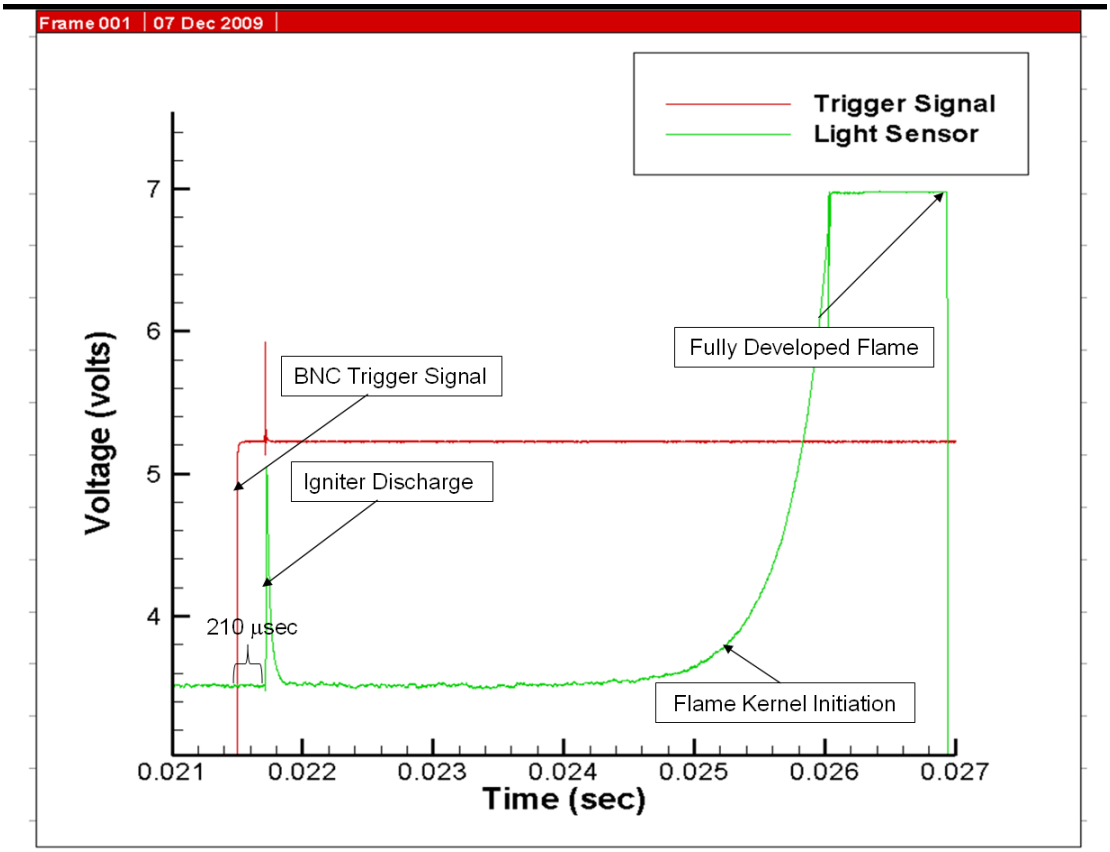

Figure 28. Typical Plot of CDI Ignition Event

The light probe and fuel/air data for the TPI system were plotted in the same manner as for the CD system. Figures 29 and 30 show the results for the TPI tests. The results were extremely erratic with several of the inlet configurations not being able to be ignited for all flow rates. Of note is the single 45° inlet, which would not ignite for any of the flow rates and therefore was left off the plot. Both the single and dual 60° inlet as well as the single 90° inlet would ignite but only at reduced flow rates.

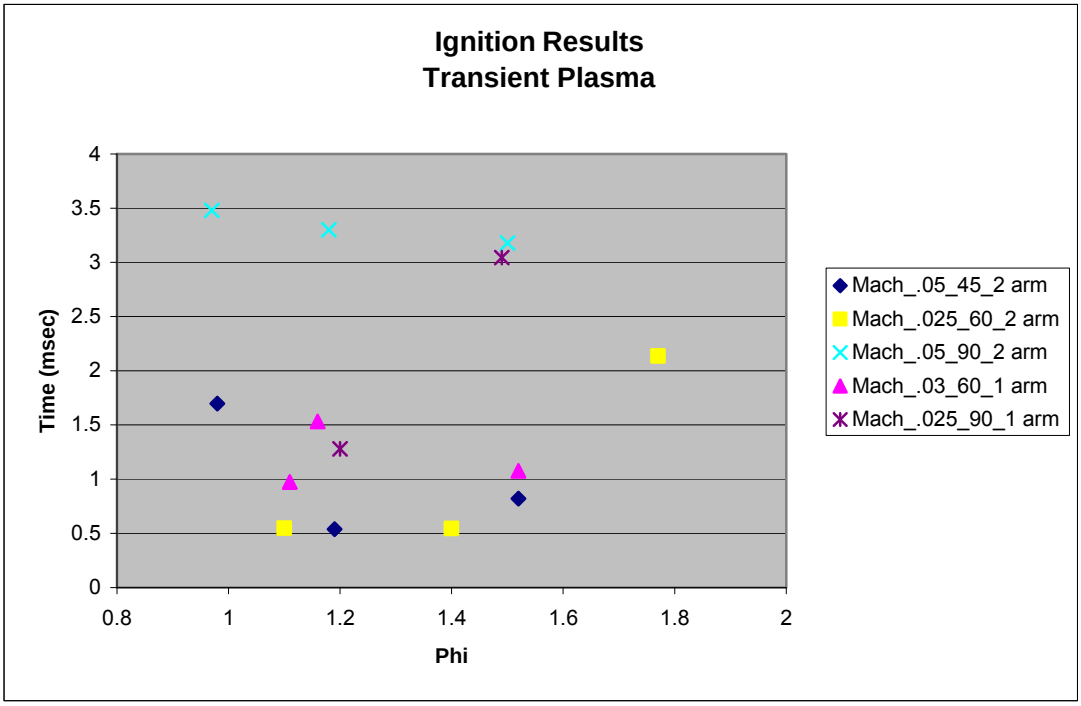

Figure 29. TPI Delay Times vs. Phi for Varying Inlet Conditions

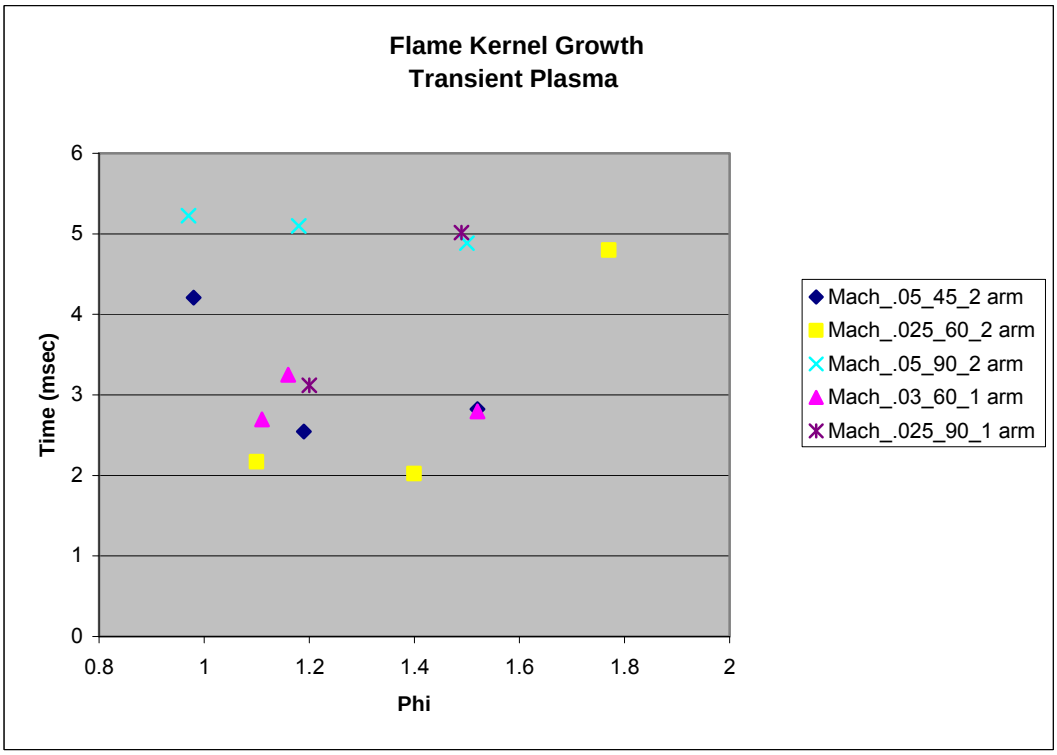

Figure 30. CD Flame Kernel Growth Times vs. Phi for Varying Inlet Conditions

A combination of two factors contributed to the TPI system not behaving as predicted. The first was the differing diameter of the inlet tubes. This difference in diameter causes the incoming flow rate to be too high to allow the mixture to ignite. Using the following Mach number to area ratio equation the Mach number the incoming fuel/air mixture (M_x) can be calculated:

$$\frac{A_y}{A_x} = \frac{M_x}{M_y}\sqrt{\left\{\frac{1+\left[(\gamma-1)/2\right]M_y^2}{1+\left[(\gamma-1)/2\right]M_x^2}\right\}^{(\gamma+1)/(\gamma-1)}} \tag{10}$$

where A_y = Area of combustor

M_y = Mach number at exit of combustor

A_x = Area of inlet tube

γ = specific heat ratio

The 45° inlet has the smallest diameter and would therefore have the highest incoming flow rate. For a single inlet 45° inlet the following values can be substituted into equation X, M_y = .05, A_y = 12.56, A_x = 3.14 and γ = 1.4 for the single 45° inlet configuration and solved for M_x giving an inlet Mach number of 0.63. The second factor affecting the TPI's ability to ignite the mixture is its size. The electrode is 8 tenths of an inch long which places the electrode in a more exposed path to the incoming mixture (Figure 31a) where as the CD igniter is protected by the head assembly (Figure 31b). The combination of the velocity of the incoming mixture and the location of the electrode caused the flame to be quenched before it has a chance to achieve sustained combustion.

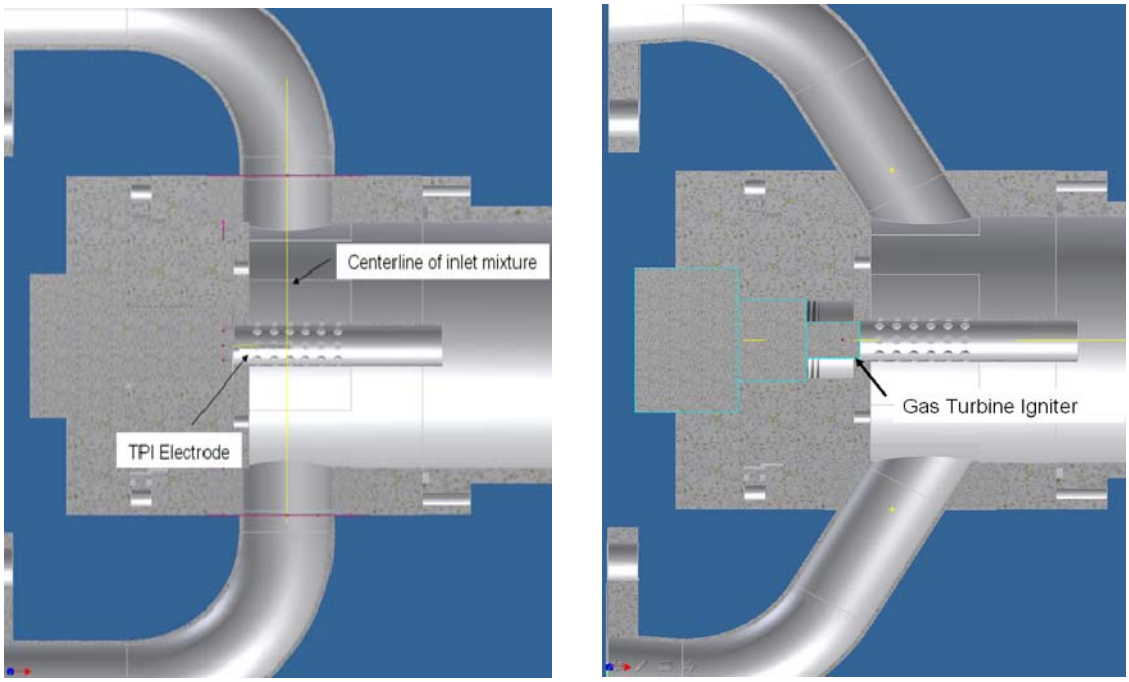

Figure 31. a) TPI and b) CDI Electrode Placement

After reviewing the side view images for the TPI cases it was seen that the flame exits the combustor can in a more uniform manner along the length of the TPI electrode than for the CDI system. This is due to the large volume in which the TPI system deposits it energy. This volume rapidly expands within the can and the exits through the holes in the can. The flame then spreads radially and axially until the entire viewing area is filled.

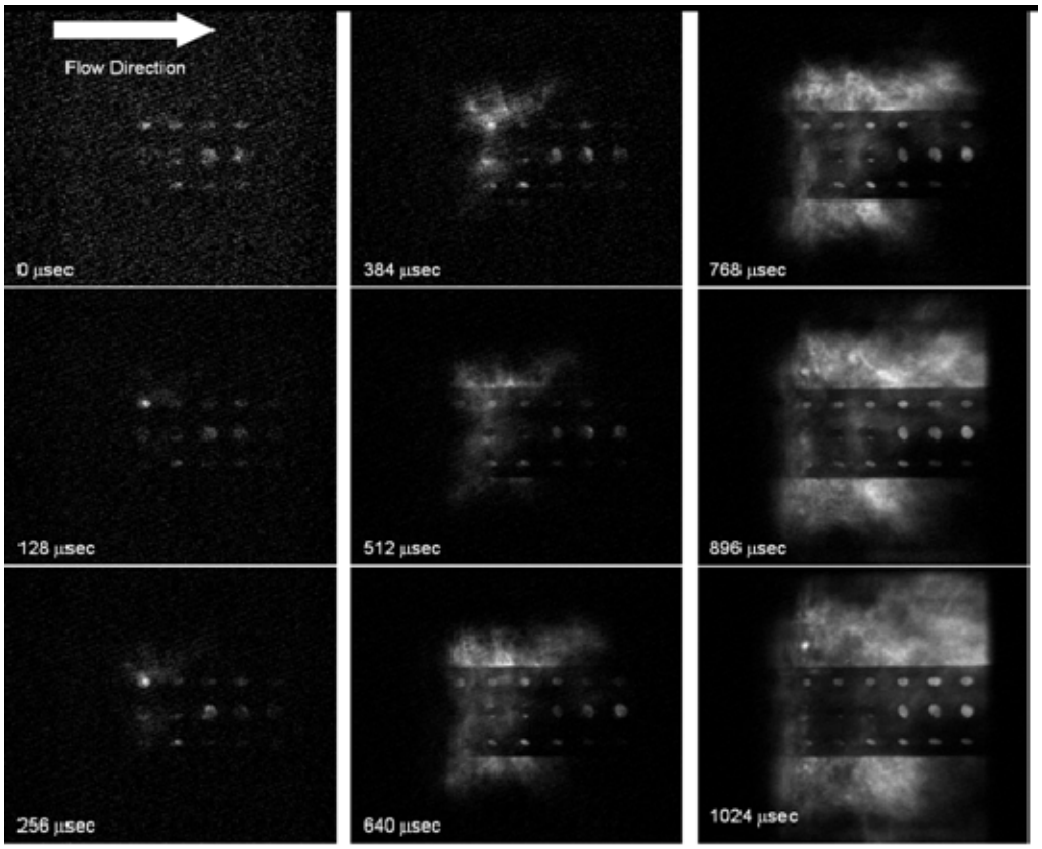

Figure 32. TPI Flame Kernel Growth Side View (C_2H_4, Phi=1.5, T=280k, P=101325Pa)

The length of the electrode caused it to have a tendency to arc instead of produce transient plasma. This arc was either due to the electrode not being centered in the combustor can which put the end of the electrode closer to the can wall, allowing a shorter path for current to flow, or due to the applied voltage being too high. When the electrode did arc, the thermal plasma was swept down the can and caused ignition further down the tube. Figure 33 shows that the flame front flashed back toward the head end of the combustor when this anomaly happened. This is not desirable because a large portion of the front of the combustor is not contributing to the DDT process.

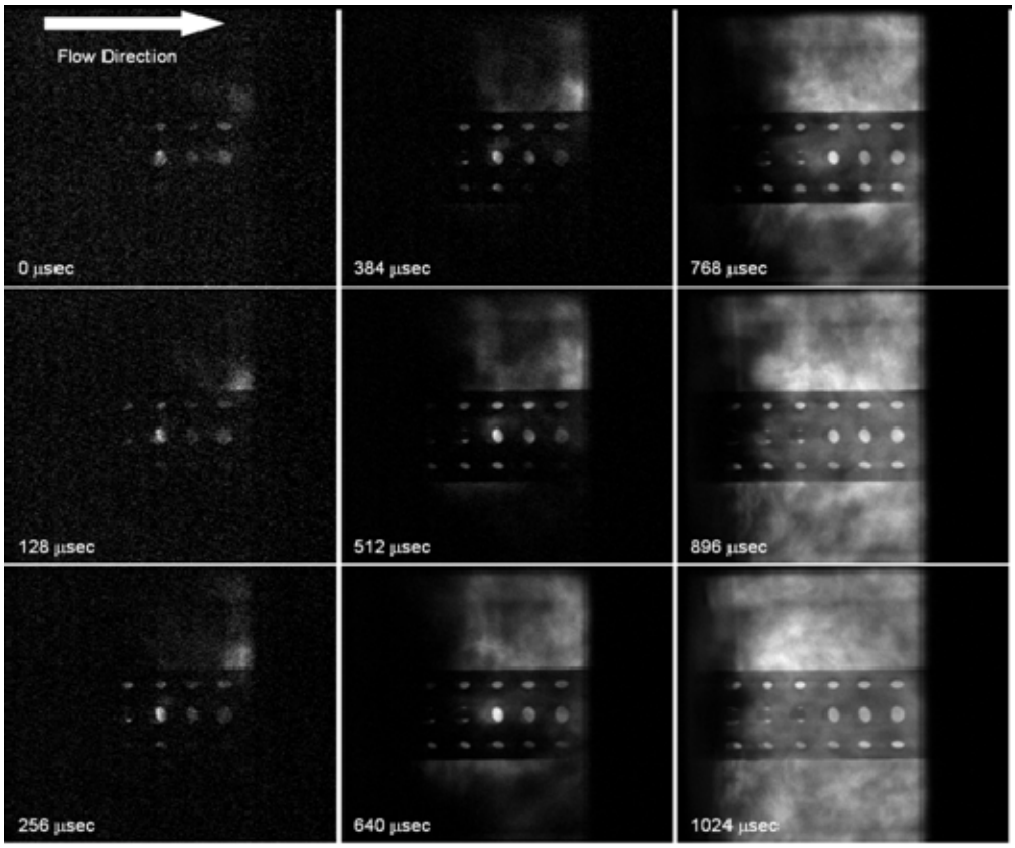

Figure 33. TPI Flame Front Flash Back (C_2H_4, Phi=1.5, T=280k, P=101325Pa)

THIS PAGE INTENTIONALLY LEFT BLANK

V. SUMMARY AND FUTURE WORK

A. SUMMARY

The results of this thesis were very useful for the design of a single inlet combustor. The CDI system gave the most consistent results while the TPI system had a hard time igniting the mixture. It is speculated that because the CDI system was installed further back into the head portion of the combustor it was "effectively" shielded from the direct path of the incoming mixture and therefore able to ignite all flow rates. The TPI electrode, although installed inside the ignition can, was not sufficiently shielded from the flow path and experienced excess flow, which caused the ignition kernel to quench before it had a chance to get going.

The single arm 45° had the best performance for ignition delay time and also preformed well for flame growth times at a Phi of 1.2 making it a good choice for a single inlet combustor. The 60° single inlet preformed the best over the full range of mixture ratios tested and would make a good inlet if the combustor would have to operate at varying mixture ratios. The 90° preformed poorly in both ignition delay and timing and therefore would not make good single inlet.

Flame imaging showed that the combustor can provide an area in which the initial combustion could begin and the spread to the rest of the combustor volume. The single inlet configurations tended to force the flame front to the opposite side of the combustor from the inlet, while the dual inlet forced the flame outward from the middle of the can. In each case vortices were formed as the flame front got caught up in the incoming fuel/air mixture.

Using a long electrode also made the TPI system more sensitive to the input voltage. If the electrode is not exactly centered in the ignition, the tip of the electrode can become too close to the can and cause the TPI to arc instead of producing the transient plasma. When this happens, the arc is forced out the end of the ignition can, igniting the

mixture further downstream. The flame front then spreads both forward down the tube and toward the head end. This situation limits the effectiveness of the combustor to achieve the DDT process.

B. FUTURE WORK

It was found that the TPI electrode was insufficiently shielded from the direct path of the incoming high Mach flow and that the CDI and TPI systems were not located at the same point in the combustor. Shorter TPI electrodes could be looked at to try and place the TPI electrode out of the main inlet stream. Also, the ignition could be redesigned to help better protect it from the direct force of the incoming mixture. This could be as simple as putting smaller or fewer holes on the side facing the inlet than on the backside of the can. The head assembly could be redesigned to place the electrode more toward the head end of the combustion chamber.

Another problem that should be addressed, is the varying inlet diameter size. In order to better compare each inlet, the incoming Mach numbers should be the same. This may involve making the inlets a shape other than round. Making the inlets an oval or kidney shape, would allow each inlet to fit into the given opening, while maintaining the areas the same. This would ensure that all of the testing was done with comparable inlet mach numbers.

APPENDIX A. DRAWINGS

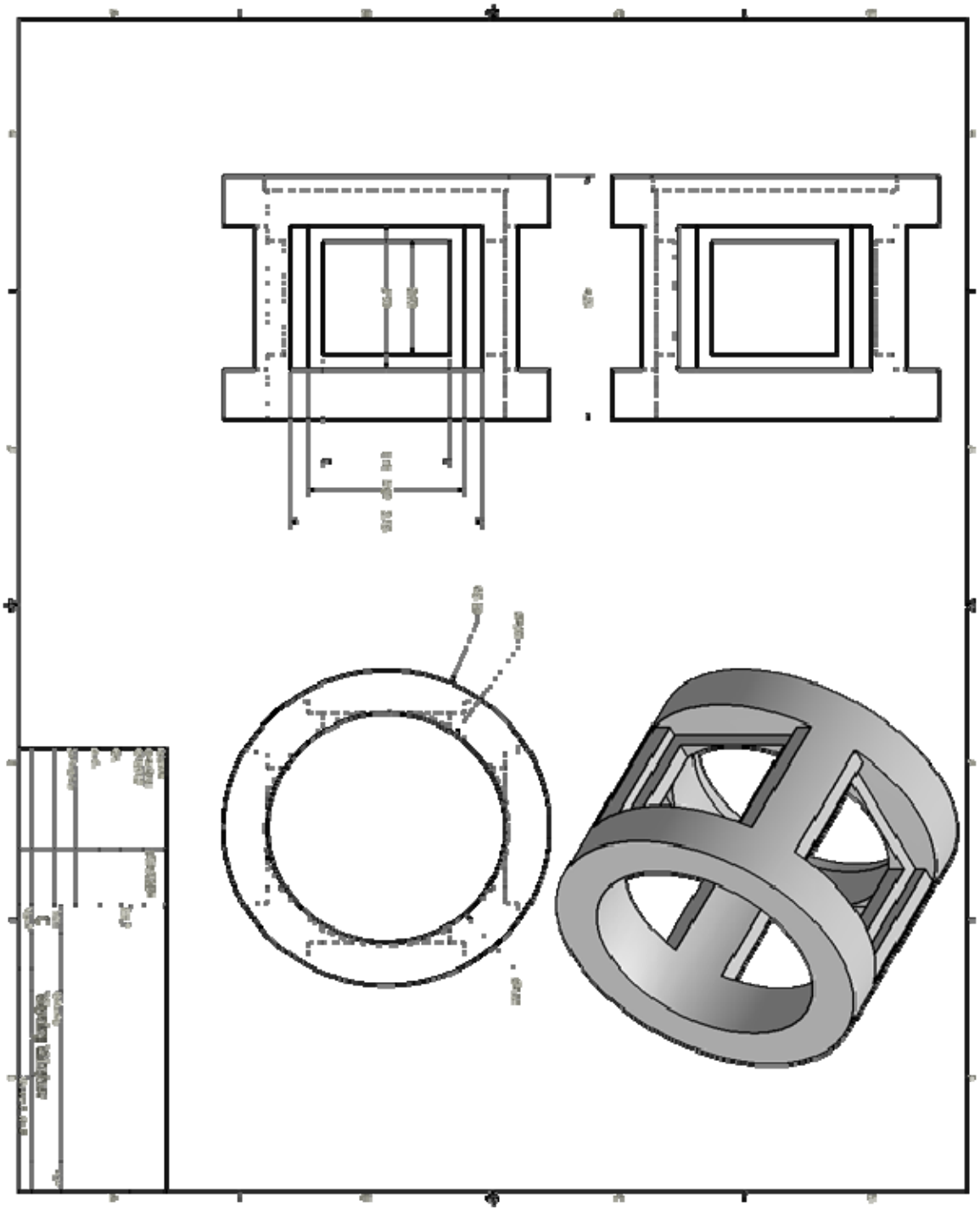

Combustor Viewing Section

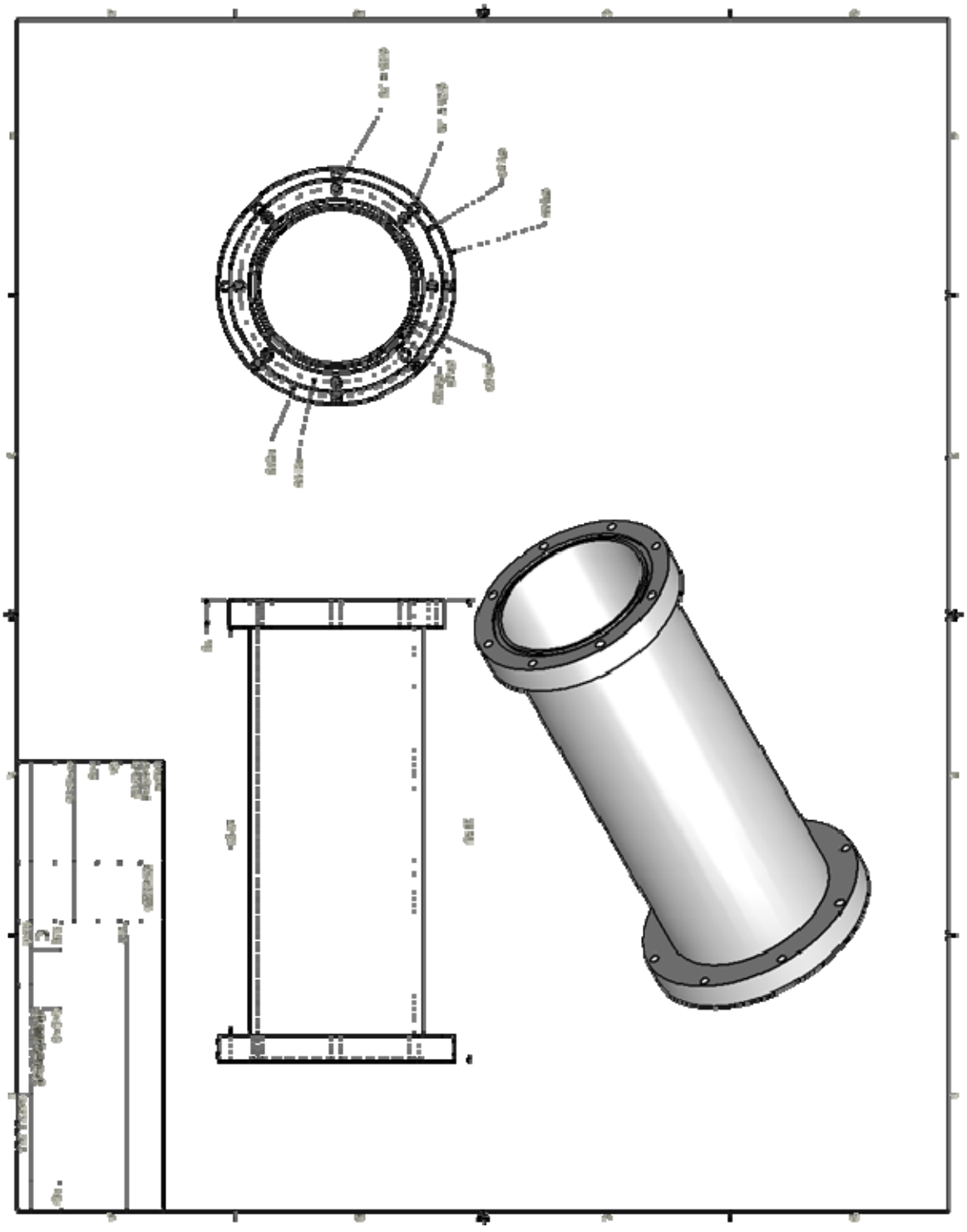

Combustor Exhaust Tube

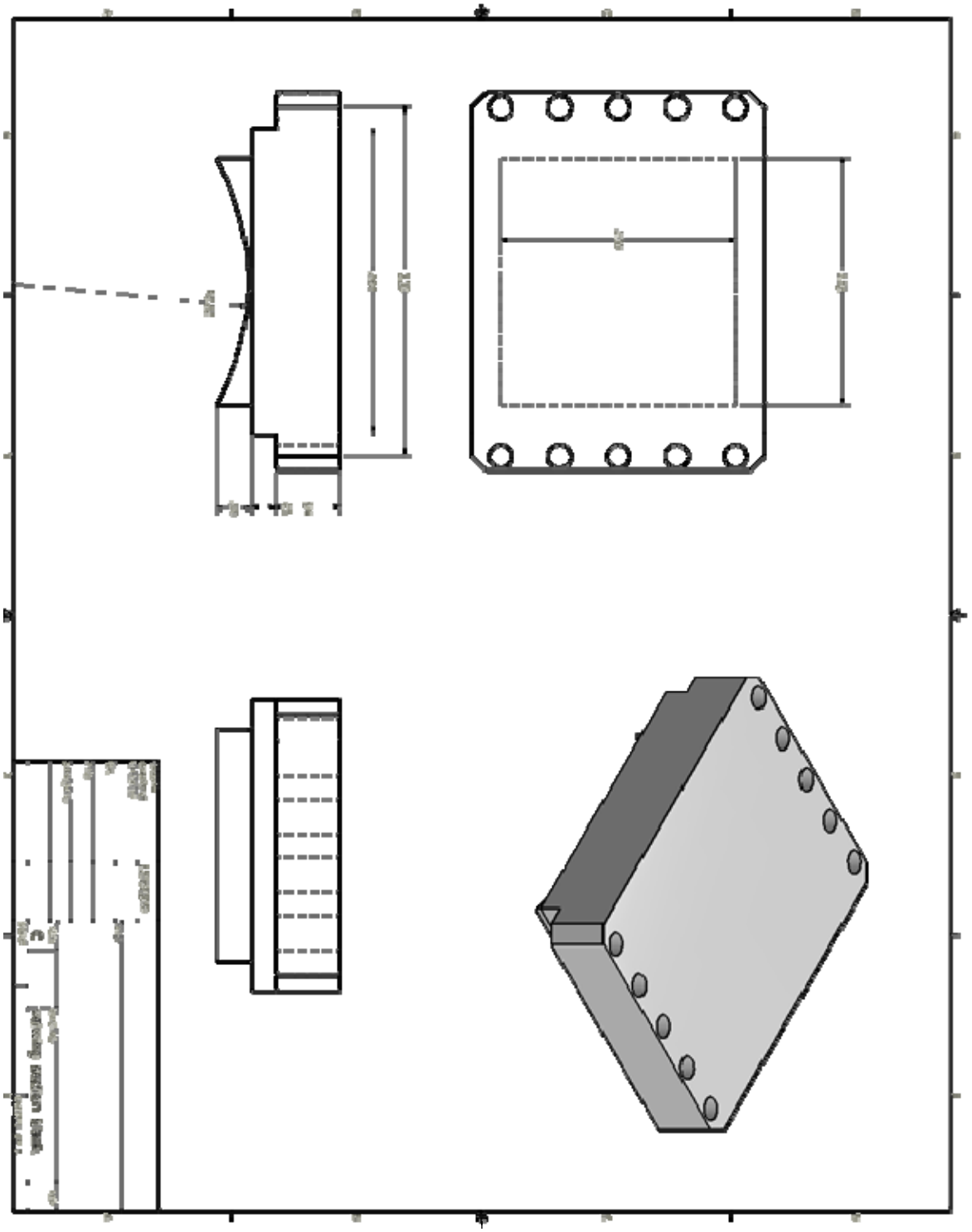

Viewing Window Blank

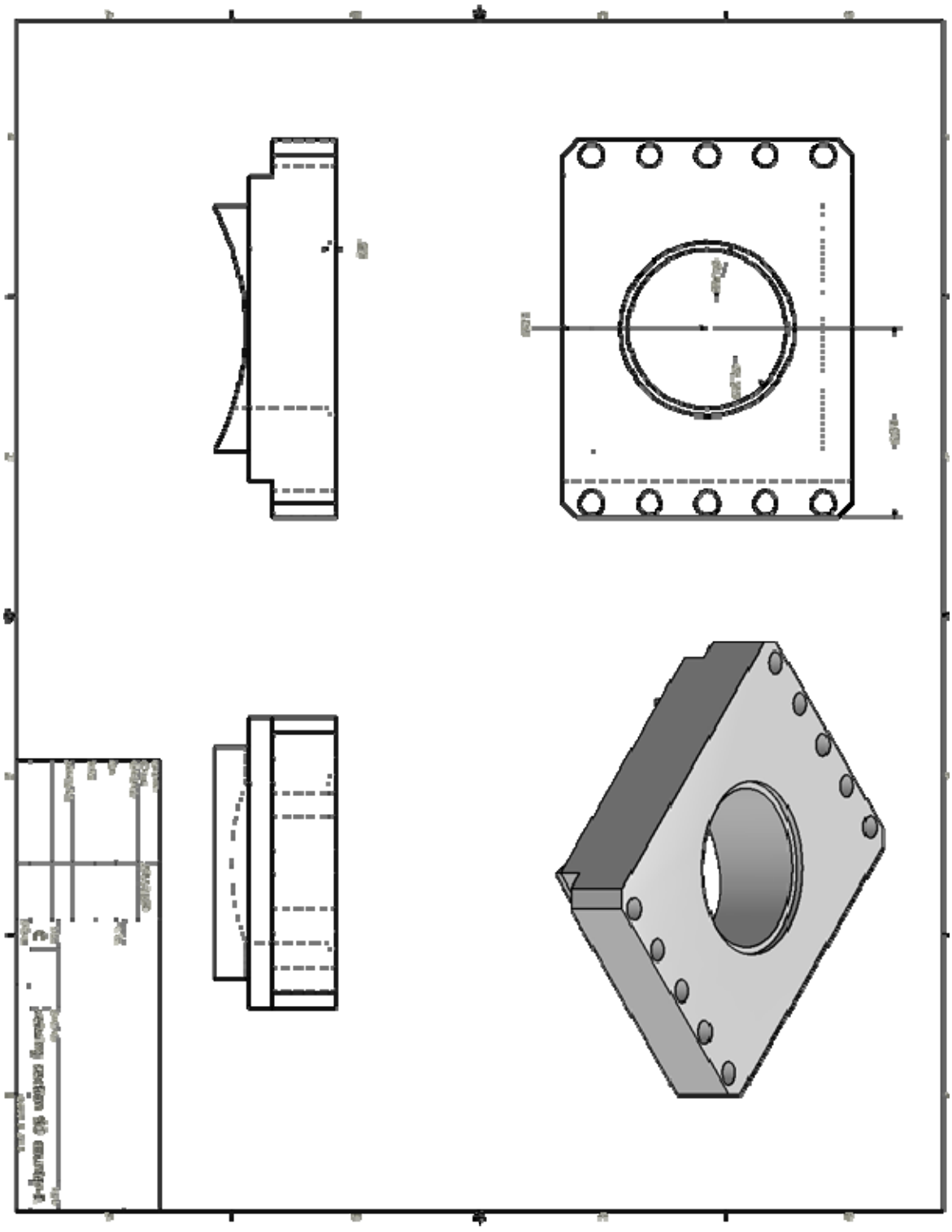

90° Inlet Port

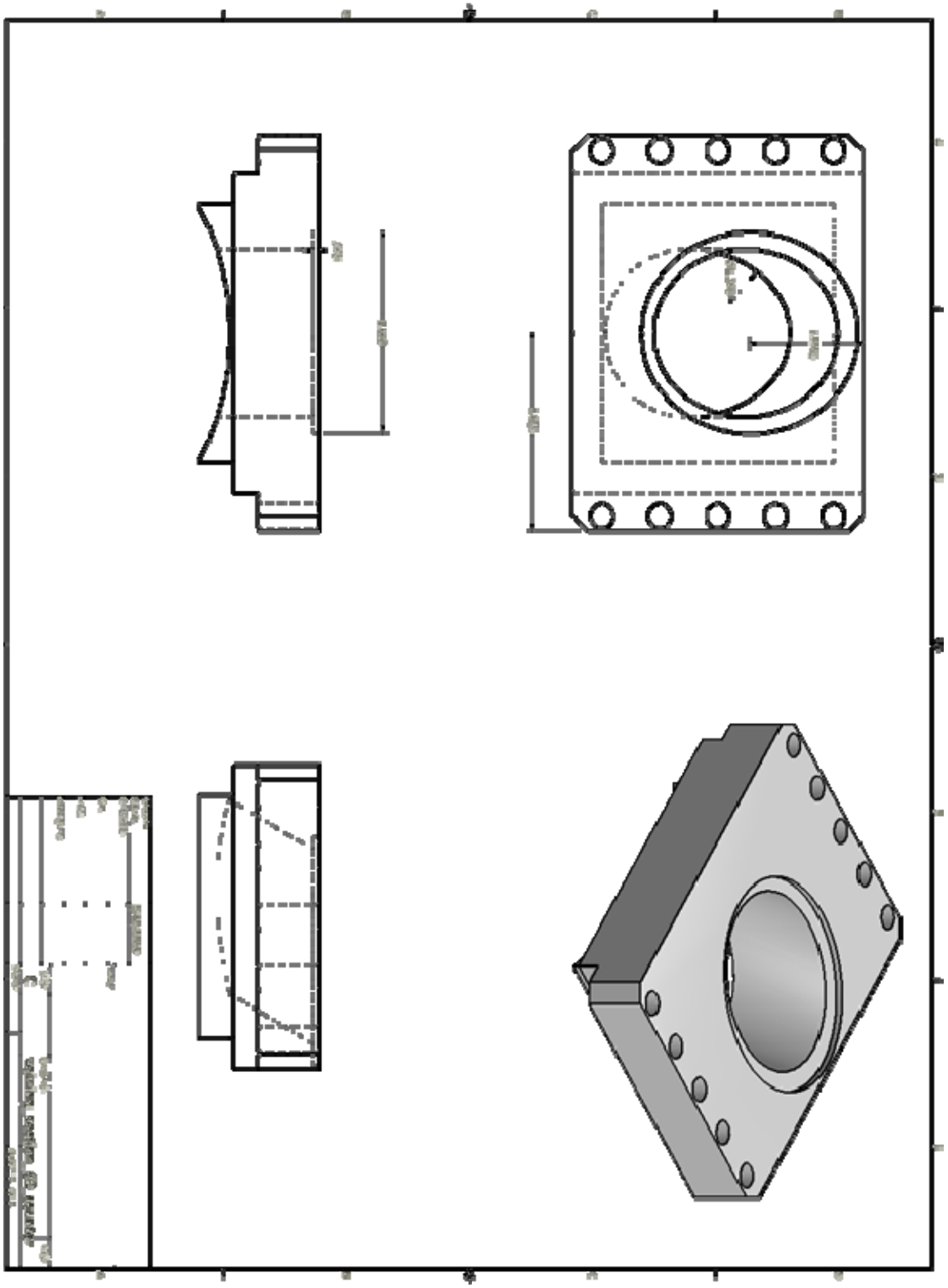

60° Inlet Port

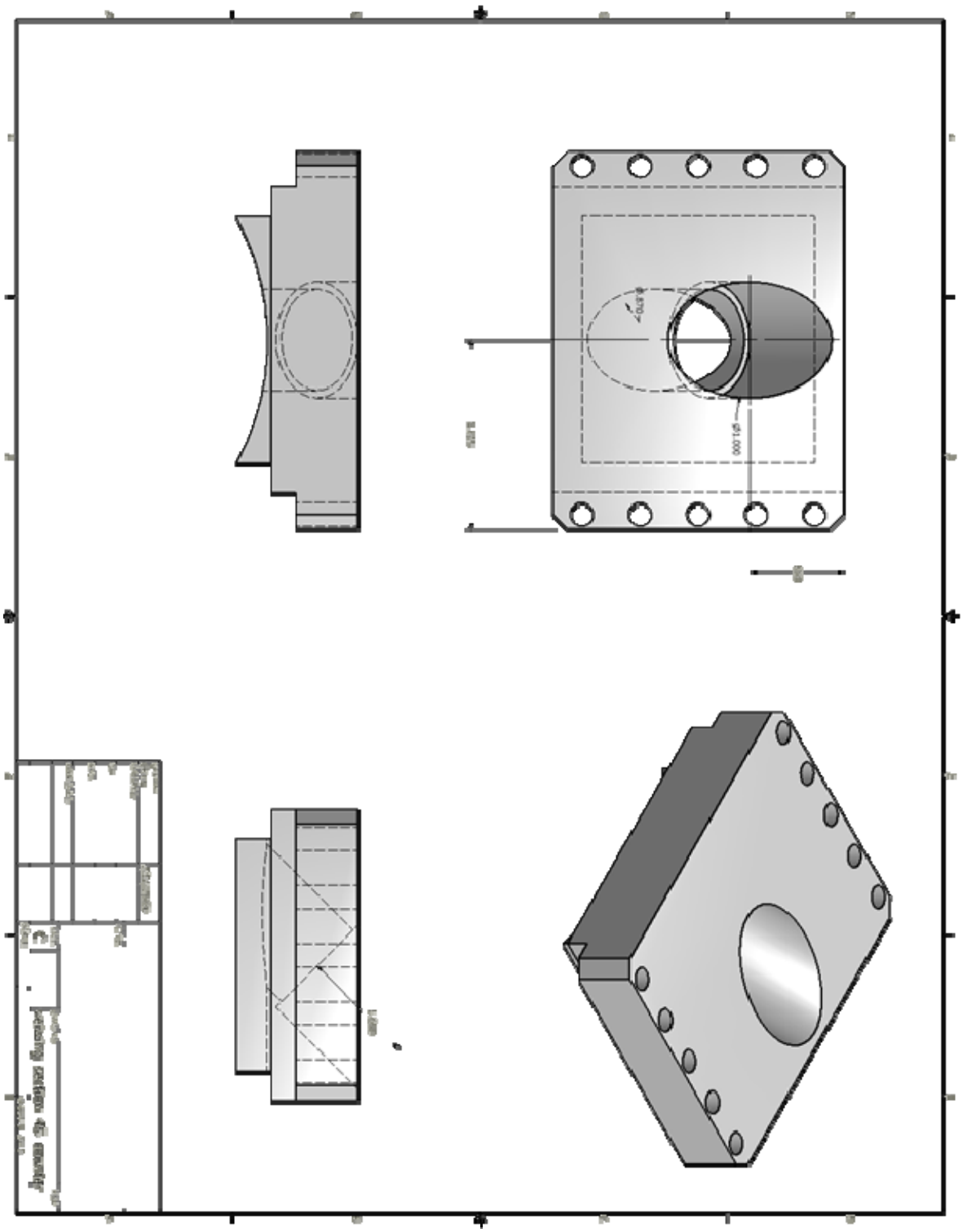

45° Inlet Port

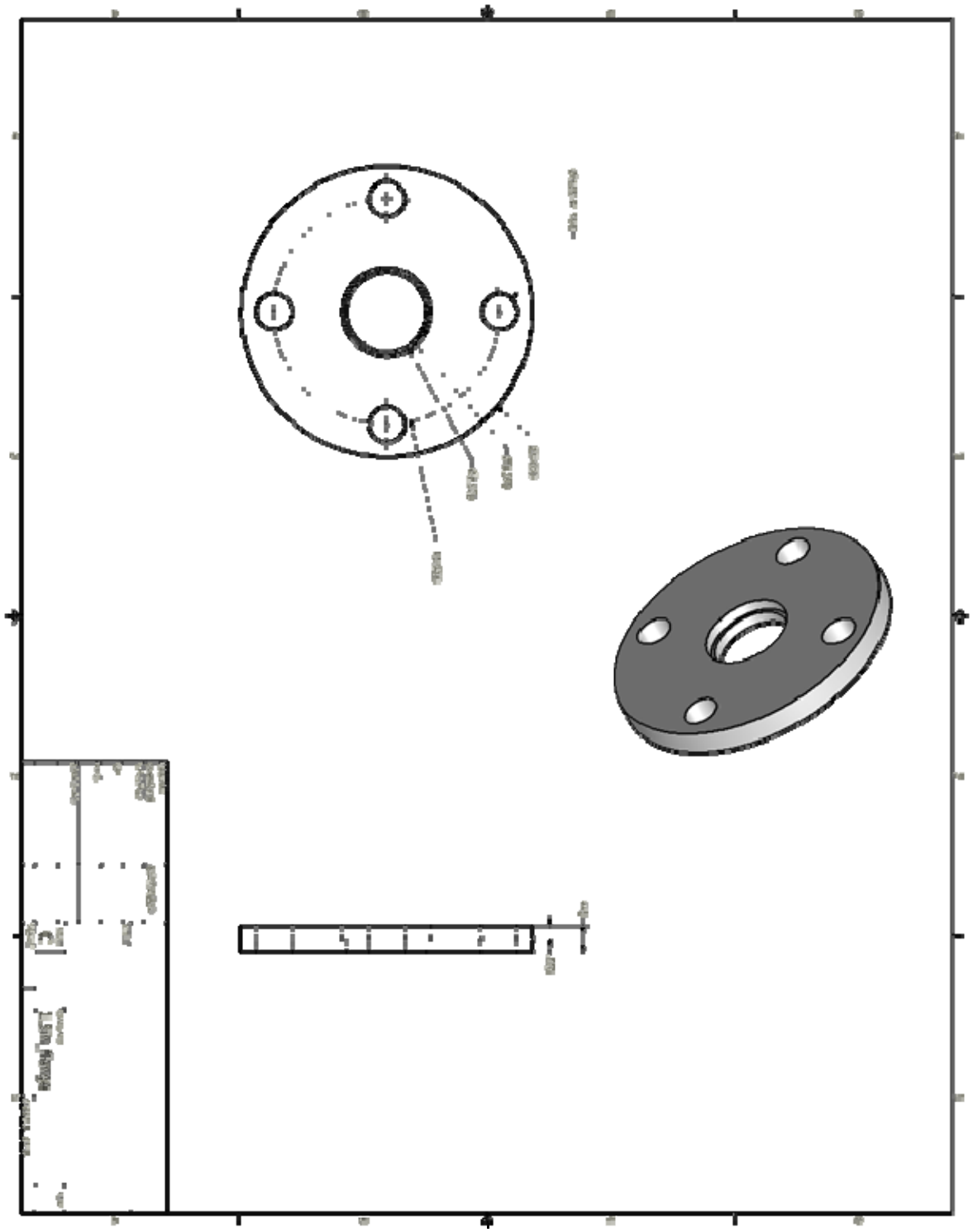

90° Inlet Flange

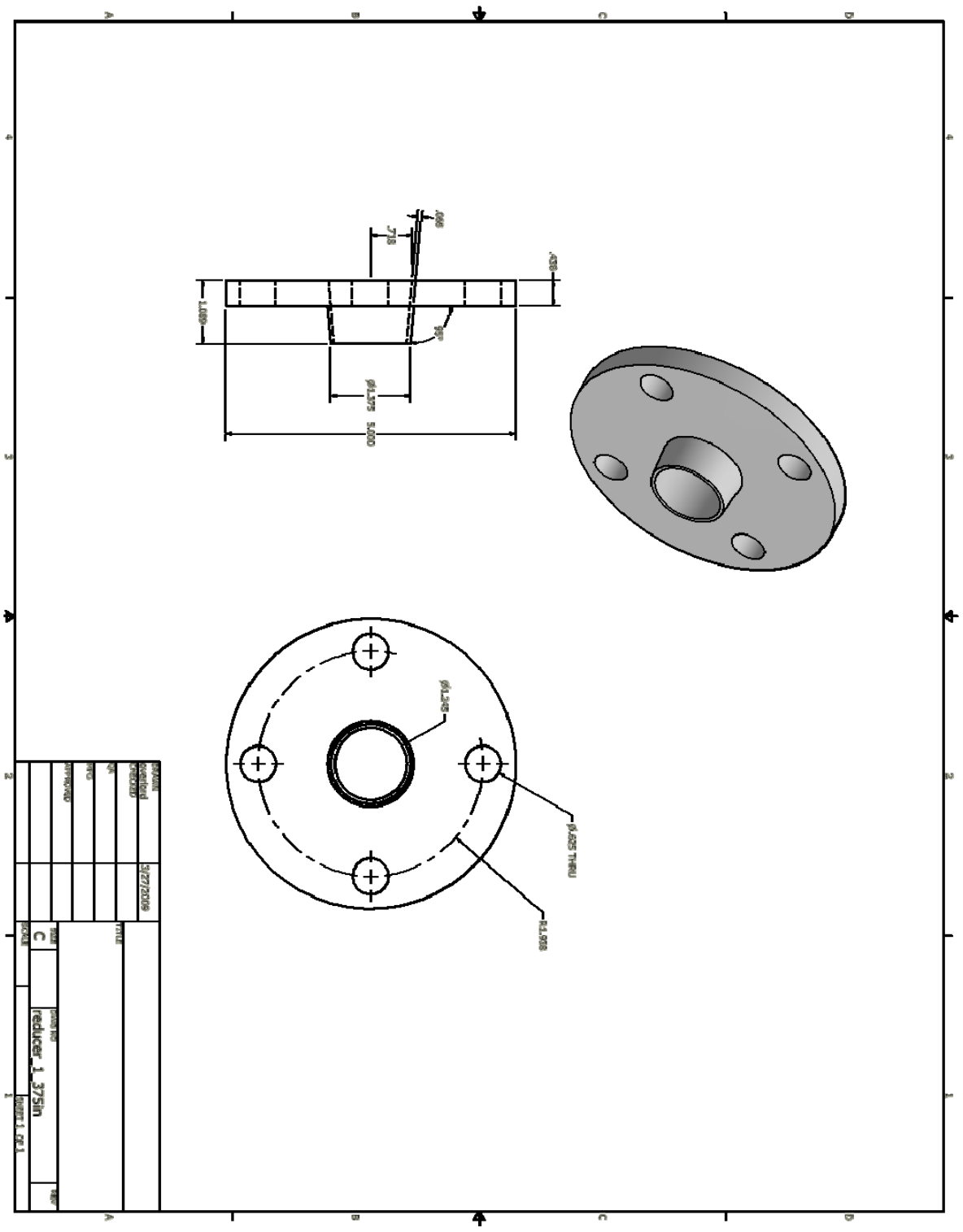

60° Inlet Flange

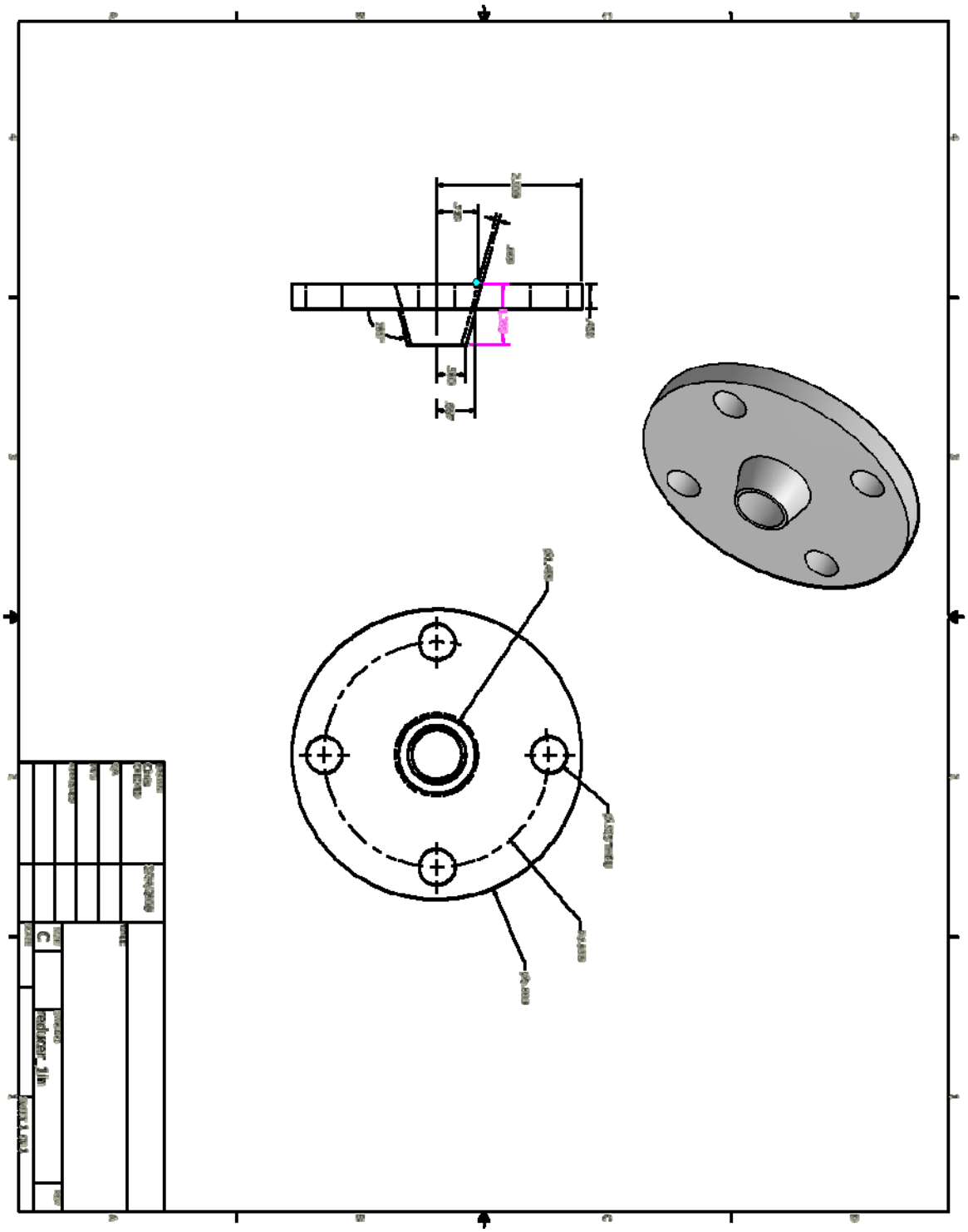

45° Inlet Flange

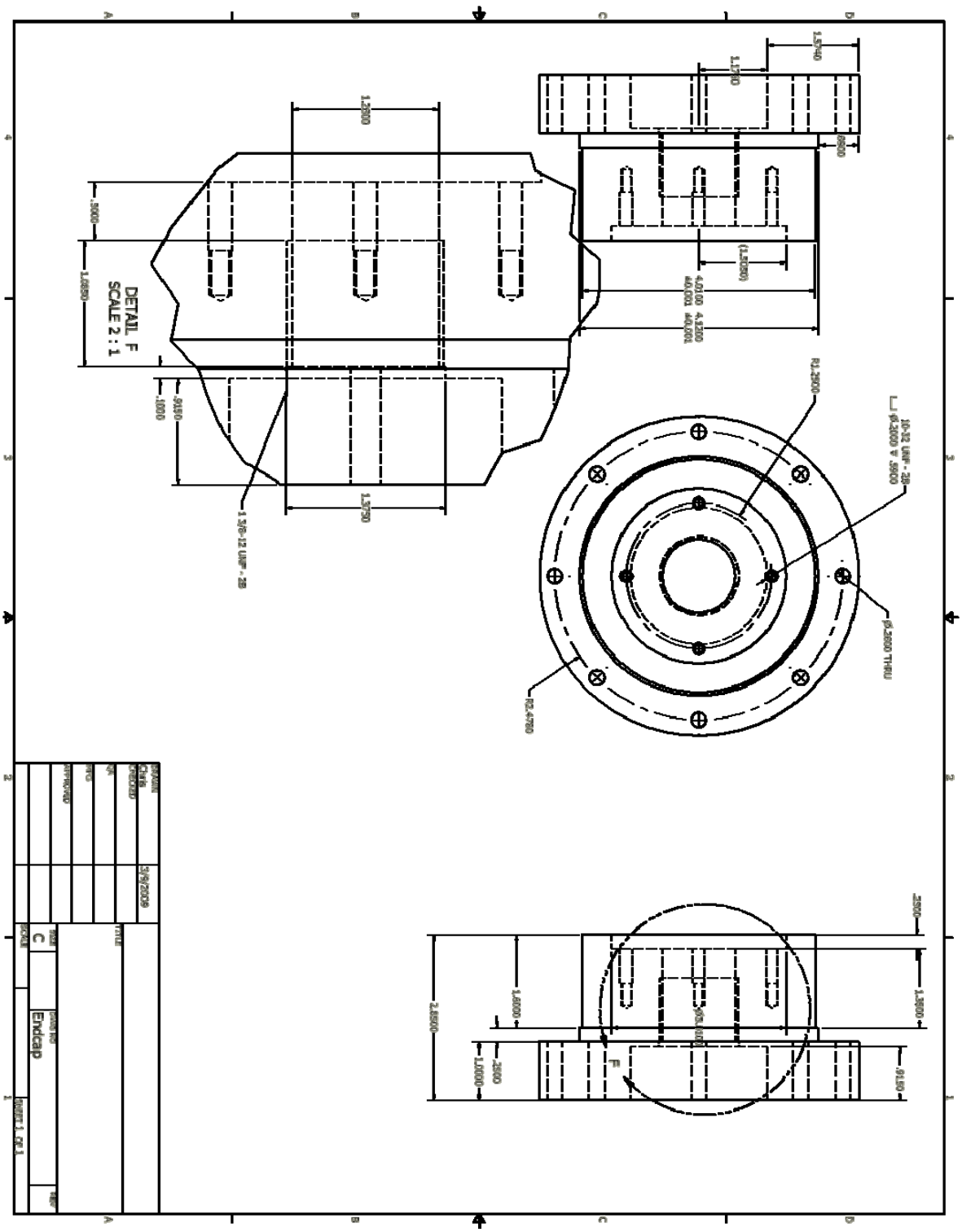

Combustor Head Assembly

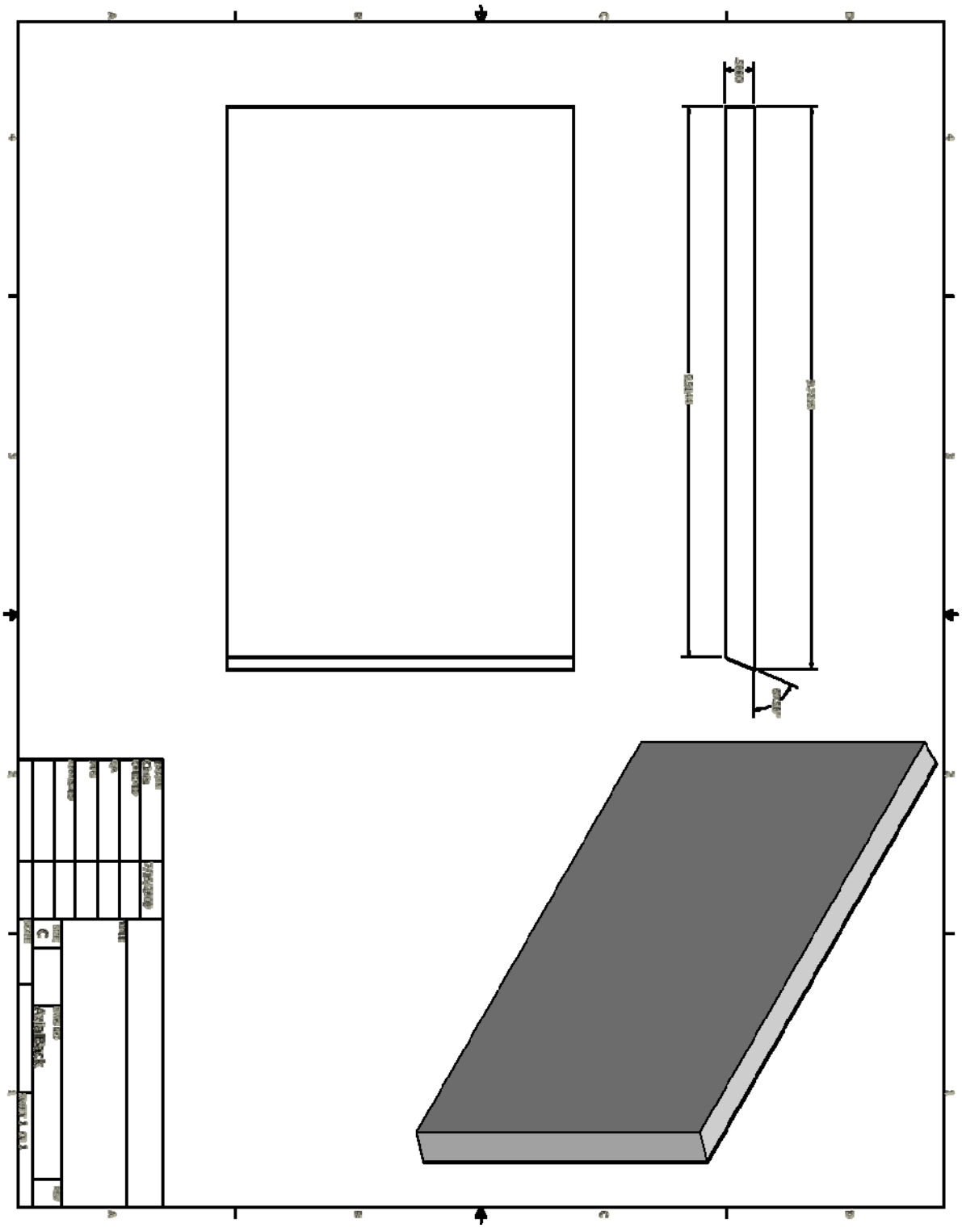

Forward Exhaust Rear Section

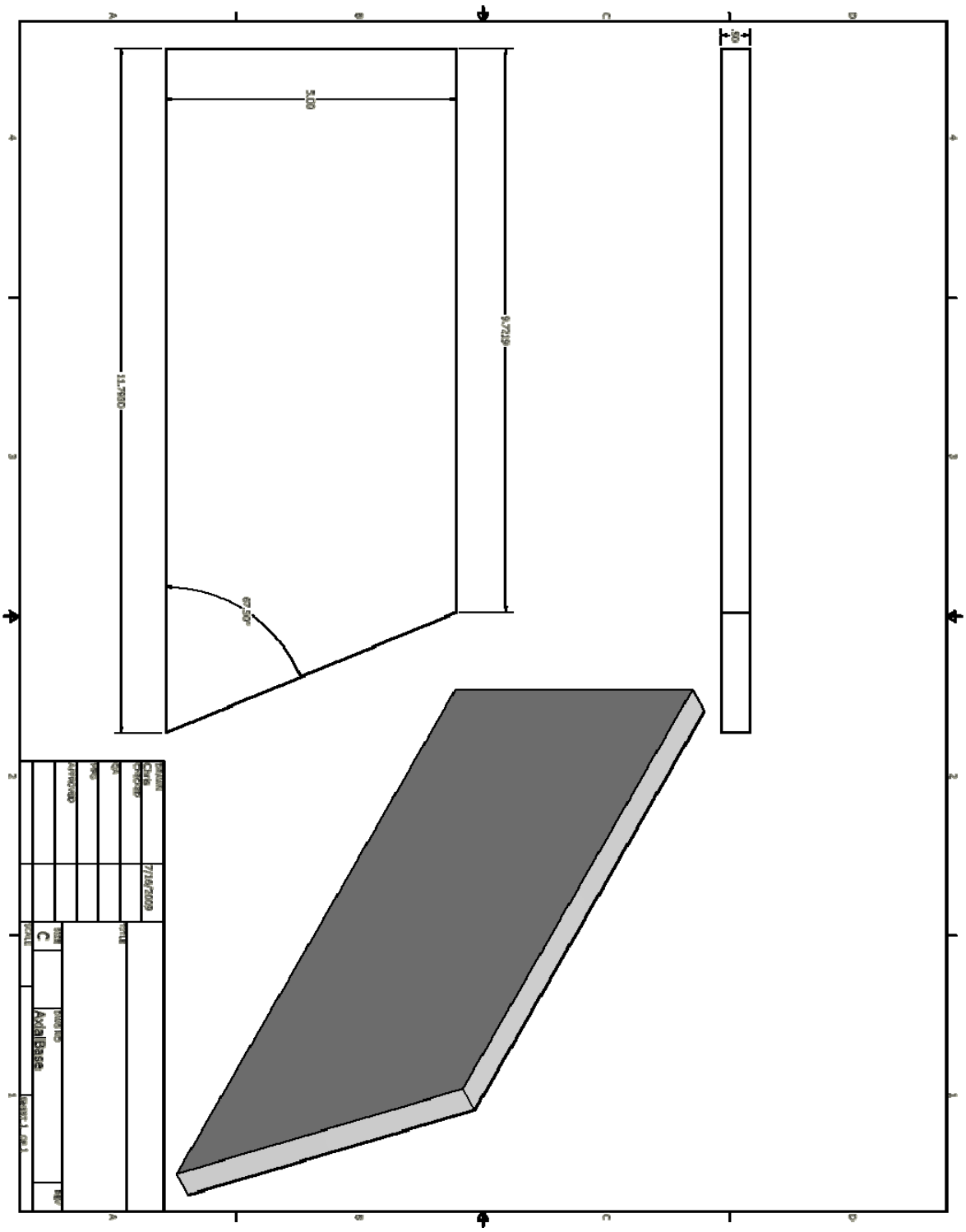

Forward Exhaust Base Section

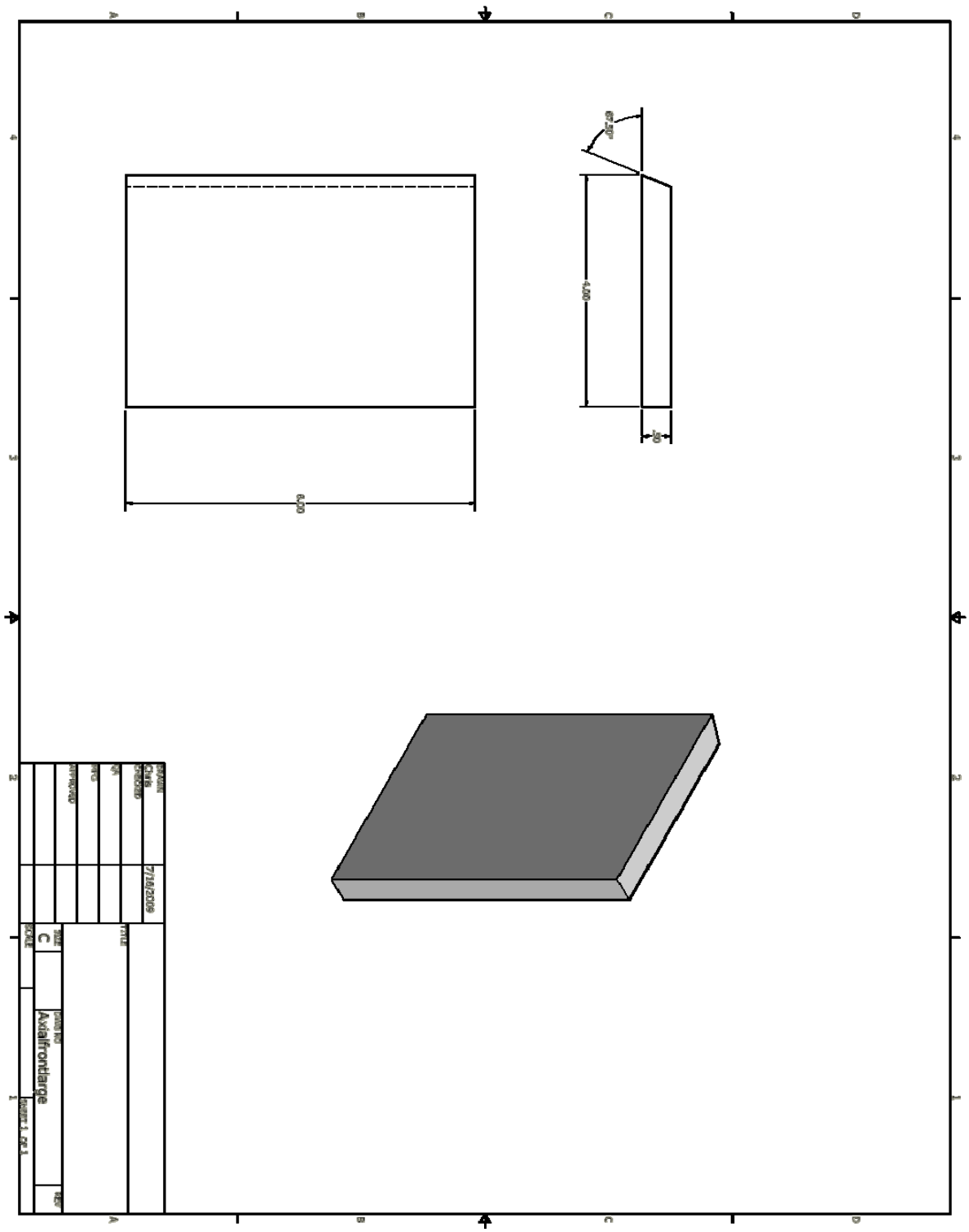

Forward Exhaust Small Rear Section

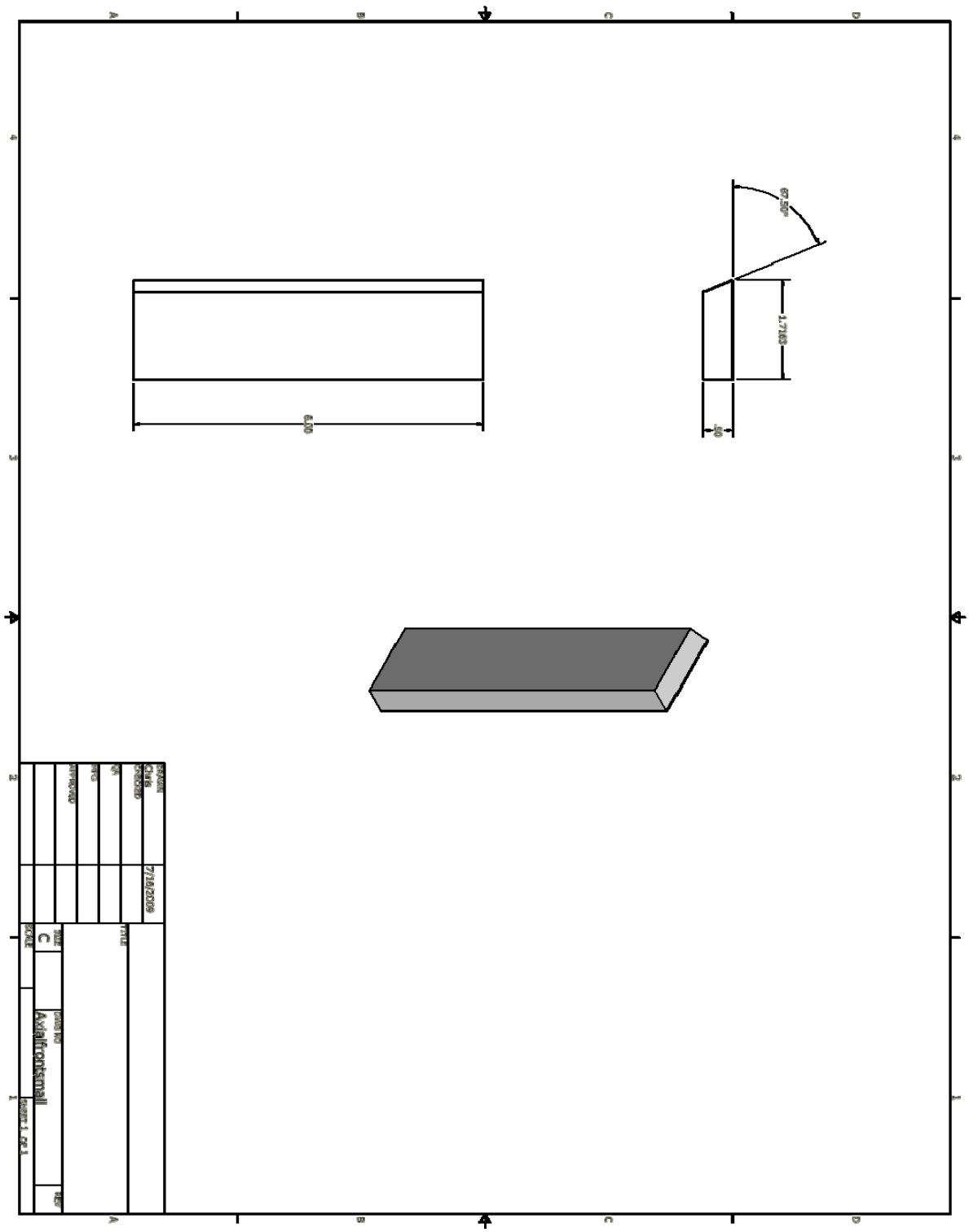

Forward Exhaust Small Front Section

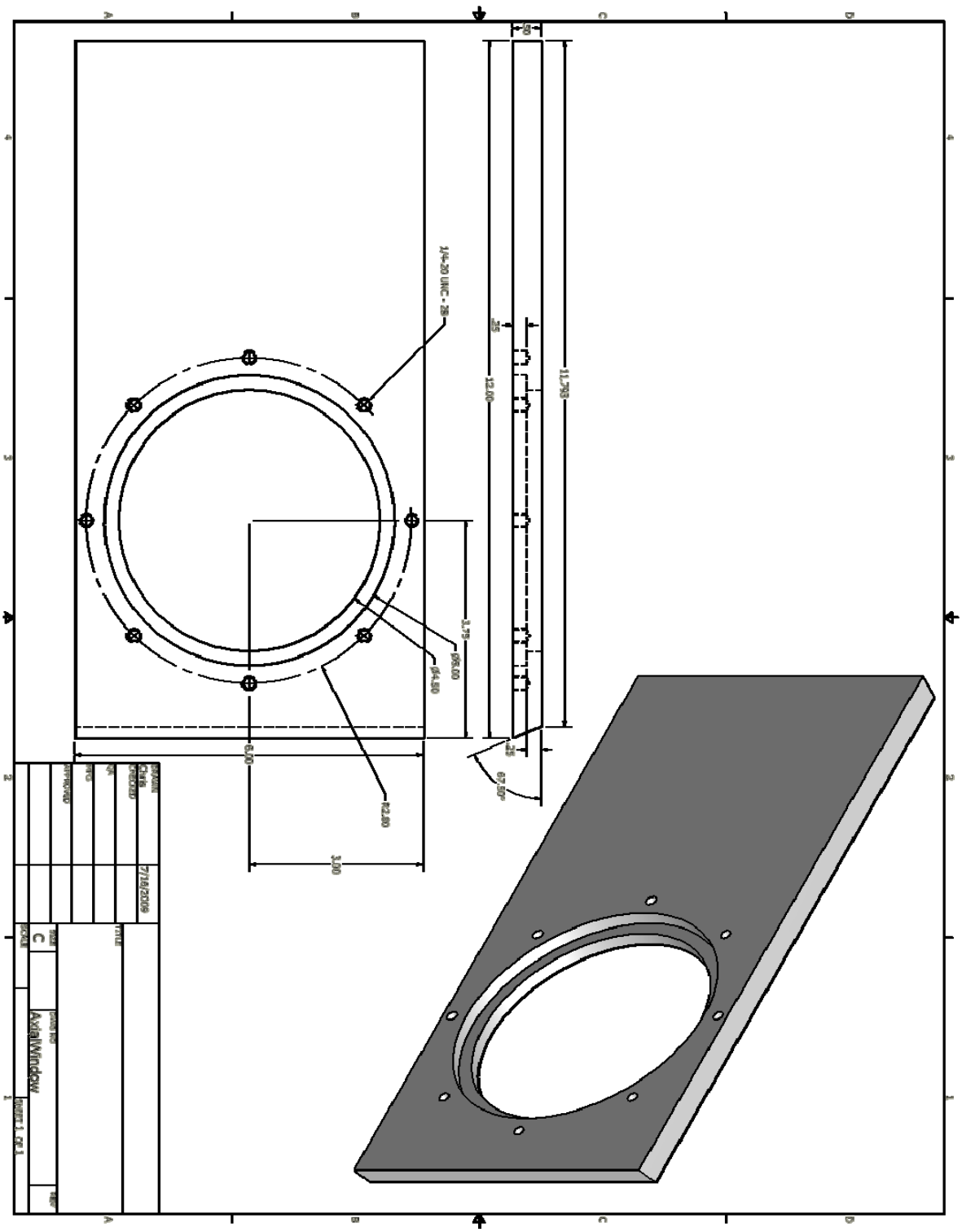

Forward Exhaust Axial Viewing Section

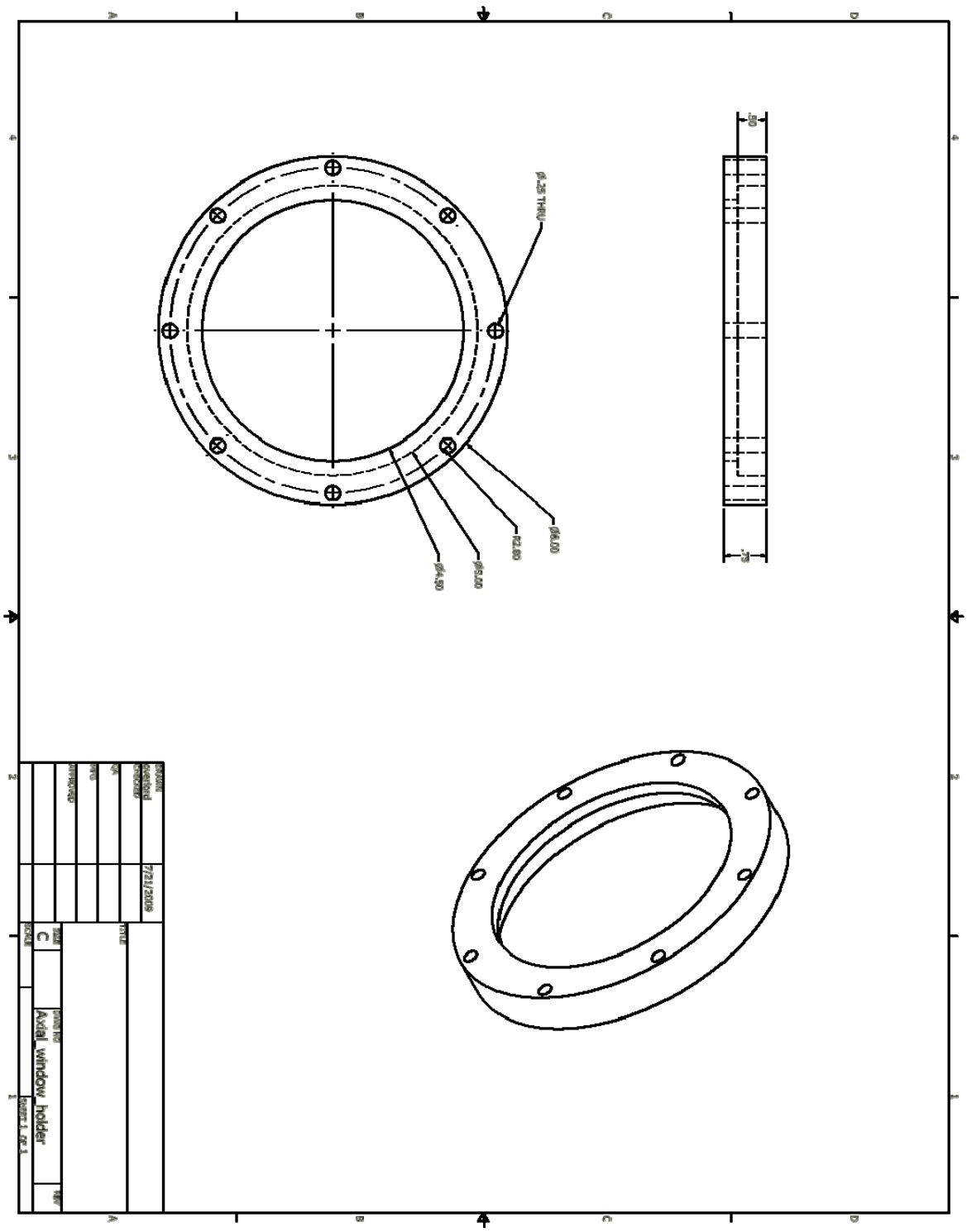

Axial Viewing Window Holder

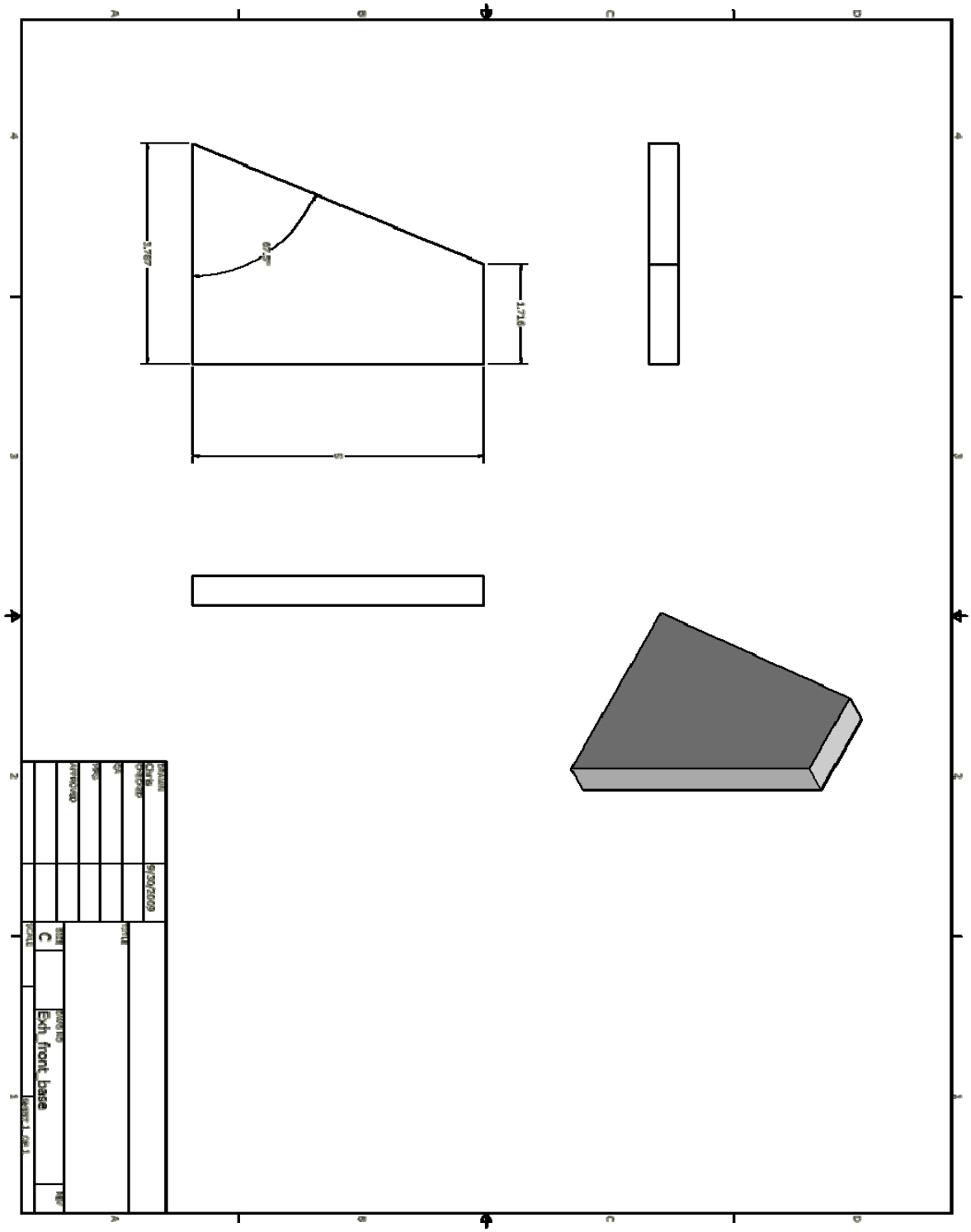

Forward Exhaust Small Base Section

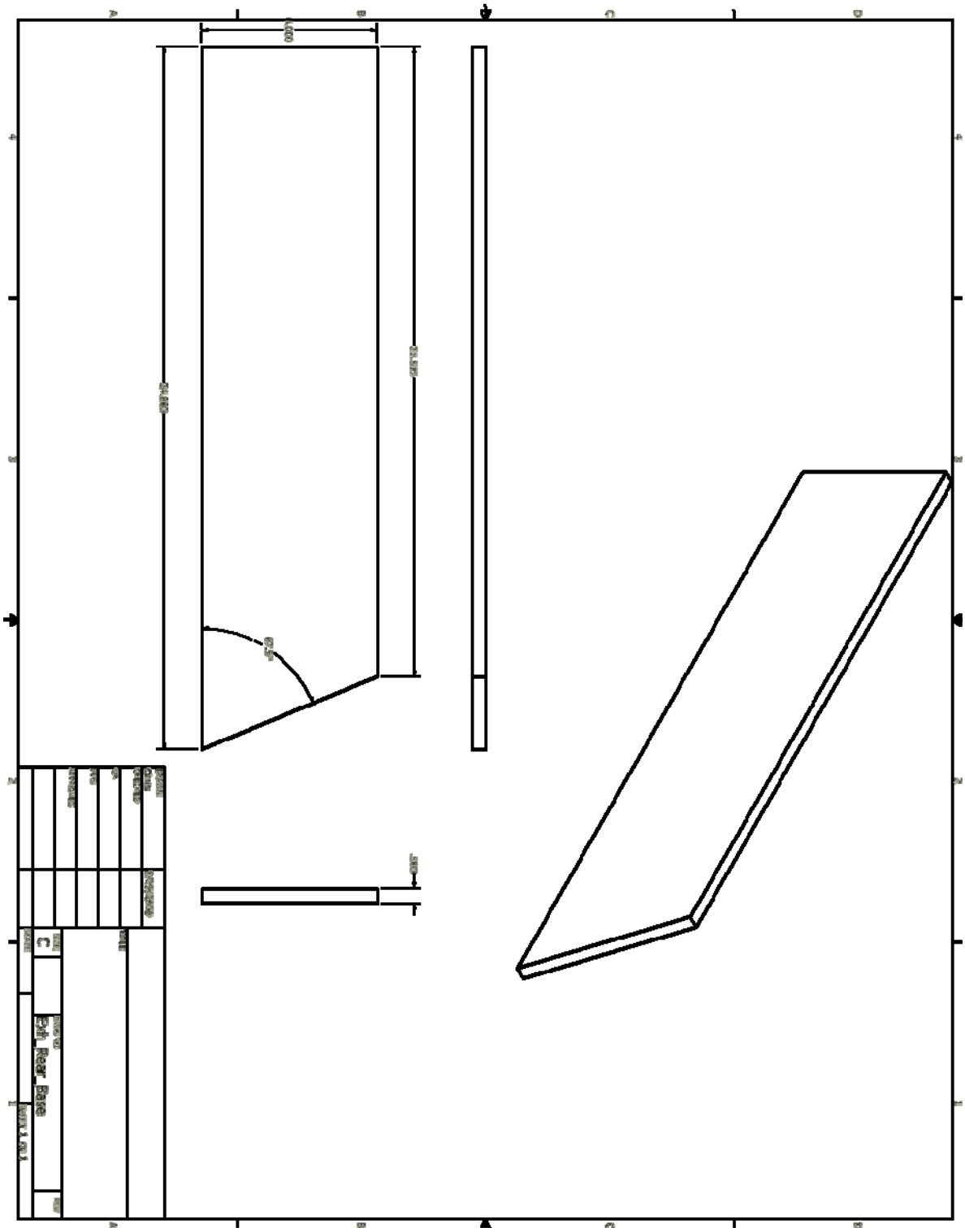

Rear Exhaust Aft Base Section

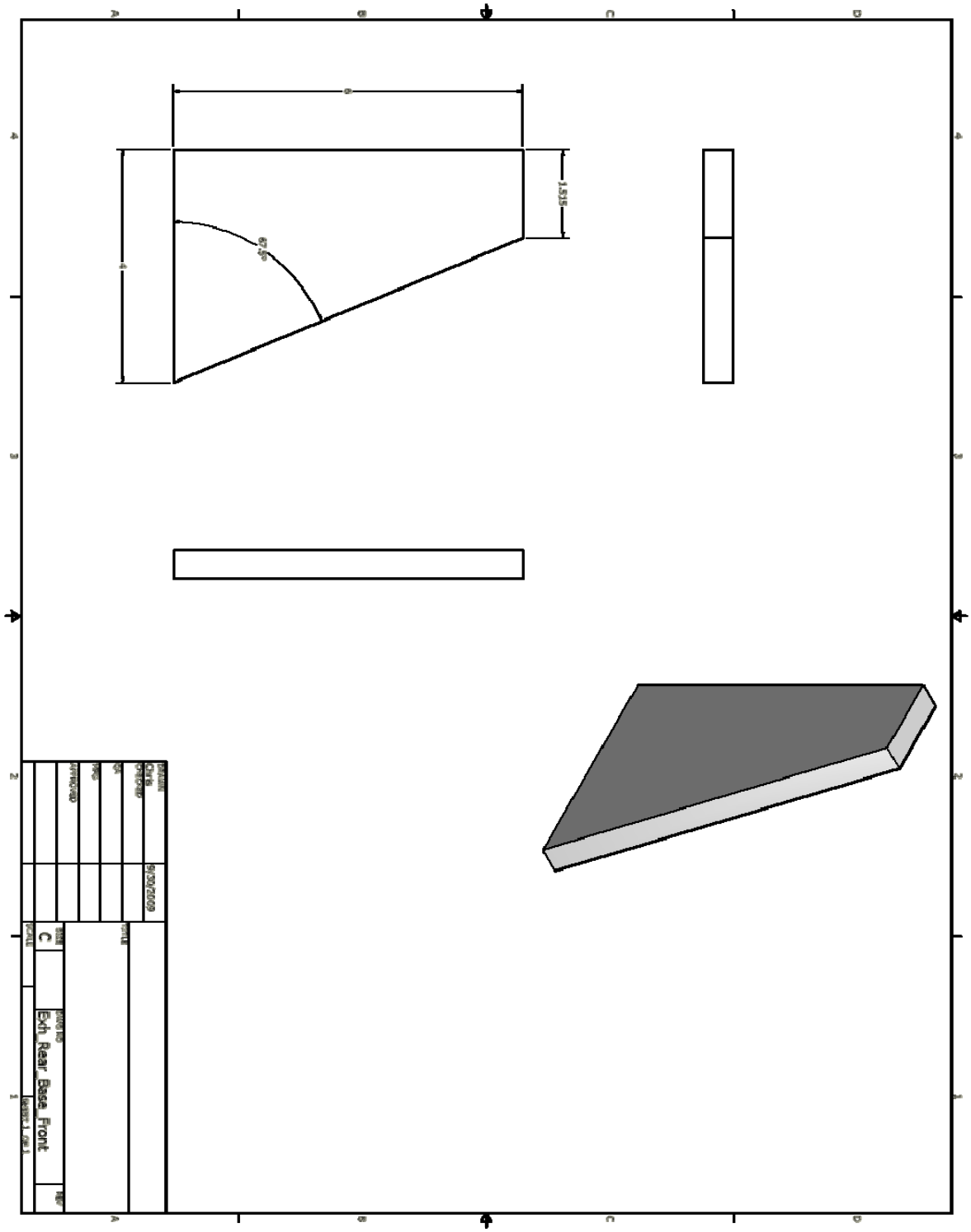

Rear Exhaust Forward Base Section

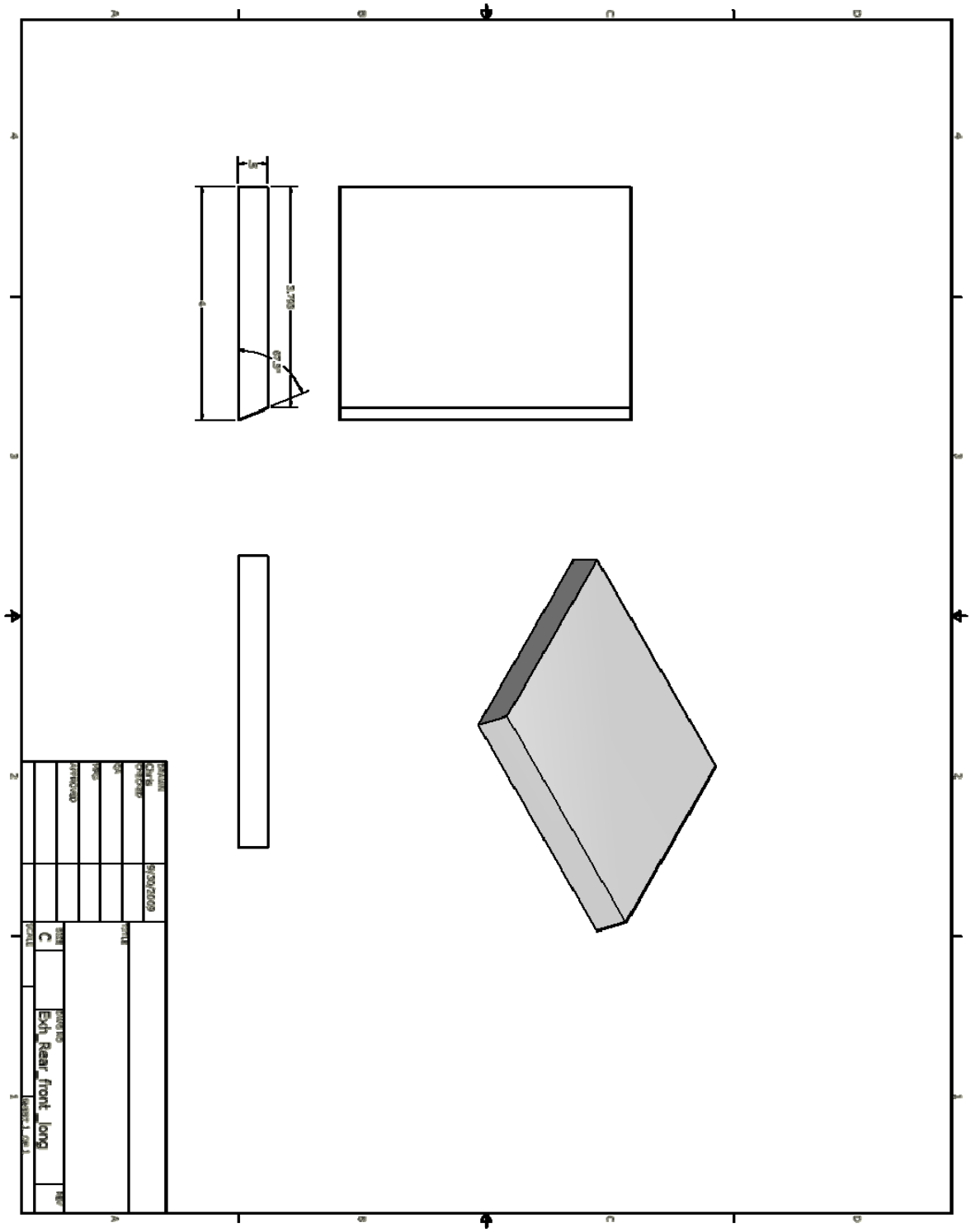

Rear Exhaust Long Forward Side Section

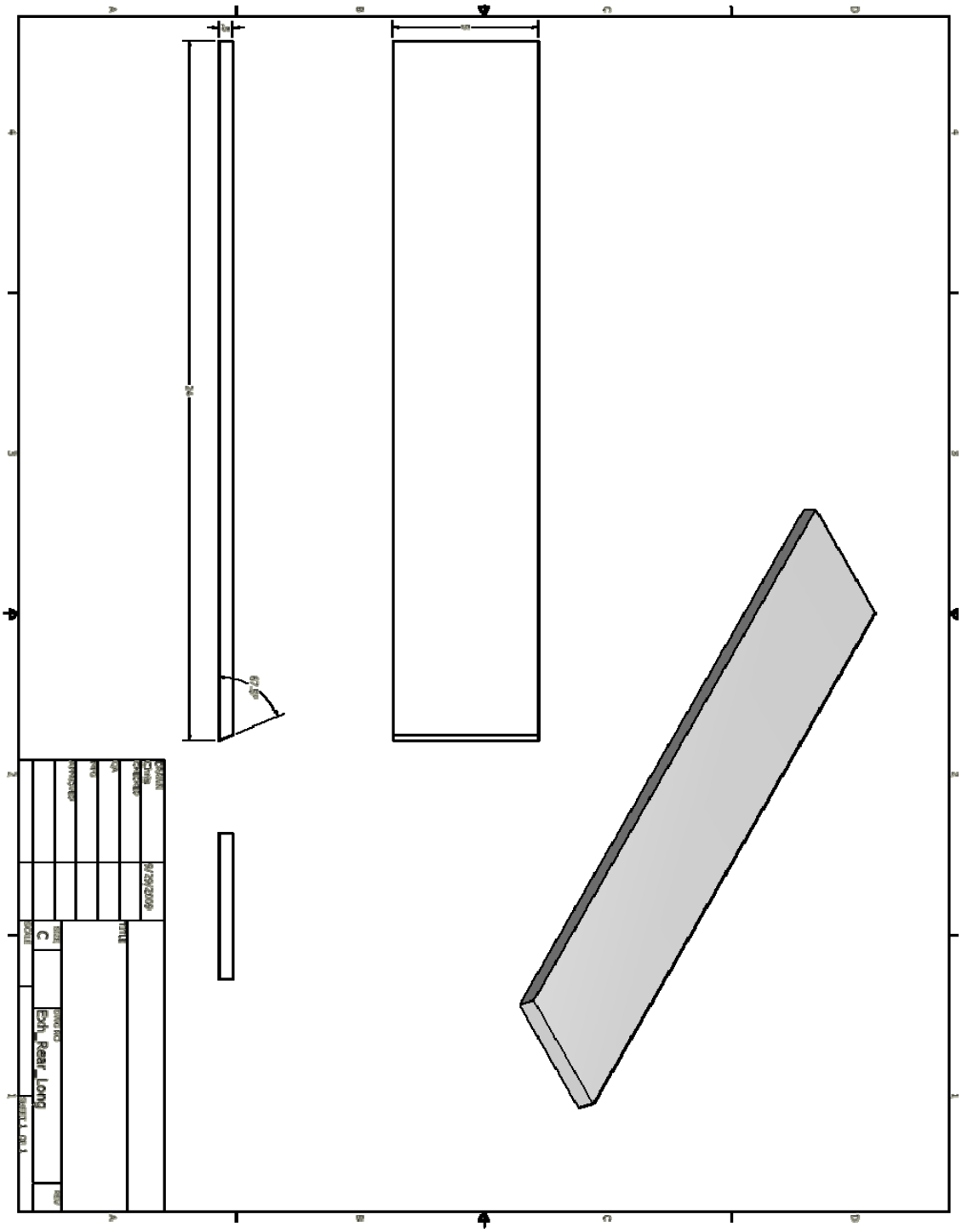

Rear Exhaust Aft Long Side Section

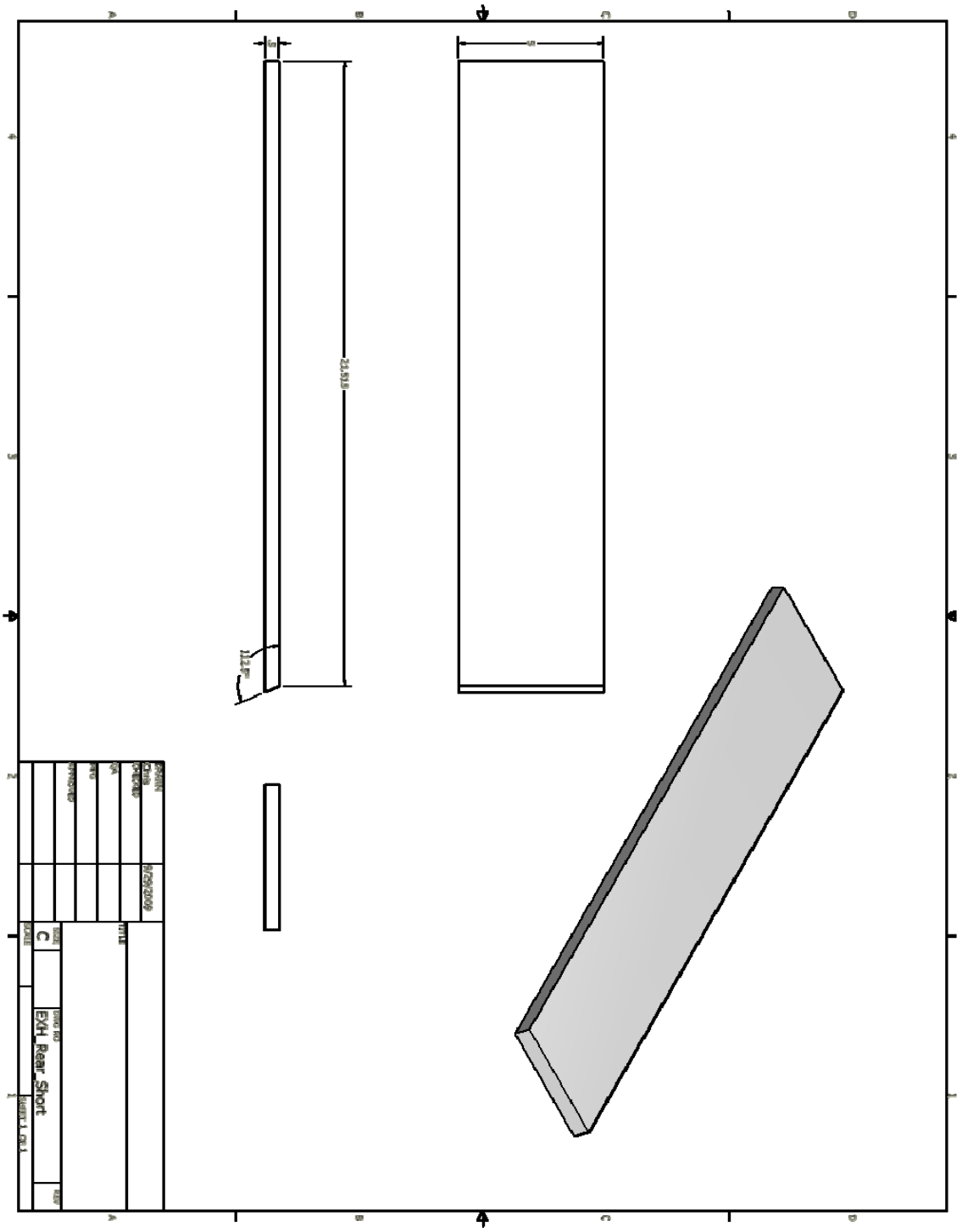

Rear Exhaust Aft Short Side Section

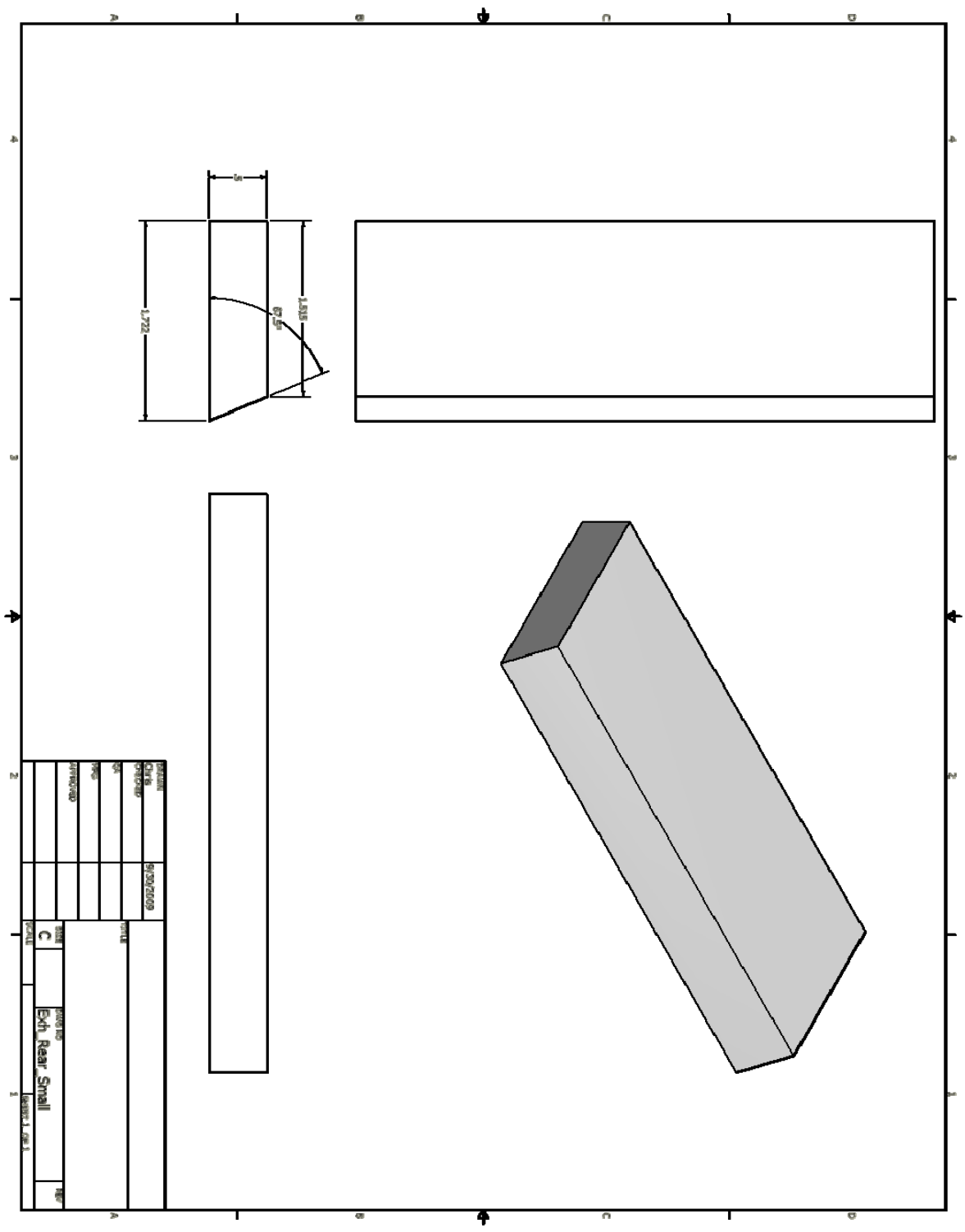

Rear Exhaust Forward Short Side Section

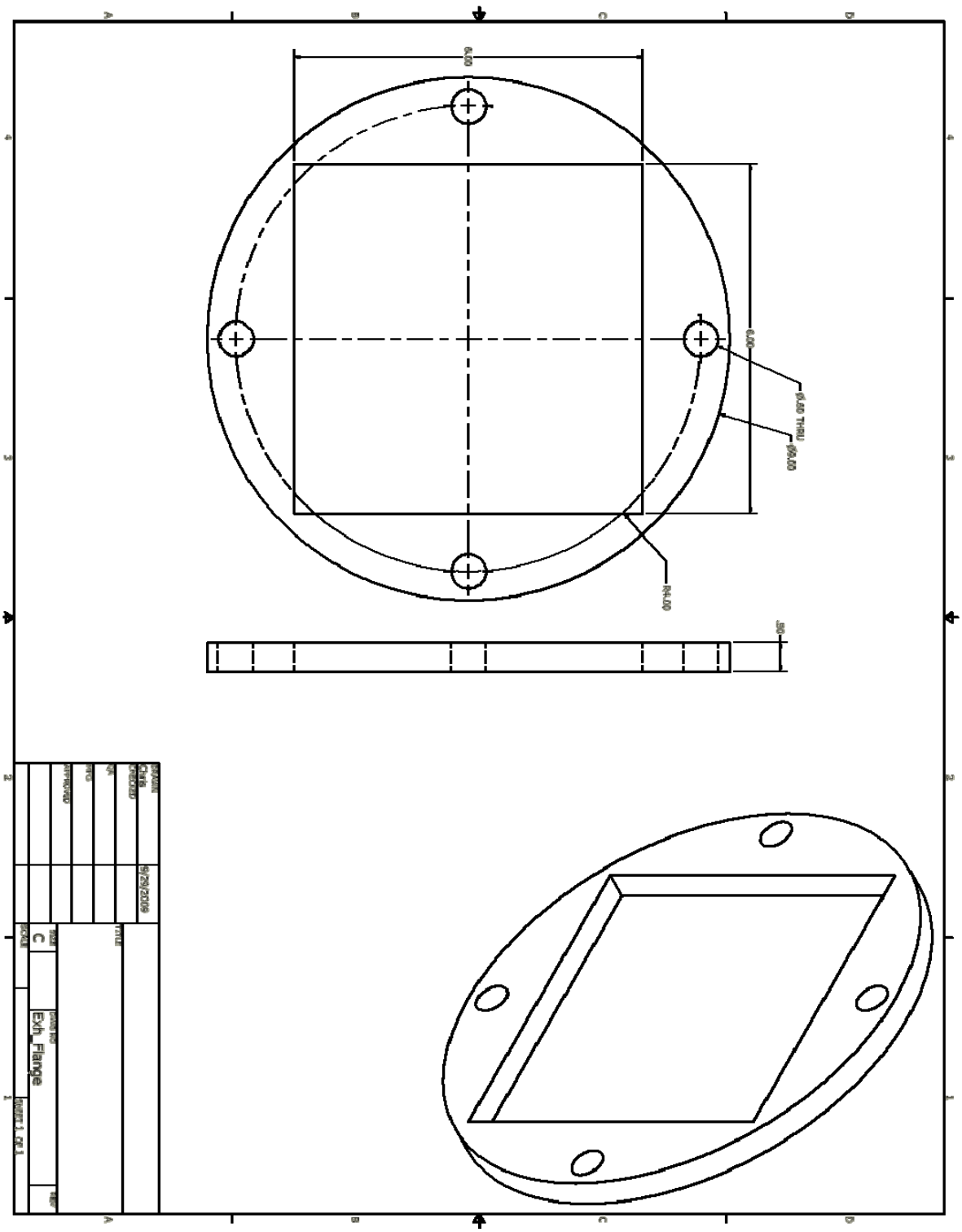

Rear Exhaust Flange

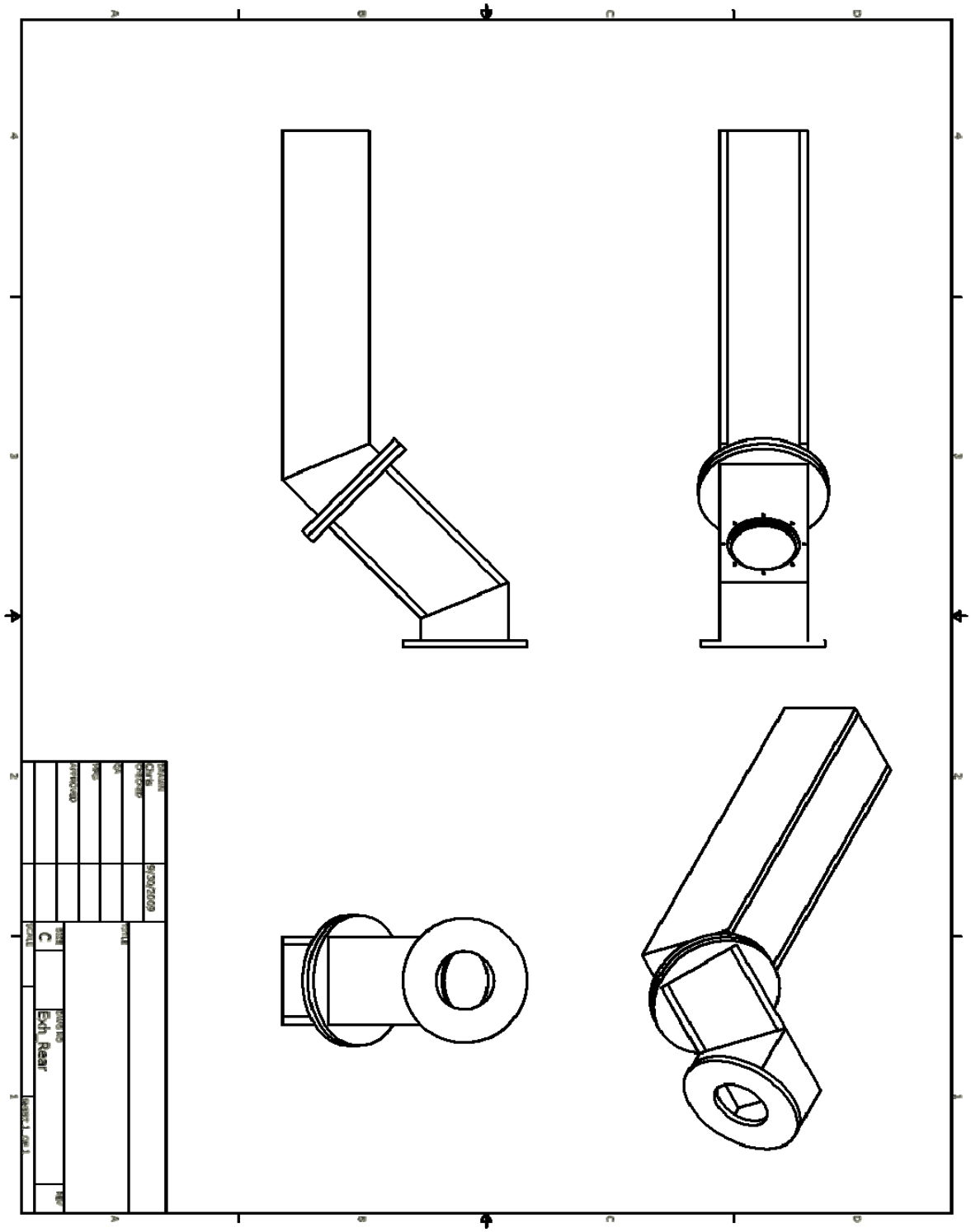

Exhaust Assembly

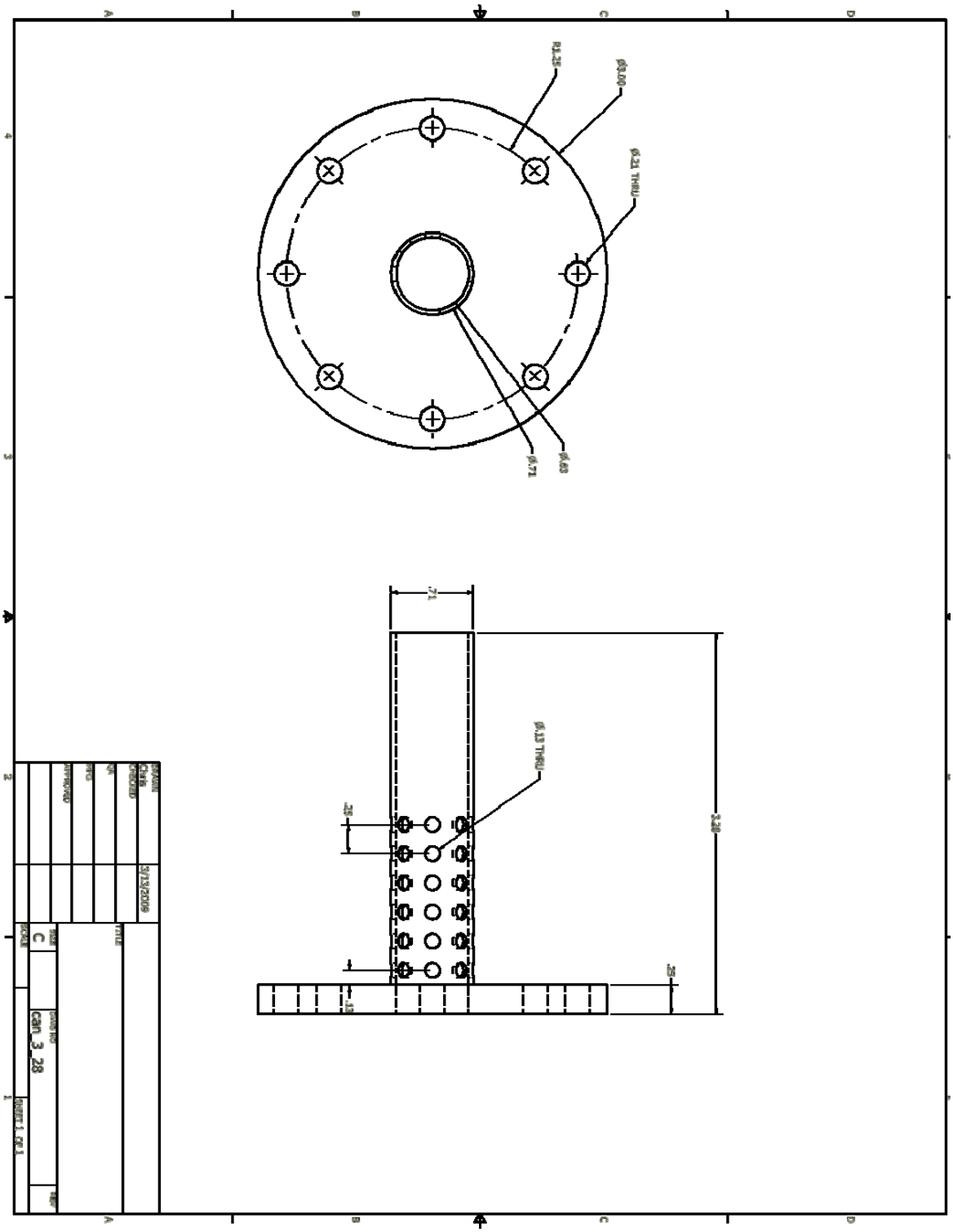
R1.25
Ø3.00
Ø.21 THRU
Ø.71
Ø.63
.71
Ø.13 THRU
.28
1.28
.25
.13
C
5/13/2006
can_3_28

Igniter Can

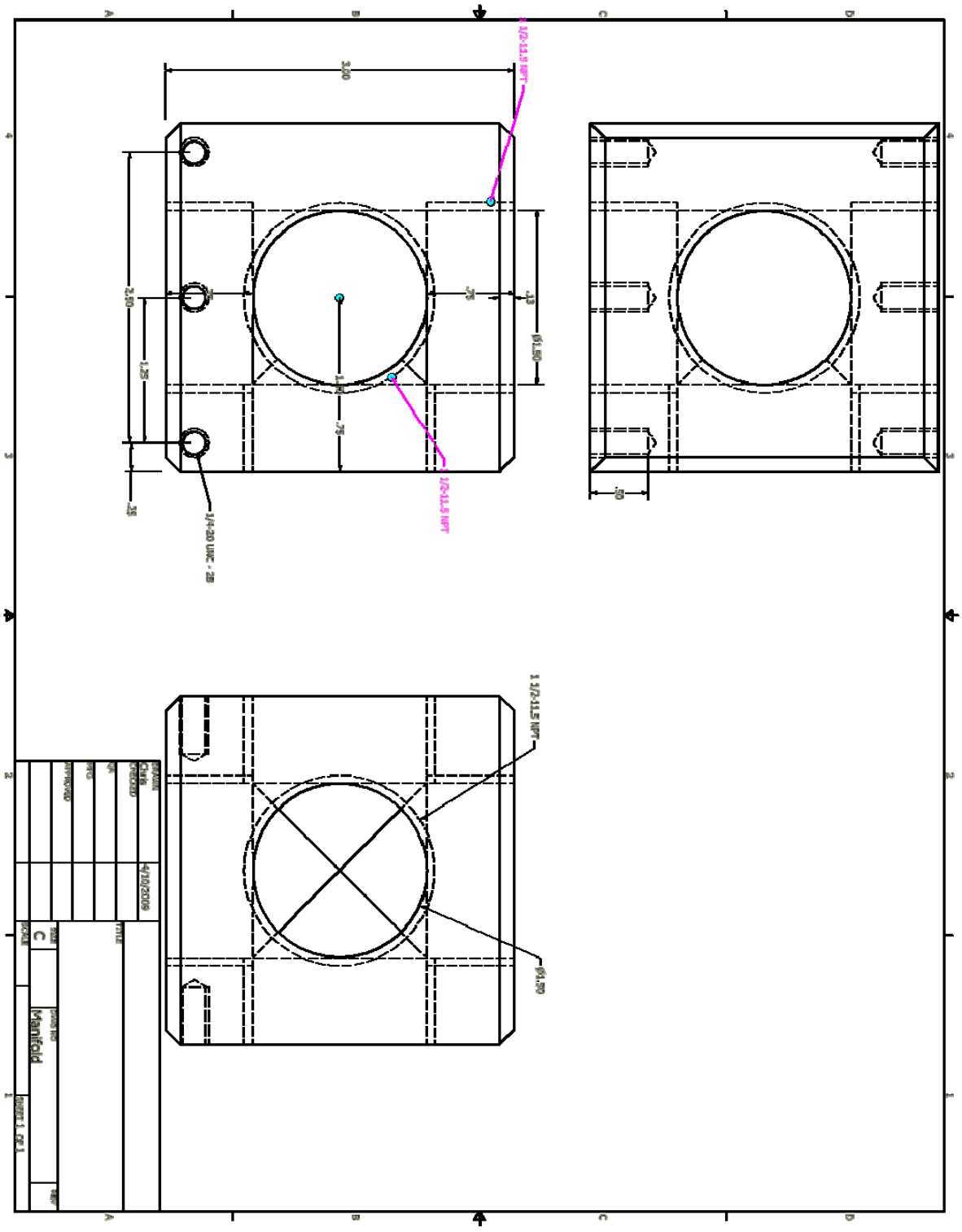

4 Way Manifold

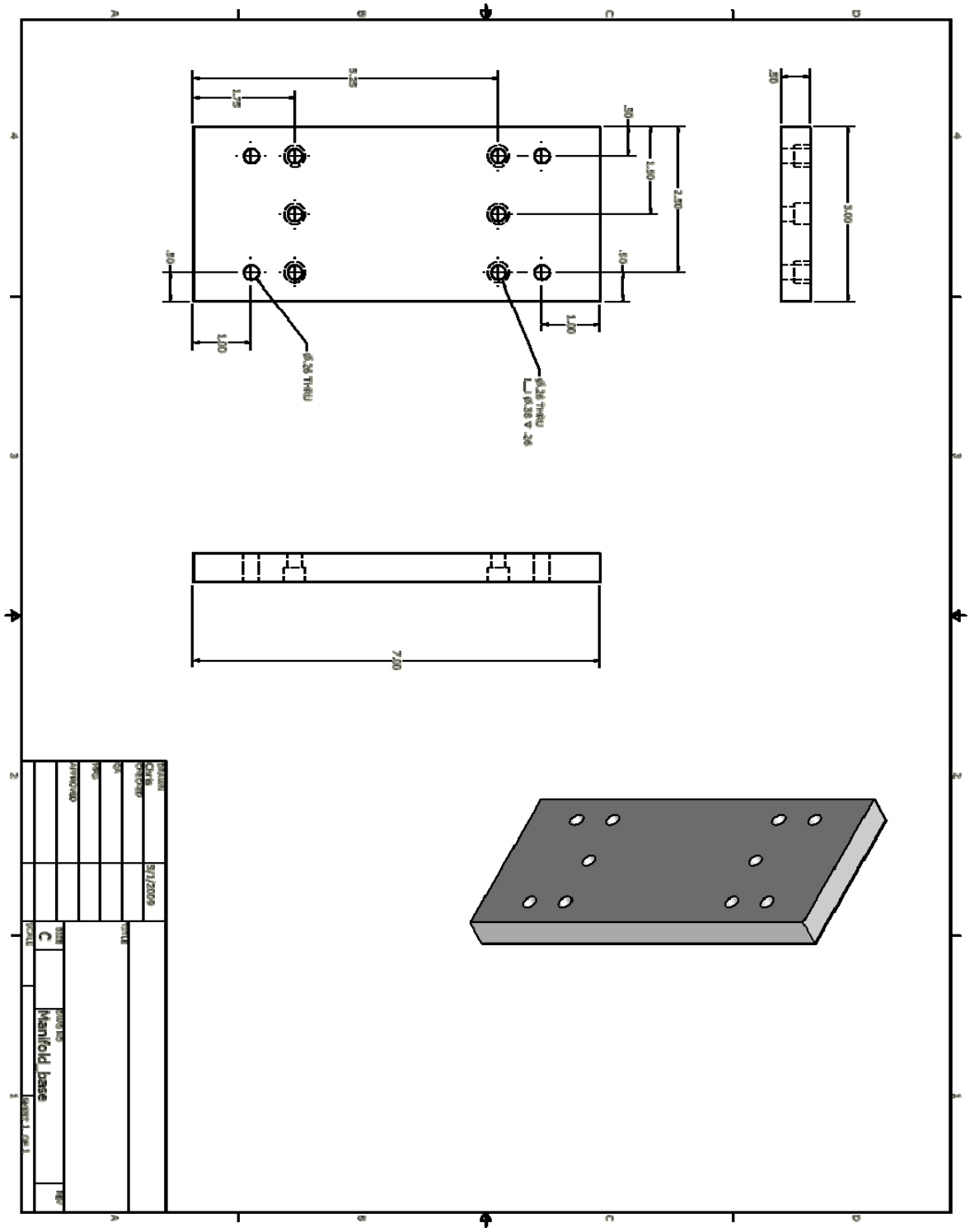

4-Way Manifold Holder Base

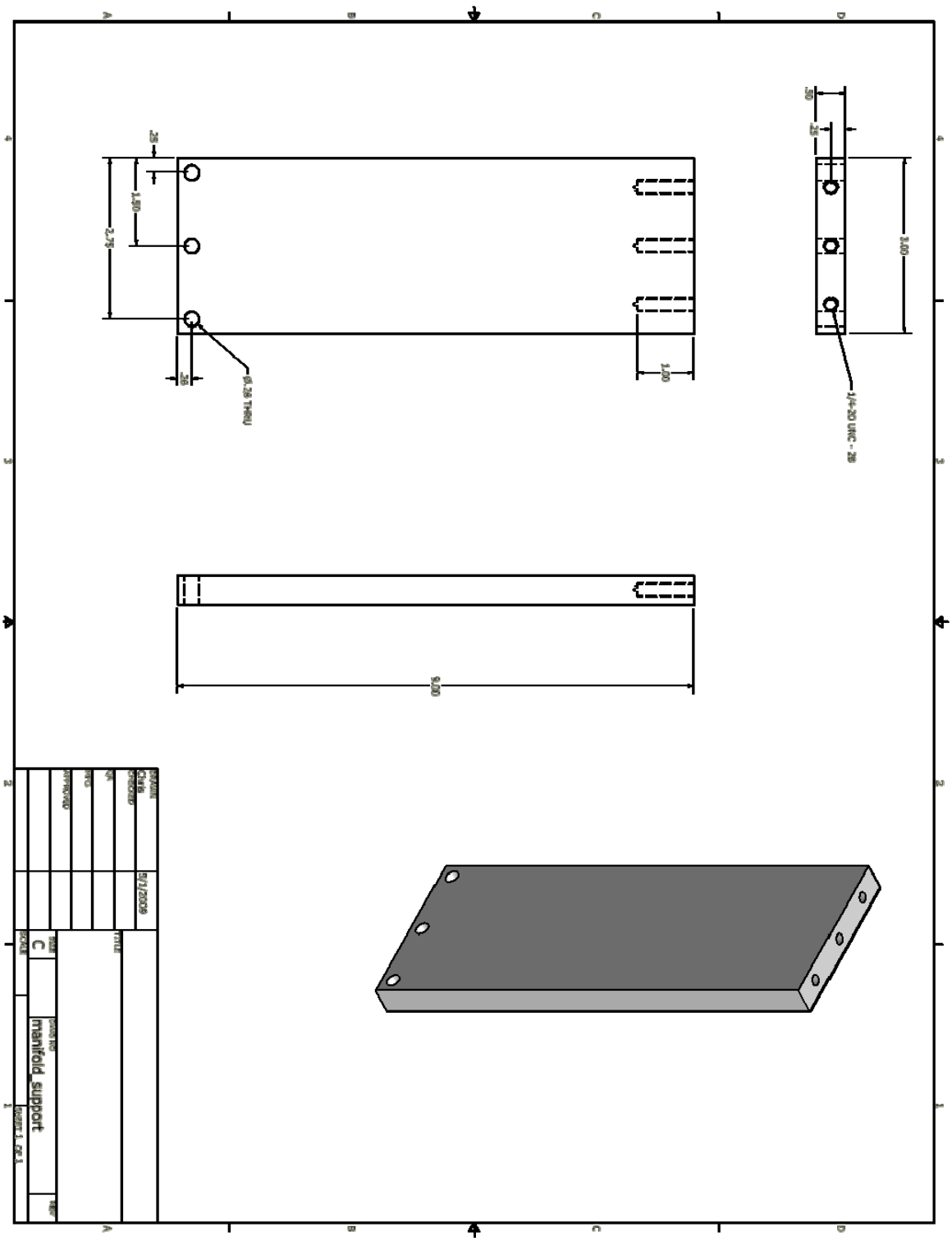

4-Way Manifold Vertical Support

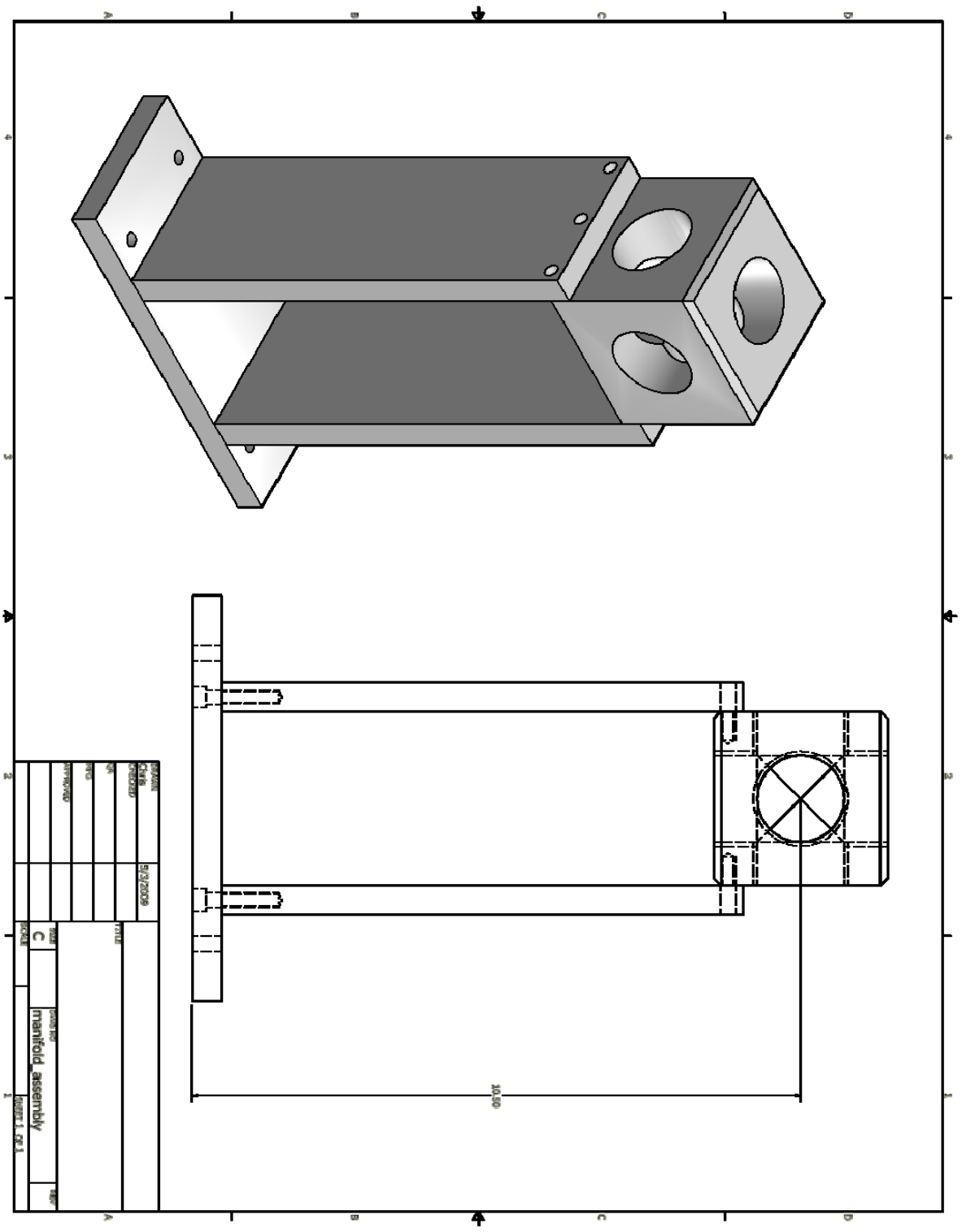

4-Way Manifold Assembly

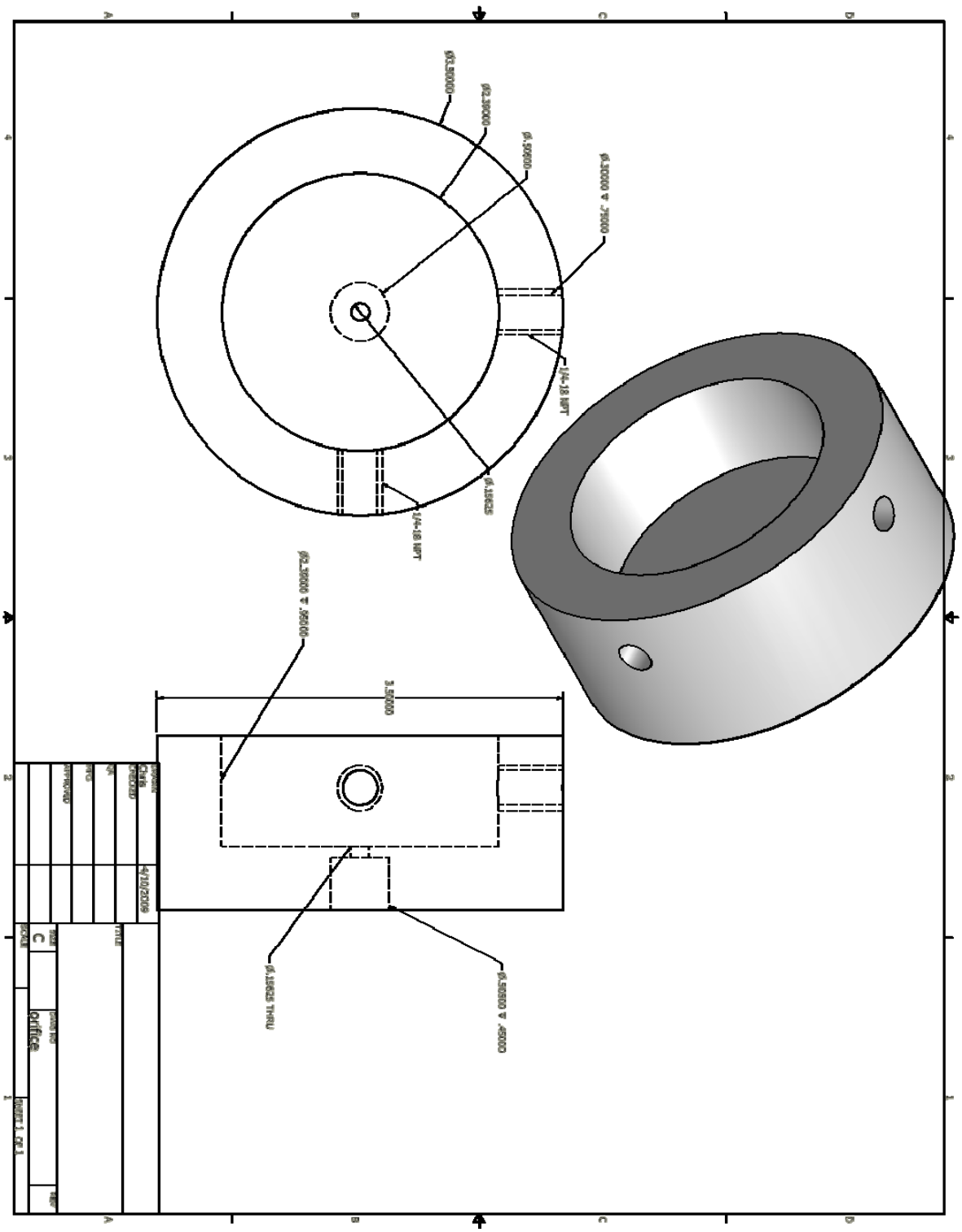

Air Choke and Fuel Inlet Assembly

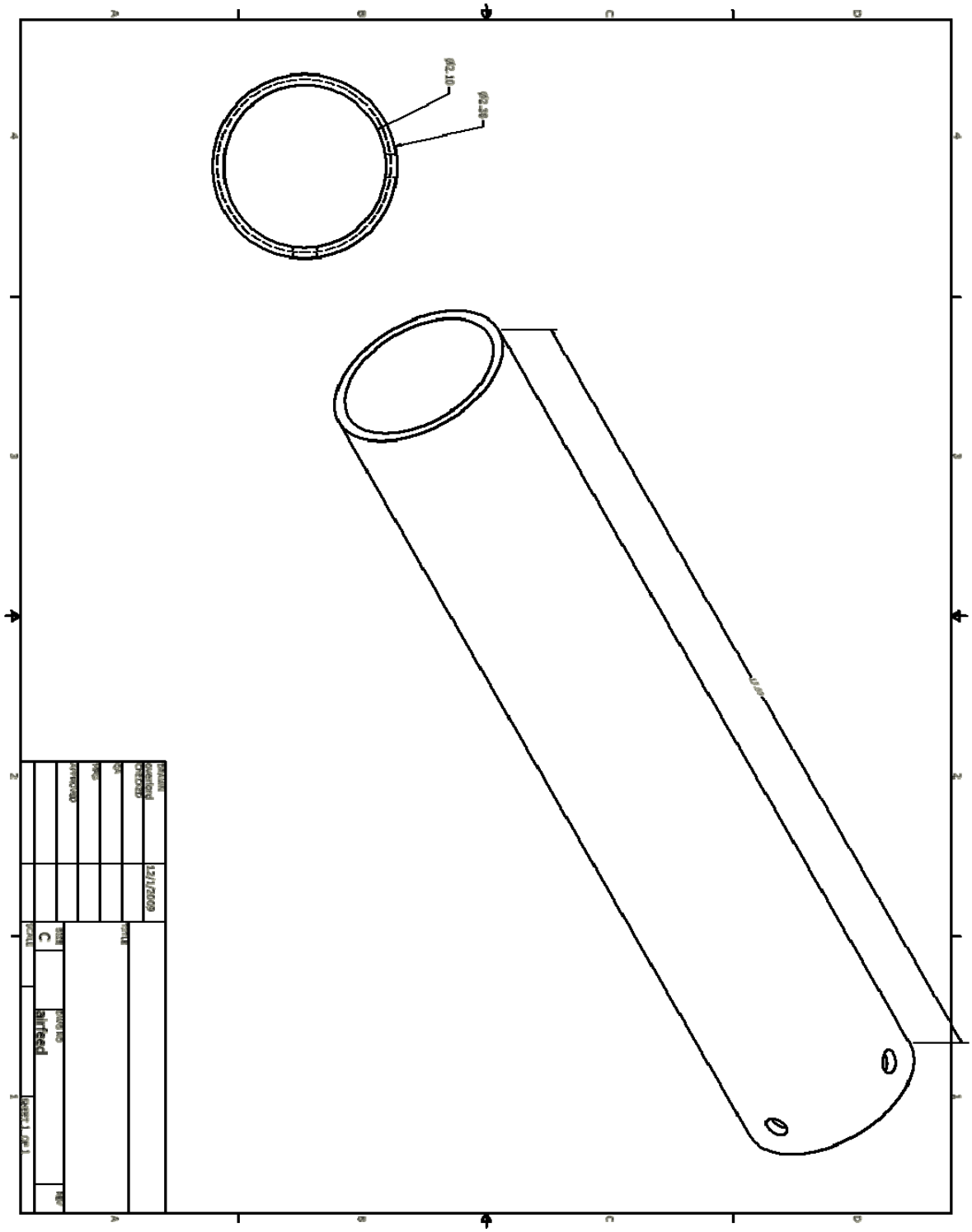

Mixing Manifold

APPENDIX B. PRESSURE TRANSDUCER CALIBRATION

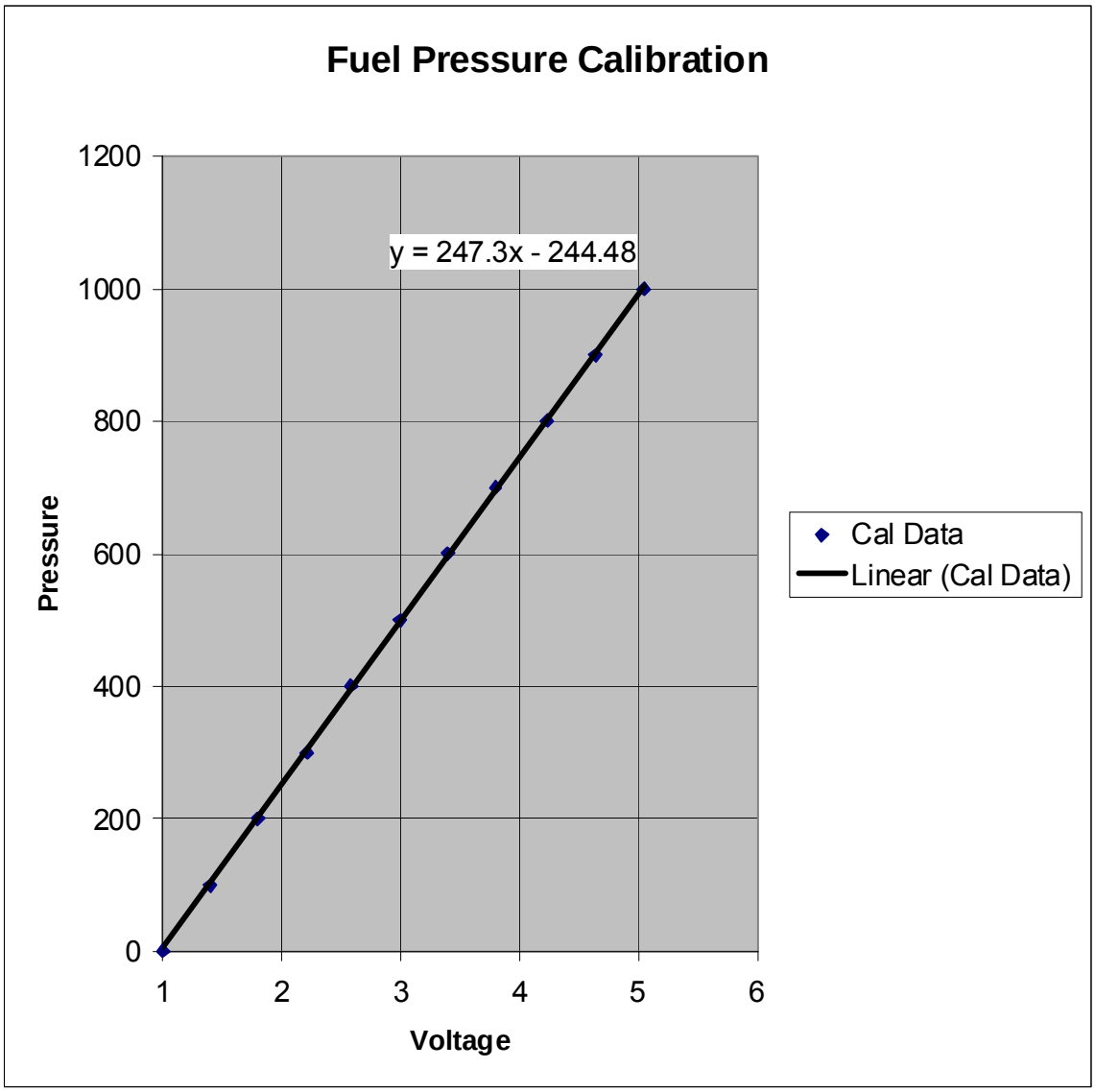

Fuel Pressure Calibration Graph (Pressure vs. Voltage)

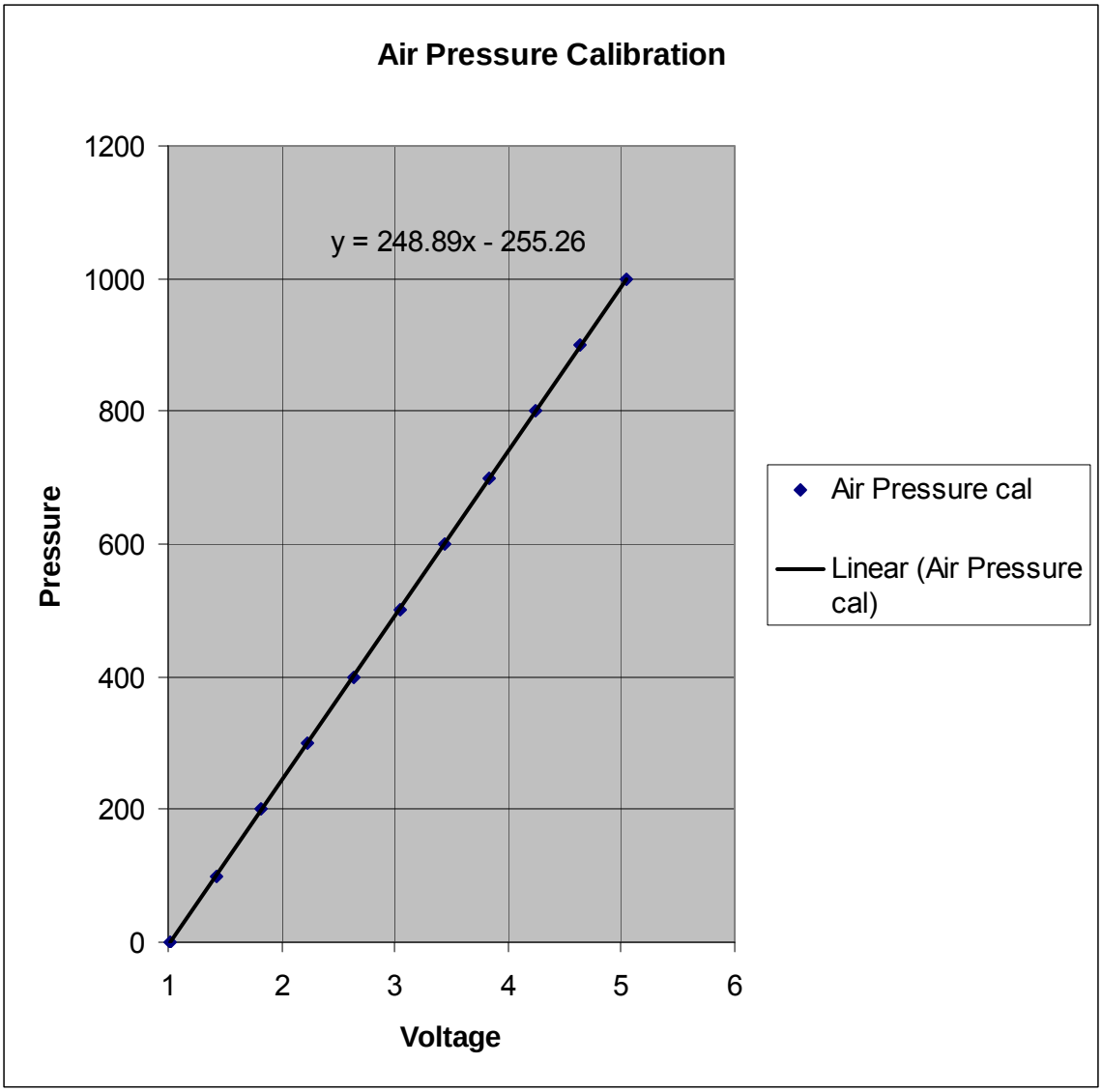

Air Pressure Calibration Graph (Pressure vs. Voltage)

APPENDIX C. STANDARD OPERATING PROCEDURE

Test Cell #1
Standard Operating Procedures (S.O.P)
Flame Viewing Test Rig
(Modification Date 4 Aug 2009)

INITIAL PREPARATIONS

1. Notify all lab personnel of intention to make test cell 1 live.
2. Turn **ON** control console
3. Turn **ON** warning lights
4. Cell #1 EMERGENCY SHUTDOWN BUTTON (Control Room)- **VERIFY IN**
5. Notify the Golf Course (x2167) (Only required if Hot Fire Test is conducted)
6. Open Test Cell Door
7. For non-TPI Test
    a. Igniter Control (Test Cell)-**VERIFY OFF** (Red Button Out)
    b. PXI-1000B Rack (Test Cell)-**VERIFY ON**
8. For TPI Test
    a. Pulse Generator - **VERIFY OFF**
    b. High Voltage Power Supply - **VERIFY OFF**
9. Shop Air-**VERIFY > 100 PSI**
10. Shop Air Valve (Test Cell)-**VERIFY OPEN**
11. Fuel Valve Control Air (On Test Bench) - **VERIFY OPEN**
12. 115 VAC Control/Cell #1 Switch (Control Room)-**ON**
13. 28VDC Power Supply/Cell #1 Switch (Control Room)-**ON**
14. Open LABVIEW

TESTING SET-UP

1. Desired testing configuration verified.

****Note: Viewing Section must be removed and slid aft in order to continue****

2. Node 4 HP Main Air Valve (under test bench) – **VERIFY OPEN**
3. Notify all personnel that gasses and TESCOM will be enabled.
4. Test Cell #2 and #3 Node 4 Air Isolation Valve (Test Cell #2)-**VERIFY CLOSED** (Cross Check Item)

****NOTE: This valve maybe left open only if Test Cell #2 or #3 is configured for active testing****

5. TRANSDUCER and TESCOM Power Switch (Test Cell #2)-**ON**
6. Set **0 (Zero)** pressures on ER3000 (Control Room) for the following:

   a. **Node 3 (Ethylene)**
   b. **Node 4 (Main Air)**
7. Main HP Air Jamesbury Valve (Outside Test Cell)-**OPEN SLOWLY**
8. For non-TPI Test
   a. Power Strip (above PXI-1000B)-**VERIFY ON**
   b. Igniter Control Light (Red LED upper left on CRYDOM in PX-1000B Rack)-**VERIFY OUT**

****DANGER: IF RED LIGHT IS ENERGIZED, MUST CLEAR USING LABVIEW BEFORE CONTINUING TO PREVENT PREMATURE IGNITION****

   c. Igniter Control (Test Cell)-**PUSH RED BUTTON IN**
   d. Igniter Control Startup Diagnostics-**OBSERVE COMPLETION OF DIAGNOSTICS**
9. For TPI Test
   a. High Voltage Power Supply – **TURN ON**
   b. Pulse Generator – **TURN ON**
10. Node 4 LP Isolation Valve – **OPEN SLOWLY**

****DANGER: OPEN VALVES SLOWLY TO PREVENT RAPID PRESSURIZATION OF DOWNSTREAM LINES****

11. Node 3 (Ethylene) Shop Air Valve (Above Bottle in Bottle Room)- **VERIFY OPEN**
12. Ethylene Bottle Isolation Valve (On Bottle)-**OPEN SLOWLY**

**** VERIFY ADEQUATE ETHYLENE PRESSURE FOR TESTING ON DOWNSTREAM GAGE LOCATED IN BOTTLE ROOM****

PRE-TESTING

1. ULTRA Camera-**TURN ON AND REMOVE COVER**
2. Start ULTRA Software
3. Verify Image on ULTRA Software
4. Verify Desired Trigger Types and Valve Durations
5. Determine Desired Fuel and Air Pressures (Mass Flow Choke Calibrations.xls)
6. Set Required Pressures on ER3000
   a. **Node 3 (Ethylene)**
   b. **Node 4 (Main Air)**
7. Insert Tape into VCR
8. Switch Monitor to B (Test Cell #1)

TESTING

1. Clear All Test Cells and Verify with Head Count
2. Flashing Red Light and Siren-**ENERGIZE**
3. Verify Golf Course is **CLEAR**
4. VCR-**RECORD**
5. Camera-**ARM**
6. In LABVIEW Enable Facility Button-**ON**
7. Test Cell #1 Emergency Shutdown Button-**TURN CLOCKWISE**
8. In LABVIEW Start Button-**CLICK TO START**

WHEN TEST COMPLETE:

9. Set Node 4 Pressure to **0 (Zero)**
10. In LABVIEW Turn Off Button-**CLICK TO SECURE**
11. In LABVIEW Enable Facility Button-**VERIFY OFF**
12. Test Cell #1 Emergency Shutdown Button-**PUSH IN**
13. Siren-**OFF**
14. VCR-**Stop/Pause**
15. Save ULTRA Image

****NOTE: If Further Testing is Required, re-perform steps 1-15 of the Testing Section****

POST TESTING

1. Set ER300 Node 3 (Ethylene) to **0 (Zero)**
2. Verify pressures on ER3000 are set to 0 (Zero) on the following:
    a. **Node 3 (Ethylene)**
    b. **Node 4 (Main Air)**
3. Node 4 LP Isolation Valve - **CLOSE**
4. Main HP Air Jamesbury Valve (Outside Test Cell)-**CLOSE**
5. Ethylene Bottle Isolation Valve (On Bottle)-**CLOSE**
6. Igniter Control (Test Cell)-**PUSH RED BUTTON OUT**

****NOTE: If Further Testing will be accomplished with a different Ramp obstacle configuration, return to the TESTING SET-UP Section. If not continue to step 7.****

7. ULTRA Camera-**TURN OFF AND INSTALL COVER**
8. TRANSDUCER and TESCOM Power Switch (Test Cell #2)-**OFF**
9. Close Test Cell Door
10. Node 3 (Ethylene) Shop Air Valve (Above Bottle in Bottle Room)-**CLOSE**
11. Secure Bottle Room
12. Exit out of ULTRA

13. EXIT out of LABVIEW
15. 28VDC Power Supply/Cell #1 Switch (Control Room)-**OFF**
16. 115 VAC Control/Cell #1 Switch (Control Room)-**OFF**

LIST OF REFERENCES

[1] Carlos A. Medina, "Evaluation of Straight and Swept Ramp Obstacles on Enhancing Deflagration to Detonation Transition in Pulse Detonation Engines," Master's Thesis, U.S. Naval Postgraduate School, Monterey CA, December 2006.

[2] John A. Anderson, "Deflagration-to-Detonation Transition Enhancement Using Low-Loss Obstacles," Master's Thesis, U.S. Naval Postgraduate School, Monterey, California, December 2007.

[3] J.B. Liu, P. Ronney, and M.A. Gundersen, "Corona Discharge Ignition of Premixed Flames," http://carambola.usc.edu/research/coronaignition/coronaignition.html, accessed September 2005.

[4] C. Cathey, J. Cain, H. Wang, M.A. Gundersen, C. Carter, M. Ryan, "Combustion and Flame," Science Direct, March 2008.

[5] D. Singleton, J.O. Sinibaldi, C.M. Brophy, A. Kuthi, and M.A. Gundersen, "Compact Pulsed Power System for Transient Plasma Ignition," Office of Naval Research, February 2009.

[6] C. Cathey, F. Wang, T. Tang, A. Kuthi, M.A. Gundersen, J.O. Sinibaldi, C.M. Brophy, E. Barbour, R.K. Hanson, J. Hoke, F. Schauer, J. Corrigan, J. Yu, "Transient Plasma Igition for Delay Reduction in Pulse Detonation Engines," Presentation to the 45th AIAA Aerospace Science Meeting and Exhibit, January 2007.

[7] G.V. Naidis, "Modeling of Transient Plasma Discharges in Atmospheric-pressure Methane-air Mixtures," Journal of Physics, July 2007.

[8] C. Cathey, J. Cain, H. Wang, M.A. Gundersen, C. Carter, M.Ryan, "Transient Plasma Induced Production of OH and its Effects on Ignition in Atmospheric CH_4-air Quiescent Mixtures," Presentation to the 46th AIAA Aerospace Science Meeting and Exhibit, January 2008.

[9] C. Cathey, T. Tang, T. Shiraishi, Tomonori, A. Kuthi, M.A. Gundersen, "Nanosecond Plasma Ignition for Improved Performance of an Internal Combustion Engine," IEEE Transactions on Plasma Science, Vol. 35, No.6, December 2007.

[10] F. Wang, J.B. Liu, J.O. Sinibaldi, C.M. Brophy, A. Kuthi, C. Jiang, P. Ronney, M.A. Gundersen, " Transient Plasma Ignition of Quiescent and Flowing Air/Fuel Mixtures," IEEE Transactions on Plasma Science, Vol. 33, No. 2, April 2005.

[11] Michael A. Fludovich, Jr., "Pulsed Detonation Engines: Investigation of Detonation Wave Diffraction with Reactive Transpiration," Master's Thesis, Monterey CA, September 2002.

[12] George P. Sutton, "Rocket Propulsion Elements," 6th ed., John Wiley and Sons, Inc., 1992.

[13] G. D. Roy, "Energy Conservation through Detonative Processes," presentation to the 1st international Energy Conservation Engineering Conference, August 2003.

INITIAL DISTRIBUTION LIST

1. Defense Technical Information Center
   Ft. Belvoir, Virginia

2. Dudley Knox Library
   Naval Postgraduate School
   Monterey, California

3. Asst. Professor Chris Brophy
   Naval Postgraduate School
   Monterey, California

4. Professor Jose Sinibaldi
   Naval Postgraduate School
   Monterey, California

5. LT Neil Hawkes
   Naval Postgraduate School
   Monterey, California